

ISSN 0280-5316  
ISRN LUTFD2/TFRT--5901--SE

# Temperature Control of a Scientific Instrument

Albert Pla Ruiz

Lund University  
Department of Automatic Control  
June 2012



<b>Lund University</b> <b>Department of Automatic Control</b> <b>Box 118</b> <b>SE-221 00 Lund Sweden</b>		<i>Document name</i> <b>MASTER THESIS</b>	
		<i>Date of issue</i> <b>June 2012</b>	
		<i>Document Number</i> <b>ISRN LUTFD2/TFRT--5901--SE</b>	
<i>Author(s)</i> <b>Albert Pla Ruiz</b>		<i>Supervisor</i> <b>Bo Bernhardsson, Dept. of Automatic Control, Lund University, Sweden</b> <b>Lars Wadsö, Division of Building Materials, Lund University, Sweden</b> <b>Anders Rantzer, Dept. of Automatic Control, Lund University, Sweden (examiner)</b>	
		<i>Sponsoring organization</i>	
<i>Title and subtitle</i> <b>Temperature Control of a Scientific Instrument (Temperaturreglering av ett vetenskapligt instrument)</b>			
<i>Abstract</i> <p>The aim of the present Master's Thesis was to improve the temperature control of a calorimetric instrument called STIC (Several Temperatures Isothermal Calorimeter). Calorimetry is the science of measuring heat, heat production rate or heat capacity; the present instrument is an isothermal calorimeter used for the measurement of thermal power from different types of processes. In the instrument, four calorimeters are placed in a temperature gradient between a warm and a cold side, both of which are temperature controlled. In order to have an open and transparent control system, new PID controllers were implemented using Simulink and dSPACE. Experiments were carried out to see the effect of external temperature changes on the STIC measurement signals. A simulation model of the STIC was also developed in MATLAB. To decrease the effect of external temperature changes, a new feed forward control was added to the cooling side. To test and tune this controller, both simulations and experiments were done. The simulation result gave an improvement of about 55% compared to the situation without feed forward-, while the experiments gave a lower improvement of about 25%. To test a possible application of the STIC, an experiment with the setting of gypsum (plaster of Paris) was carried out.</p>			
<i>Keywords</i>			
<i>Classification system and/or index terms (if any)</i>			
<i>Supplementary bibliographical information</i>			
<i>ISSN and key title</i> <b>0280-5316</b>			<i>ISBN</i>
<i>Language</i> <b>English</b>	<i>Number of pages</i> <b>1-131</b>	<i>Recipient's notes</i>	
<i>Security classification</i>			



# Preface

This Master's Thesis has been carried out as collaboration between the Division of Building Materials and the Department of Automatic Control at Lund Institute of Technology, and it represents the last step of my five years degree in Engineering (Ingeniería Industrial) at Escola Tècnica Superior d'Enginyeria Industrial de Barcelona. The work has been supervised by Professor Lars Wadsö at the Division of Building Materials, with the advice of Professors Bo Bernhardsson and Anders Rantzer at the Department of Automatic Control.

First of all I would like to thank both my former university, Escola Tècnica Superior d'Enginyeria Industrial de Barcelona, and the Faculty of Engineering, LTH, at Lund University for giving me the opportunity to finish my studies in such a wonderful country and more important, to let me grow academically but also as a person through this amazing Erasmus experience.

To Lars Wadsö, thanks for your patience, guidance and help through the entire project, but especially in those moments when a wall appeared in the way and the frustration began to grow. Thank you also for writing the first version of the MATLAB simulation model.

To Bo Bernhardsson and Anders Rantzer, thanks for giving me the chance to do this project, and also thanks for your guidance and advice that made it possible for me to solve also the more difficult problems that I encountered.

To all the staff in the Division of Building Materials, thank you for making me feel comfortable during all these months being part of the division and thanks for helping me in whatever I had needed.

To my parents, thank you for your support during my childhood and adolescence, but especially thanks for your support during these hard five years of university studies, thank you for being there in the moments of frustration and desperation, and never letting me down. Although you have been far away during the realization of this thesis, I have felt you so close, and I have felt your support through the screen of the laptop.

And last but not least, I dedicate this thesis to my two newborn cousins, who have been born while this thesis was being done. Inés and Emma, I cannot wait to meet you!

Lund, in June 2012  
Albert Pla Ruiz



# Contents

<b>1. Isothermal Calorimetry.....</b>	<b>6</b>
1.1 Description of an isothermal calorimeter.....	7
<b>2. Description of the STIC.....</b>	<b>10</b>
2.1 Physical components.....	10
2.2 Insulation.....	20
2.3 Sensors.....	21
2.4 Data loggers.....	24
2.5 Electric schema of the STIC.....	26
<b>3. PID Controller in dSPACE Platform.....</b>	<b>28</b>
3.1 dSPACE and MATLAB Simulink.....	28
3.2 Electrical and electronic devices.....	28
3.3 Control algorithm.....	33
3.4 Temperature sensor calibration.....	37
3.5 Results.....	40
<b>4. Simulation Model.....</b>	<b>46</b>
4.1 Model.....	46
4.2 Test and validation.....	52
<b>5. Control System Improvement.....</b>	<b>56</b>
5.1 Feed forward control.....	56
5.2 Relationship between ambient temperature and TEC duty cycle.....	57
5.3 Feed forward control algorithm.....	58
5.4 Feed Forward simulation.....	59
5.5 Feed forward tuning experiment.....	62
<b>6. Gypsum plaster setting experiment.....</b>	<b>72</b>
6.1 Description of gypsum plaster.....	72
6.2 Experimental procedure.....	72
6.3 Results and discussion.....	73
<b>7. References.....</b>	<b>76</b>
<b>8. Software.....</b>	<b>78</b>
<b>9. Annexes.....</b>	<b>80</b>
9.1 Material's properties.....	82
9.2 Simulation model.....	84
9.3 STIC drawings.....	92



# 1. Isothermal Calorimetry

Calorimetry is the science of measuring the heat of chemical reactions or physical changes, as well as heat capacity, by using a calorimeter. This field of knowledge is said to have been founded in the middle 18th century by the Scottish physician and scientist Joseph Black, who was the first to notice the difference between heat and temperature [1]. Black also discovered latent heat, which was the operational base of the world's first calorimeter, the ice-calorimeter created by Antoine Lavoisier and Pierre-Simon Laplace in the winter of 1782-83. This calorimeter was able to determine the heat evolved in various processes [1]. The operation of the calorimeter was as follows (see Figure 1-1, from reference [2]): the heat produced by the animal (or any other process) inside the closed inner chamber was proportional to the mass of liquid water emerging from the melting ice in the inner of the two chambers with ice and water surrounding the inner chamber [2].



**Figure 1- 1** Lavoisier-Laplace ice calorimeter.

Since the 18<sup>th</sup> century there has been a significant advancement in calorimetric techniques and there are today several types of modern calorimeters, such as differential scanning calorimeters, adiabatic or semi-adiabatic calorimeters, indirect calorimeters and nuclear calorimeters. The instrument studied in this project is an isothermal conduction calorimeter.

Isothermal calorimetry is the measurement of heat and thermal power at (essentially) constant temperature conditions [3]. This type of calorimeter is based on the work of Professor Albert Tian in the early 1920's. Tian described his compensation isothermal microcalorimeter for the first time in 1922 while studying the metabolism of insects, and then brought further improvements to this thermocouple instrument in 1924 and 1926. Tian's successor Edouard Calvet introduced the differential setup and a rational construction of the two twinned calorimetric elements in the 1940's, transforming the Tian's appliance into a true laboratory instrument [4]. This technique can be applied in several fields, due to the fact that almost all processes, whether physical, chemical or biological, produce heat. For example, isothermal calorimeters are used in food science, polymer science, for the study of cement hydration, in microbiological studies and in pharmaceutical technology.

There are some aspects of the isothermal calorimeters that made the isothermal calorimetry one of the most useful types of calorimeters. Besides of being a general method with multiple fields of application, the measurement is non-destructive, often sensitive, one can manipulate the sample during the experiment, and the results can be processed in order to do thermodynamic calculations.

## 1.1 Description of an isothermal calorimeter

First of all, one should define three concepts, heat, heat flow rate and thermal power:

- Heat  $Q$ : The form of energy that can be transferred from one system to another as a result of a temperature difference [5]. The SI unit of heat is the joule (J).

- Heat flow rate  $\Phi$ : The amount of heat transferred per unit time [5]. The SI unit of heat flow rate is the watt (W),  $1 \text{ W} = 1 \text{ J/s}$

- Thermal power  $P$ : The amount of heat rate produced by the process (physical, chemical or biological) subject of the study. The SI unit of the thermal power is the watt (W).

$$P = \frac{dQ}{dt}$$

Isothermal calorimeters of the heat conduction type consist, as shown in Figure 1.1-1, of five different components: the sample, the reference, the heat sink and two heat flow sensors. The sample is an amount of the material which one wants to study the thermal power from. The reference is an inert sample (no heat production) with thermal properties similar to the sample. Common references are water or sand.

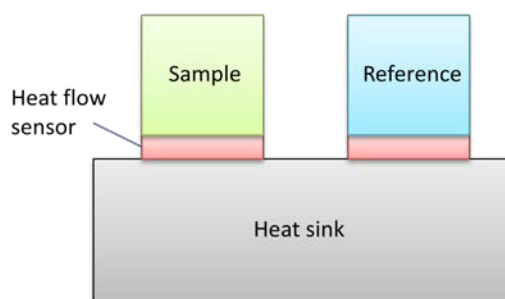


**Figure 1.1-1** Isothermal calorimeter.

The whole set-up must be essentially isothermal, so the temperature of the heat sink is maintained constant by a thermostat. The heat flow sensors are thermocouples based on the Seebeck effect, which will be described later.

The working principle is the following. Heat is produced in the sample and a temperature difference develops across the heat flow sensor which results in a voltage output while heat flows out to the heat sink [3]. Let us use the following nomenclature:  $\Phi$  is heat flow (W);  $\Delta T$  is temperature difference (K);  $U$  is voltage (V); and  $P$  is thermal power (W). At steady-state, the heat flow rate across the sensor is the same as the thermal power of the sample:  $\Phi = P$ . Heat flow rates are proportional to the existence of temperature difference:  $\Phi \sim \Delta T$ . The output voltage of the thermocouple is proportional to the temperature difference:  $U \sim \Delta T$ . Then, the voltage output is proportional to the heat flow across the sensor:  $U \sim \Phi$ . And finally, the measured output voltage is proportional to the thermal power:  $U \sim P$ .

So in conclusion, at steady-state (when the thermal power is constant), the thermal power ( $P$ ) is the output voltage of the heat flow sensors ( $U$ ) multiplied by a constant, which we call the calibration coefficient ( $\varepsilon$ )

$$\Phi = \varepsilon \cdot U$$

However, at unsteady-state (when the thermal power changes as a function of time), the measured signal is delayed with respect to the actual thermal power of the sample, and will therefore lag behind when the thermal power changes. To remove this effect, the Tian correction is used. This correction gives the true

thermal power of the sample from the delayed curve, and consists of a correction for the time-lag of the calorimeter based on the time constant ( $\tau$ ) [3].

$$\Phi = \varepsilon(U + \tau \cdot \frac{dU}{dt})$$

The aim of using a reference and to measure the difference between the sample-signal and the reference-signal is primarily to have less noise from external disturbances, but also to get a faster response in the measurements.



## 2. Description of the STIC

The STIC (Several Temperature Isothermal Calorimeter) is a device that can make measurements in four isothermal calorimeters at four different temperatures at the same time. It was designed by Lars Wadsö around 2005 with funding from The Crafoord Foundation. Its general working principle is described in reference [6] together with examples of its use in biological science. It is basically an aluminum square tube with four isothermal calorimeters inside, equidistantly placed along the length of the tube (Figure 2-1). The free space between them is filled with thermal insulation. To get each calorimeter at a different temperature, a temperature gradient is created between the ends of the tube, by heating in one side and cooling in the other. With both the effect of the gradient and the insulation, one obtains a different temperature in each calorimeter, but also that each calorimeter is (essentially) isothermal.

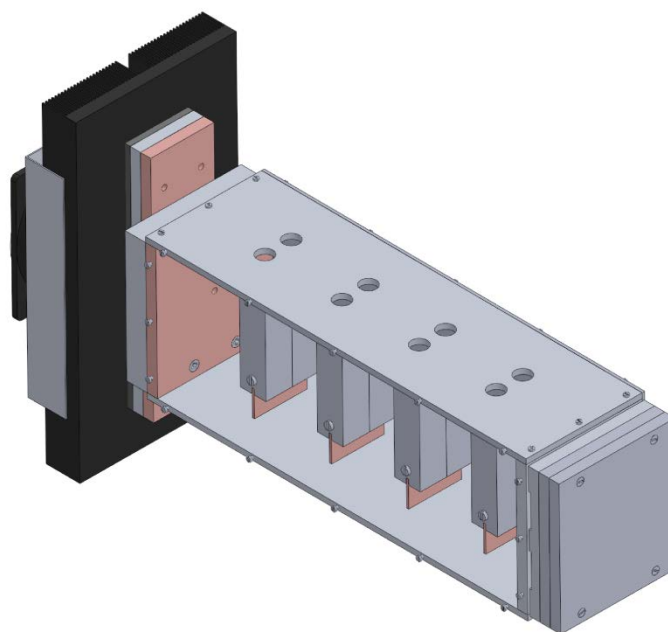


**Figure 2-1** *Several Temperature Isothermal Calorimeter (STIC)*

In the next sections all parts and components of the STIC will be described as well as being discussed in terms of their function and operation.

### 2.1 Physical components

The STIC structure is formed by a square aluminum tube, the four calorimeters, the heater, the TEC (Thermoelectric Cooler) and some metal plates (Figure 2.1-1).

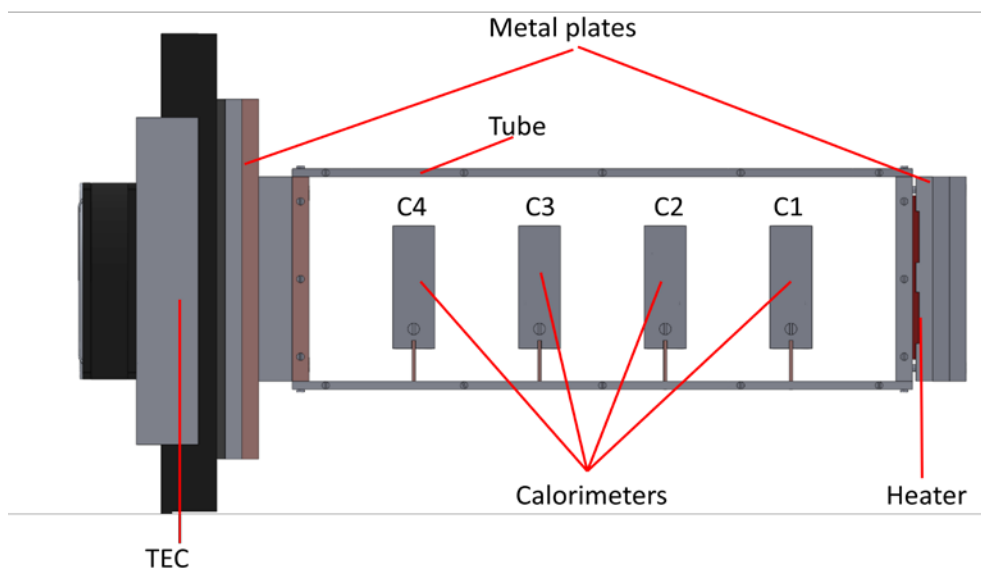


**Figure 2.1-1** Physical components of the STIC.

Each one of the components of the STIC will be briefly described in the next pages. The exact dimensions and properties are given in an annex.

### Calorimeter

The calorimeter is the part of the instrument in which the measurements are made. It is a heat conduction calorimeter based on the same principle discussed above. The sample and the reference ampoules are placed in sample holders, which are placed on heat flow sensors, which are in contact with the heat sink. Each assembly (one for the sample and one for the reference) is situated inside a tube with a square cross section and kept together by a screw. The resulting assembly is connected to the heat gradient tube by a copper heat conduction plate (Figure 2.1-2).

All parts of the assembly are made of aluminum, except the screw (steel), the sensor (BiTe and  $\text{Al}_2\text{O}_3$ , description below) and the copper heat conduction plate.

The heat flow sensors give a voltage signal proportional to the heat flow from the sample to the heat sink. Between the two cubic heat sinks there is a little space where a Pt-100 temperature sensor is placed to measure the temperature of the calorimeter (which is essentially constant in the whole calorimeter).

There are four calorimeters in the STIC placed equidistantly along the tube. They are numbered from 1 to 4 with calorimeter 1 closest to the hot side (where the heater is placed) and calorimeter 4 closest to the cold side (where the TEC is placed).

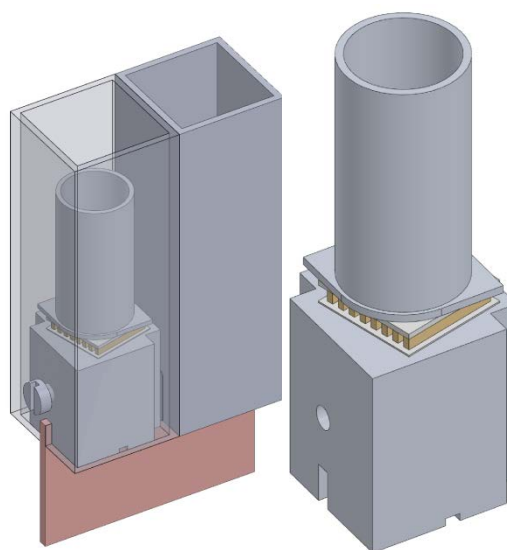


**Figure 2.1-2** Calorimeter.

## Tube

The tube is the main structure of the STIC. As shown in Figure 2.1-3, it consists of four aluminum plates, two vertical plates of 370x135x2 mm and two horizontal plates of 370x110x5 mm. The upper cover has eight circular holes, concentric with the sample holders, so that one can put in and take out the ampoules. The lower cover has four rectangular holes to fit the copper heat conduction plates of the calorimeters. The aluminum plates are held together by small screws.

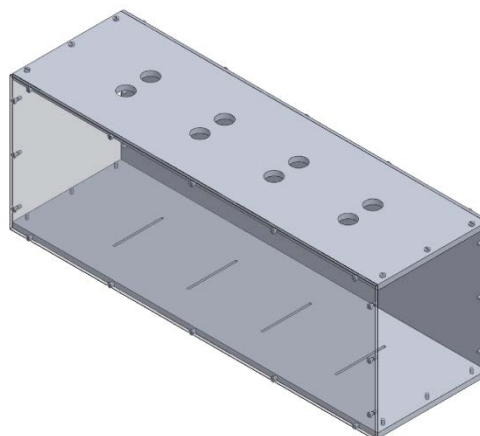


Figure 2.1-3 Tube.

## Metal plates

The metal plates placed at the ends of the main tube are made of aluminum or copper. Their function is both to help the heat flow between the heater-tube and the tube-TEC, and to add thermal inertia to the device in order to reduce the effect of external noise and perturbations that could influence the calorimetric measurements. Their positions in the STIC are shown in the Figure 2.1-4. Their dimensions are given in an annex.

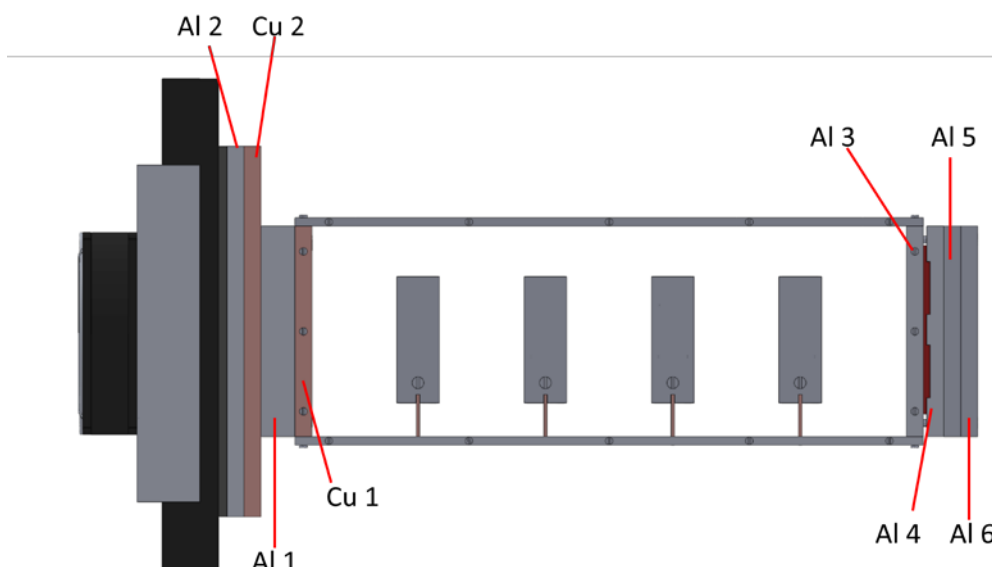


Figure 2.1-4 Metal plates in the STIC.

## TEC

The TEC (ThermoElectric Cooler) is a device whose function is to cool the cold side of the STIC. The present TEC is manufactured by Laird Technologies and has the item number DA-075-24 [7]. It consists on several TEMs (Thermoelectric Modules) that are able to extract heat from one of their surfaces and produce heat at the other surface; they are therefore a type of heat pump. As shown in Figure 2.1-5, the TEC also has a finned heat sink with a fan on the external side in order to improve the dissipation of the heat, as it will be explained in the next sections.

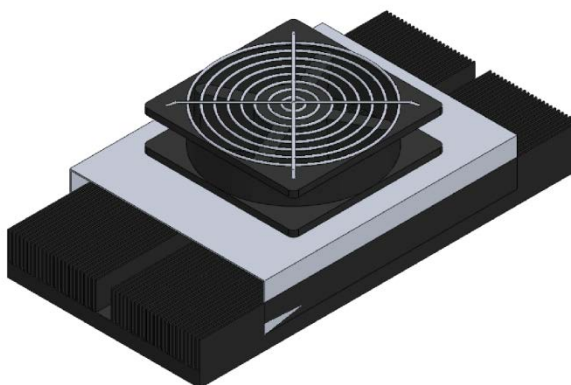


Figure 2.1-5 ThermoElectric Cooler (TEC).

### -TEM (ThermoElectric Module)

A thermoelectric module is a device composed of thermoelectric couples based on the Peltier effect: when a current flow through a circuit made of two different materials with two junctions, heat is generated at one of the junctions (at  $T_1$ ) and absorbed at the other junction (at  $T_0$ ). This is shown in Figure 2.1-6, from reference [8].

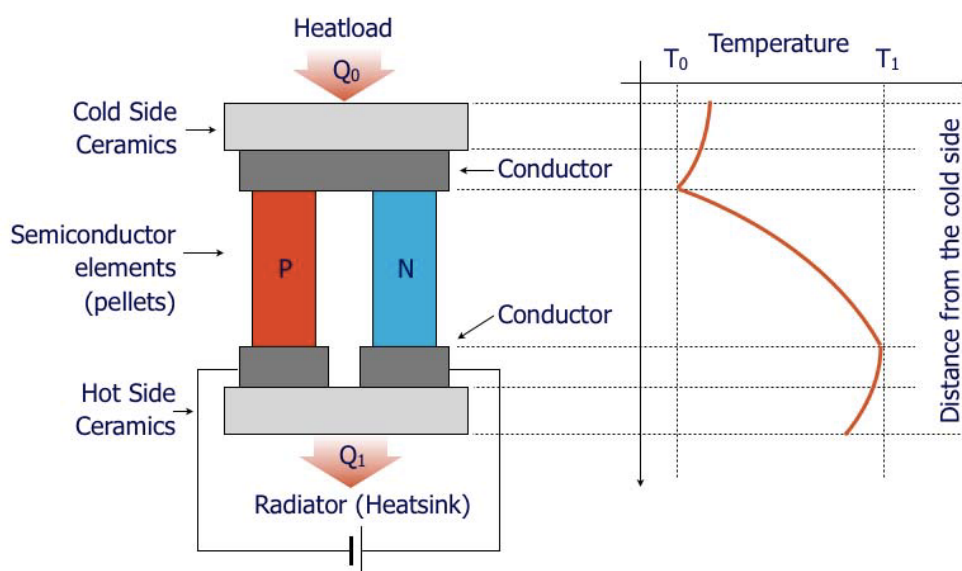


Figure 2.1-6 Simplified scheme of TEM and the temperature differential along it.

In contrast to Joule heating, which is proportional to the square of the current ( $P_J = RI^2$ ), the Peltier heat ( $P_P$ ) is a linear function of the current and its sign also changes with the current:

$$P_P = p \cdot I$$

Here  $I$  is the current through the junction (A) and  $p$  is the Peltier coefficient (V), which depends on the junction materials' nature and the junction temperature. It can be calculated from the Seebeck coefficient:

$$p = S \cdot T$$

where  $S$  is the Seebeck coefficient which depends on the materials, their properties and the junction temperature (V/K), and  $T$  is the junction temperature (K).

The thermoelectric couples are made by n and p-type semiconductor pellets, usually bismuth telluride ( $\text{Bi}_2\text{Te}_3$ ), connected electrically in series and thermally in parallel. The pellets are fixed by soldering and sandwiched between two ceramic plates (Figure 2.1-7, from reference [8]), with high thermal conductivity and high electrical resistivity. These plates are usually made by aluminum oxide ( $\text{Al}_2\text{O}_3$ ), and they provide mechanical integrity to the module.

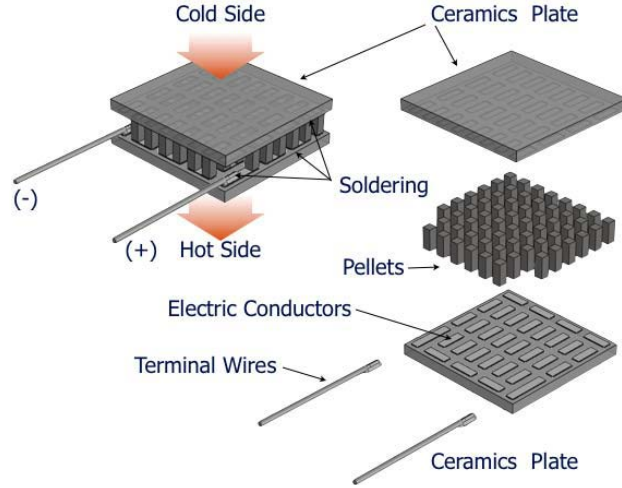


Figure 2.1-7 TEM construction.

If one calls the cold side  $C$  (the side where heat is absorbed) and the hot side  $H$  (where the heat is released), one can calculate the heat flows at these two sides as [9]:

$$\begin{aligned}\Phi_C &= SIT_C - \frac{1}{2}R_e I^2 - K(T_H - T_C) \\ W_e &= SI(T_H - T_C) + R_e I^2 \\ \Phi_H &= \Phi_C + W_e\end{aligned}$$

where  $\Phi_C$  is the heat power absorbed in the cold side,  $W_e$  the electric power applied to the TEC,  $\Phi_H$  the heat power released in the hot side,  $S$  is the Seebeck coefficient,  $I$  is the current through the pellets,  $T_C$  and  $T_H$  are the temperatures in the cold side and the hot side,  $R_e$  is the overall electrical resistance of the module and  $K$  is the thermal conductivity of the module.

From the above equations one can see that the heat absorbed  $\Phi_C$  is composed of three different terms: the heat absorbed by the Peltier effect ( $SIT_C$ ) minus half of the Joule heating ( $\frac{1}{2}R_e I^2$ ) and minus the heat transferred between the hot and the cold side ( $K(T_H - T_C)$ ) because of the temperature difference (there is always a conductive heat flow from the hot side to the cold side). So it is clear that the actual heat absorbed, and so the cooling power of the TEC, is lower than the theoretical Peltier effect as there also appears other heat production/transfer terms that makes the power decrease.

The electric power  $W_e$  is the voltage applied to the TEC to overcome the Seebeck effect and the resistive voltage drop, multiplied by the current. The heat released is the heat created by the Peltier effect ( $SIT_H$ ) plus half the Joule heating ( $\frac{1}{2}R_e I^2$ ) minus the heat transferred between the hot and the cold side ( $K(T_H - T_C)$ ).

The properties  $R_e$ ,  $K$  and  $S$  of the module can be calculated from the electrical resistivity and the Seebeck coefficient of the n-doped and p-doped  $\text{Bi}_2\text{Te}_3$  and the geometrics of the pellets [9]. Therefore:

$$S = N(S_p + |S_n|)$$

$$r_e = N \frac{L}{A} (\rho_p + \rho_n)$$

$$K = 2nN \frac{A}{L} k$$

where  $N$  is the number of thermocouples (note that each thermocouple consists of two pellets, one n and one p),  $n$  is the number of TEMs,  $r_e$  is the electrical resistance of one TEM (in  $\Omega$ ),  $S_p$  and  $S_n$  are the Seebeck coefficients of the p-doped and n-doped  $\text{Bi}_2\text{Te}_3$  (in V/K),  $\rho_p$  and  $\rho_n$  the electrical resistivity of the p-doped and n-doped  $\text{Bi}_2\text{Te}_3$  (in  $\Omega \cdot \text{m}$ ),  $k$  is the thermal conductivity of both n- and p-doped  $\text{Bi}_2\text{Te}_3$  (in W/K·m),  $L$  is the length of the pellets (in m) and  $A$  is the perpendicular area of the pellets (in  $\text{m}^2$ ).

In the TEC of the STIC there are four TEMs ( $n = 4$ ) electrically connected as Figure 2.1-8 shows. The electrical resistance of each branch is

$$R_e = 2 \cdot r_e$$

and as there are two branches (the resistance is the same in each branch), the total heat absorbed in all the TEC (the four TEMs) and the electrical power are:

$$\Phi_c = 2 \cdot (2SIT_c - \frac{1}{2}R_e I^2) - K(T_H - T_C)$$

$$W_e = 2 \cdot (2SI(T_H - T_C) + R_e I^2)$$

In Table 2.1-1-2 one can see the values of the parameters and properties discussed above. The TEMs used are produced by Laird Technologies and are called CP12.161.055 ( 161 thermocouples, the length of the sides of each pellet is 1.2 mm, and the length of the pellets is 0.55 inch=1.4 mm).

Parameter	Value
$n$	4
$N$	161
$S_p$	165e-6 V/K
$S_n$	-238e-6 V/K
$\rho_p$	0.53e-5 $\Omega \cdot \text{m}$
$\rho_n$	1.2e-5 $\Omega \cdot \text{m}$
$k$	1.5 W/K·m
$L$	0.0014 m
$A$	0.0012 <sup>2</sup> $\text{m}^2$
$U$	24 V

**Table 2.1-1** Parameters and properties of bismuth telluride and the used TEMs ( from the literature [10]).

Parameter	Value
$S$	0.2595 V/K
$K$	1.9872 W/K
$r_e$	2.708 $\Omega$

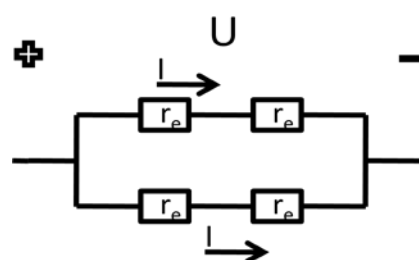


**Figure 2.1-8** Electrical connection of the TEMs.

$R_e$	5.416 $\Omega$
$I_{max}(= U/R_e)$	4.43 A

**Table 2.1-2** Calculated parameters for the used TEM.

- Heat sink

The heat sink of the TEC consists on a plate of aluminum with several fins and a fan. The dimensions can be seen in an annex. The goal of this component is to dissipate the heat released in the hot side of the TEMs to the ambient air.

To help this dissipation, there are 48 fins placed along the heat sink. The heat transference between the heat sink and the ambient is due to convective heat transfer, which follows the following equation [5]:

$$\Phi_{conv} = h \cdot A \cdot (T_{surf} - T_{\infty})$$

Where  $\Phi_{conv}$  is the dissipated heat flow (W),  $h$  is the convection coefficient ( $\text{W/m}^2 \cdot \text{K}$ ),  $A$  is the contact area between the object and the ambient ( $\text{m}^2$ ),  $T_{surf}$  is the temperature of the surface of the object (K) and  $T_{\infty}$  is the temperature of the ambient air (K).

To increase the dissipation, one has two options: increase the contact area or increase the convection coefficient. By using the fins, one increases the contact surface with the ambient, and with the action of the fan, one increases the convective coefficient, since the convective coefficient increases with the Reynolds number, which is proportional to the velocity of the air.

-TEC PID SuperCool controller:

The TEC of the STIC was originally regulated by a PID controller (Laird Technologies PR-59, [11]) and software (Laird Technologies SC Interface) from the TEC manufacturer. The goal of the controller was to achieve and maintain a desired temperature at the cold side of the TEM (when the TEC is used as a cooler as it is in the present application). The reference temperature is specified by the user in the software, and is here called  $T_d(t)$ . The controller has an input signal, which comes from a thermistor placed close to the cold side of the TEM, in the STIC it is placed in the aluminum plate Al2. This signal gives the actual value of the cold side temperature  $T_s(t)$ , and is used as a feedback signal.

Once the reference is fixed, the controller compares the reference with the temperature of the sensor obtaining a new signal called the signal error  $e(t)$ .

$$e(t) = T_d(t) - T_s(t)$$

This error signal is then sent to the PID controller, in order to calculate an output that will bring the error signal towards zero ( $e(t) \rightarrow 0$ ). The PID controller has a proportional part P, an integral part I and a derivative part D. The proportional term makes a change to the signal that is proportional to the current error value using a proportionality constant  $K_p$ :

$$P = K_p \cdot e(t)$$

With only the proportional part one can often achieve a steady value (temperature), but one cannot reach the target value, as the output signal retains a steady-state error. In terms of time, the P depends on the present error.

The integral term is the sum of the instantaneous error over the time multiplied by a constant  $K_i$ :

$$I = K_i \cdot \int_0^t e(\tau) \cdot d\tau$$

This part of the controller accelerates the movement of the process towards the set point and eliminates the residual steady-state error given by the proportional part. In terms of time, I depend on the accumulation of past errors.

The derivative term is calculated by determining the slope of the error over time and multiplying this rate of change by a constant  $K_d$  :

$$D = K_d \cdot \frac{d}{dt} e(t)$$

This part slows the rate of change of the controller output and reduces the magnitude of the overshoot produced by the integral term. However, it may amplify the signal noise, so it is common to use just a *PI* controller instead of the complete *PID*.

As a result of the three parts one will get the output of the PID controller  $p(t)$  as:

$$p(t) = P + I + D = K_p \cdot e(t) + K_i \cdot \int_0^t e(\tau) \cdot d\tau + K_d \cdot \frac{d}{dt} e(t)$$

The output  $p(t)$  of the PID is the suitable cooling power to move towards the desired temperature. This signal is divided by the maximum power that can be given  $P_{max}$  in order to have a function  $f(t)$  that expresses the fraction of the maximum power that is needed.

$$P_{max} = \frac{U^2}{R_e}$$

$$f(t) = \frac{p(t)}{P_{max}}; |f(t)| \leq 1 \forall t > 0$$

Multiplying the signal  $f(t)$  with the maximum current that can be given  $I_{max}$ , one gets the signal  $i(t)$ , the current necessary in the TEM to get the desired temperature  $T_d(t)$  (actually, with this current one regulates the heat absorbed  $\Phi_C(t)$ , which is related with the temperature  $T_d(t)$ ):

$$i(t) = f(t) \cdot I_{max}$$

The signal  $i(t)$  is created by the PWM (Pulse Width Modulation) technique: the output has only three values, 0 and  $\pm U$ . In order to change the effective value of the output, the output only gives  $\pm U$  during a part of its period. The amount of time the signal is giving  $\pm U$  is defined by the function  $f(t)$ , and so is the sign of the voltage. Note that when a TEC is only used for cooling (or only used for heating),  $U$  does not need to change sign.

For example, if  $f(t_i) = 0.5$ , for each second, one will have half a second of  $U$  and half a second without voltage. As the voltage and the current are proportional (Ohm's law), when one has  $U$  one also has  $I_{max}$ , so the output  $i(t)$  will be  $I_{max}$  during half second and 0 A during the other half. Mathematically:

$$\text{If } T \text{ is the period of } i(t) \text{ and } f(t) = x \text{ then } i(t) = \begin{cases} I_{max}, & 0 \leq t \leq x \\ 0, & x < t < T \end{cases}$$

Once the signal  $i(t)$  is calculated, it is sent to the TEMs, where it creates a heat flow  $\Phi_C(t)$ , and then the sensor signal  $T_s(t)$  is measured to start the process again. Figure 2.1-9 shows the scheme of the PID regulator control.

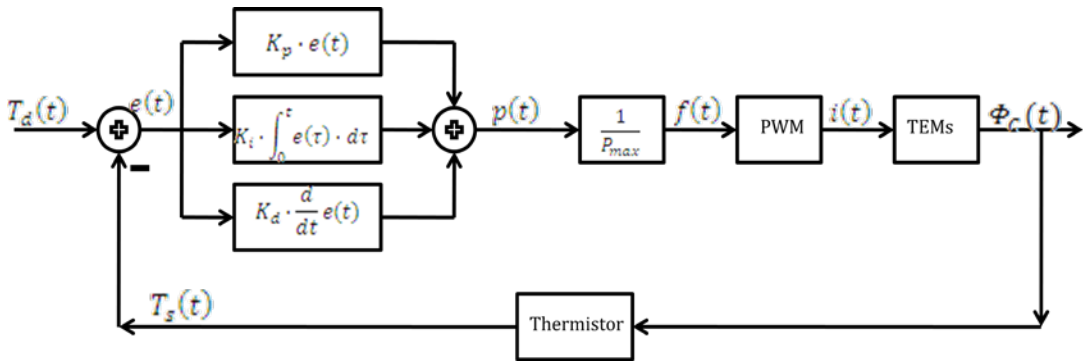


Figure 2.1-9 Scheme of the PID regulator control system of the TEC.

**Heater**

The heater used in the STIC is an electrical film heater (resistance) with a rubber protection (Figure 2.1-10) based on the Joule effect. The rate of heat dissipation ( $\Phi_J$ ) in a resistive conductor is proportional to the square of the current ( $I$ ) through it and to its resistance ( $R$ ).

$$\Phi_J = RI^2$$

The heater is located in one of the ends of the STIC and its function is to produce heat on the warm side of the instrument to create the temperature gradient. In order to keep the temperature stable, the heater is controlled by a PID regulator.

The PID has a maximum voltage value of  $V = 48$  V, and the resistance of the heater is  $R = 57.0 \Omega$ . The dissipated heat is  $P = RI^2$ . Applying the Ohm's law  $I=V/R$ , the maximum heat that the heater can dissipate is

$$\Phi = \frac{V^2}{R} = \frac{48^2}{57} = 40.4 \text{ W}$$

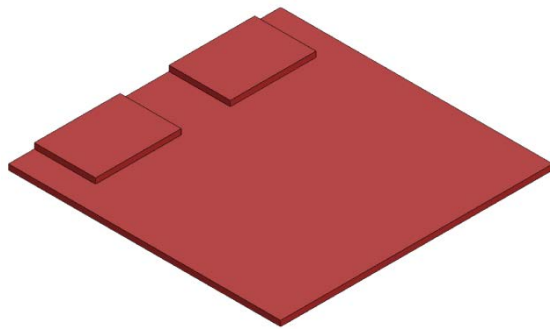


Figure 2.1-10 Heater.

**-PID Regulator**

The heater was originally controlled by a PID regulator with has four resistance decades (10x10 k $\Omega$ ; 10x1 k $\Omega$ ; 10x100  $\Omega$ ; 10x10  $\Omega$ ) so the user could choose any resistance between 11110 and 99990  $\Omega$ . This resistance is part of a Wheatstone bridge in which a thermistor close to the heater is one of the other resistances, and it is the balance between these two resistances that determines the output of the bridge. The resistance of the used type of thermistor is shown in the Table 2.1-3 as a function of temperature. So the desired temperature is set by setting the decade resistances equal to the thermistor resistance at that temperature. If one wants a temperature of 30  $^{\circ}\text{C}$  in the heater, one should select 39710  $\Omega$  in the regulator.

Desired temperature in heater ( $^{\circ}\text{C}$ )	Resistance in the regulator ( $\Omega$ )
25	50000
30	39711
40	25524

50	16795
60	11295
70	7750,9

**Table 2.1-3** Relationship desired temperature-resistance in the Heater PID regulator [12].

Once the desired temperature is chosen, the *PID* regulates the temperature of the heater. The input of the regulator is the signal of a thermistor placed in the Al 4 plate, which measures the temperature in the heater. This signal is the feedback of the controller. The heater PID controller works in the same way as the TEC PID controller.

The signal  $u(t)$  is used to regulate the duty cycle in order to get the appropriate output  $i(t)$  to control the power on the heater. In this case,  $V_{max} = 48$  V. If the sensor temperature  $T_s(t)$  is one degree or more above the desired temperature  $T_d(t)$  ( $e(t) \leq -1$ ), one needs to cool down the heater so the duty cycle would be 0% (no power given). On the other hand, if the sensor temperature  $T_s(t)$  is one degree or more below the desired temperature  $T_d(t)$  ( $e(t) \geq 1$ ), one needs to keep heating to get to the desired temperature, so the duty cycle would be 100% (all the time giving the maximum power). Finally, if the sensor temperature  $T_s(t)$  is within  $\pm 1$  K of the desired temperature  $T_d(t)$  ( $|e(t)| < 1$ ), the controller regulates the power by adapting the duty cycle to the needs.

The signal  $i(t)$  is sent to the heater where it creates a heat flow  $\Phi_J(t)$  due to the Joule effect, which is related with the desired temperature  $T_d(t)$ . In Figure 2.1-11 the scheme of the heater PID regulator control is shown.

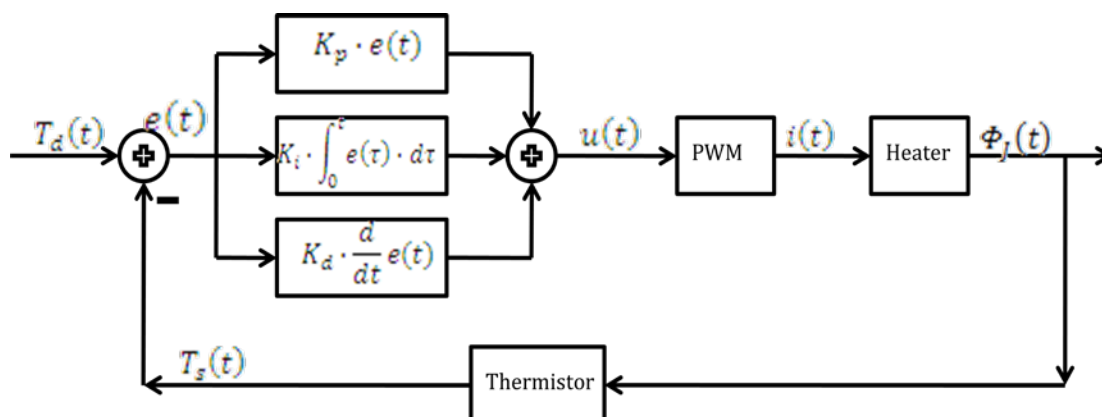


**Figure 2.1-11** Scheme of the PID regulator control system of the heater.

## Heat Transfer Compound

A heat transfer compound is a kind of grease fluid made by a blend of synthetic fluids as a base and powdered metal oxides as thermo-conductive component. Such a product (Electrolube non-silicone Heat Transfer Compound) was applied on all contact surfaces within STIC, such as the connection between of the vertical sides and the horizontal covers of the tube and between the temperature sensors and the surfaces whose temperature one want to measure. Because of its high thermal conductivity, it reduces the thermal contact resistance between the surfaces. It has a wide operational temperature range and has a high conductivity at high temperature, and it is not toxic [13].

## 2.2 Insulation

The STIC device is filled by thermal insulation on the inside and surrounded by thermal insulation on the outside. The insulation used is XPS (Extruded Polystyrene Foam) with a low thermal conductivity (lower than  $0.04 \text{ Wm}^{-1}\text{K}^{-1}$ ). The XPS has a relatively high stiffness, and can be used up to  $70 \text{ }^\circ\text{C}$  (continuously).

On the inside of the temperature gradient tube, the insulation fills all the space left between the tube and the calorimeters, with the exception of the eight holes above the sample holders, in order to enable the charging and removal of the ampoules. The goal of insulation inside of the tube is to remove convection so that each calorimeter is maintained at different temperature determined by the temperature gradient of the tube.

As it is shown in Figure 2.2-1, the insulation is divided in prismatic shaped parts so that it is possible to fill all the space, but also to allow the sensor wires to leave the instrument.

On the outside of the instrument, the insulation covers all the surfaces that are in contact with the air, except the external part of the TEC and the fan (Figure 2.2-2). The aim of the outside isolation is to reduce (almost avoid) the heat losses from the STIC to the ambient, and to decrease the effect of external (room temperature) perturbations on the measurements. Such

perturbations can be caused by a door being opened or a large increase or decrease of the outdoor temperature. The external finned surface of the TEC cannot be insulated since it has to get rid of heat from its inside to the ambient air.

Just as for the inside insulation, the outside insulation is also made from prismatic shaped parts which cover all the surfaces. The dimensions of each part are given in an annex.

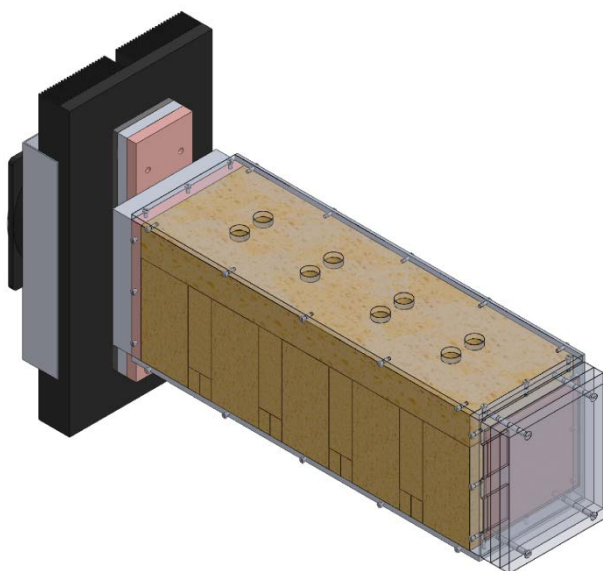


Figure 2.2-1 STIC internal insulation.

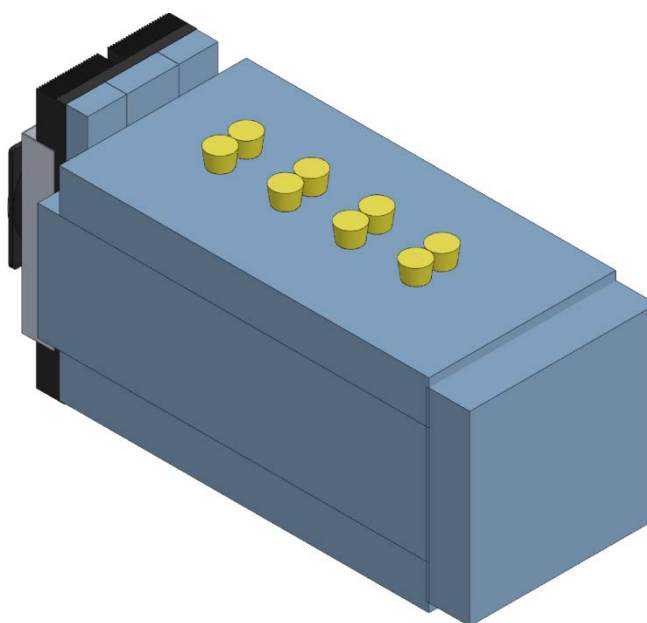


Figure 2.2-2 STIC external insulation.

## 2.3 Sensors

### Heat flow sensor

The heat flow sensors are thermocouple plates consisting of many thermocouples.. The thermocouples are based in the Seebeck effect: a temperature difference between two junctions of two different electrical conductors or semiconductors produces a voltage difference between the two junctions [14]. These sensors are essentially the same type of devices as used in the TEC, but used in the opposite way.

The voltages created by the Seebeck effect in the calorimeter are small, in the order of microvolt ( $\mu\text{V}$ ), and depends on the temperature, as the following expression shows:

$$V(T) = \int_{T_1}^{T_2} (S_B(T) - S_A(T))dT$$

where  $S_A(T)$  and  $S_B(T)$  are the Seebeck coefficients (V/K) of the two different materials as a function of temperature and  $T_1$  and  $T_2$  are the temperatures of the two junctions. Note that the Seebeck coefficients depend on the temperature and the materials.

As shown in Figure 2.3-1, the heat flow sensors are made as thermocouple plates containing many semiconductor thermocouples made of n- and p-doped bismuth-telluride ( $\text{Bi}_2\text{Te}_3$ ). The thermocouples are soldered to two covers made of aluminum oxide ( $\text{Al}_2\text{O}_3$ ), which is a very good thermo-conductor but also an electrical insulation.

Each sensor used in the STIC has 31 thermocouples. In the STIC there are in total 8 such heat flow sensors, two in each calorimeter, one between the sample holder and the heat sink and the other between the reference holder and the heat sink.

As was mentioned above, the output of the sensors is a voltage proportional to the temperature difference between the two junctions. The lower junction of each sensor is in contact with the heat sink, so they are at the same temperature. One way of measure the thermal power of the sample is to get the signal of the sample and the signal of the reference, and calculate the difference between the signals. However, there is a better way to get this measurement: if one connects the negative poles of both the sample sensor and the reference sensor, and measure the voltage between the positive pole of each sensor, one will directly get a voltage proportional to the temperature difference between the

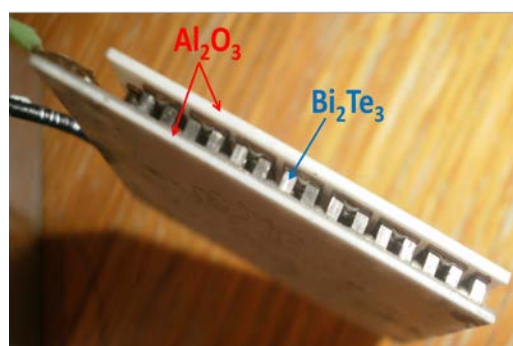


Figure 2.3-1 Heat flow sensor.

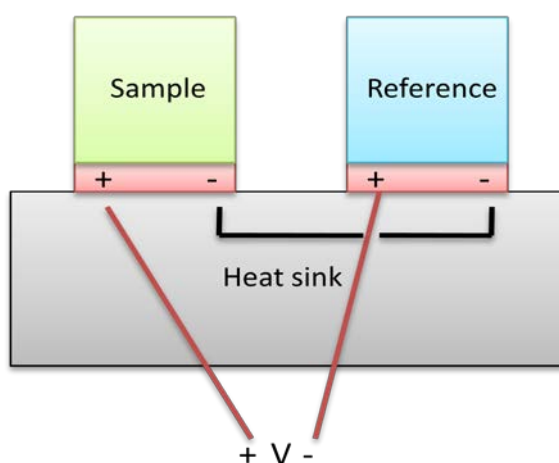


Figure 2.3-2 Heat flow sensor connection.

sample and the reference and, therefore, proportional to the thermal power of the sample (Figure 2.3-2). This configuration has two advantages: there are only two output wires, and the subtraction is done electrically and not by a software afterwards, reducing the error. The aim of this twin design is to make the response of the instrument faster, reduce the noise due to external perturbations, and to remove the influence of a non-constant temperature of the heat sink [3].

### Pt-100 Sensors

The Pt-100 sensors (Figure 2.3-3) are resistance temperature sensors (RTDs). The RTDs are made of pure metals whose resistance changes with the temperature. If one knows the value of the resistance as a function of temperature, one can calculate the temperature of a RTD by measuring its resistance [15].



Figure 2.3-2 Pt-100 sensor.

A Pt-100 is made of platinum, which is the best metal for RTDs because it has an almost linear resistance to temperature relationship over a wide temperature range. Its work-range is from -200 °C to +850 °C [16].

The principle of operation is to measure the resistance in the platinum element. The Pt-100 sensor has a resistance of 100.0 Ω at 0 °C and 138.4 Ω at 100 °C, and the relationship between temperature and resistance is approximately linear in a small temperature range. If one needs precision measurements, the non-linearity has to be taken into account.

As the sensors used in the STIC are connected to a Pico data logger, this linearization is done automatically in software. The equation of the linearization is [16]:

$$R_t = R_0(1 + At + Bt^2 + C(t - 100)t^3)$$

where:

- $R_t$  is the resistance at temperature  $t$
- $R_0$  is the resistance at 0 °C (100 Ω)
- $A = 3.9083 \text{ E-}3$
- $B = -5.775 \text{ E-}7$
- $C = -4.183 \text{ E-}12$  ( for  $t$  below 0 °C), or  $C = 0$  (for  $t$  above 0 °C)

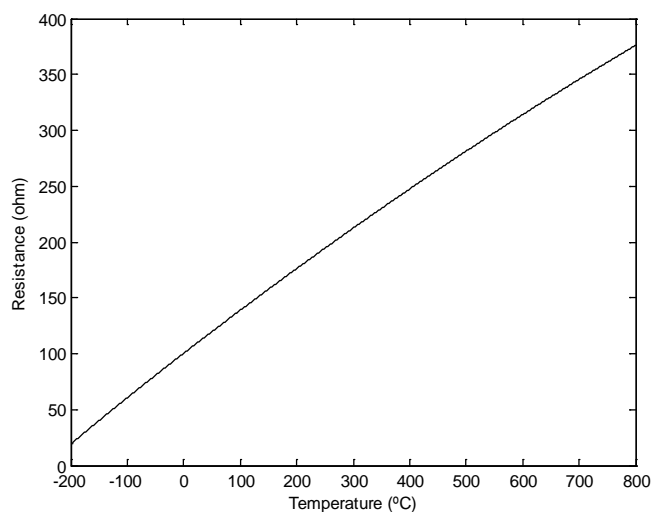


Figure 2.3-3 Linearization in the working range.

In Figure 2.3-4 one can see the result of the linearization in the working range.

In the STIC, there are eight Pt-100 sensors. Four of them are placed between the two square holders that form each twin calorimeter, and they give the temperature of each of the calorimeters. The other four are placed:

- Inside the aluminum plate next to the heater (Al4) which contains the heater control thermistor, giving the temperature of the heater.

- Inside the aluminum plate (Al2) next to the Super Cool, giving the temperature of that plate.
- Over the STIC, between the calorimeters 2 and 3, giving the air temperature.
- In front of the fan, giving the temperature of the air that goes into the fan.

All the sensors are connected in a four-wire configuration. Two of them conduct the current through the sensor that is used to measure the resistance, and the other two measure the voltage across the sensor. Using this configuration, the resistance error due to lead wire resistance is zero [16]. This is shown in Figure 2.3-5.

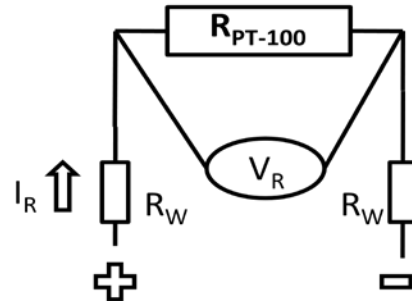


Figure 2.3-5 Four wire configuration.

One can calculate the true resistance of the Pt-100  $R_{Pt-100}$  by measuring the voltage on the sensor  $V_R$  (2 wires), and dividing by the intensity  $I_R$  (2 wires), avoiding the effect of the wire resistance  $R_W$ :

$$R_{Pt-100} = \frac{V_R}{I_R}$$

All the sensors are connected to PT-104 data loggers from Pico Technology (there are two loggers with four sensors measured in each), which measures the current and the voltage, calculates the resistance and finds the temperature.

### Thermistor TC-NTC-1

A thermistor is a type of resistor whose resistance varies significantly with temperature. Similarly to the RTDs, this variable resistance makes it possible to use them as temperature sensors [17].

The main difference between RTDs and thermistors is the material: while the RTDs are made of pure metal, the thermistors are generally made from a semiconductor. The temperature response is also different, thus thermistors achieve a higher precision within a limited temperature range, for example between  $-90\text{ }^{\circ}\text{C}$  to  $130\text{ }^{\circ}\text{C}$ , but their resistance-temperature characteristics are non-linear.

Several equations for fitting thermistor data have been proposed. Here the Steinhart-Hart equation is used. The Steinhart-Hart equation is a model of the resistance of a semiconductor at different temperatures published in 1968 by John S. Steinhart and Stanley R. Hart [18].

The equation is:

$$\frac{1}{T} = A + B \ln(R) + C (\ln(R))^3$$

where:

- $T$  is the temperature (in Kelvin)
- $R$  is the resistance at  $T$  (in ohms)
- $A$ ,  $B$ , and  $C$  are the Steinhart-Hart coefficients which vary depending on the type and model of thermistor and the temperature range of interest.

Depending on the sign of  $A$ , thermistors are classified in two types:

-PTC (positive temperature coefficient): the resistance increases with increasing temperature.

-NTC (negative temperature coefficient): the resistance decreases with increasing temperature.

The thermistors used in the STIC are NTC, and there are two of them: one used to control the heater, and the other to control the TEC (one more NTC as a feed forward control was implemented).

In Figure 2.3-6, one can see the relation between resistance and temperature of the thermistor TC-NTC-1 used in the STIC [19], and the representation of the Steinhart-Hart equation with the parameters that best fitted the data of the thermistor, which are:

$$A = 0.00137038$$

$$B = 0.000242169$$

$$C = 7.70625e-8$$

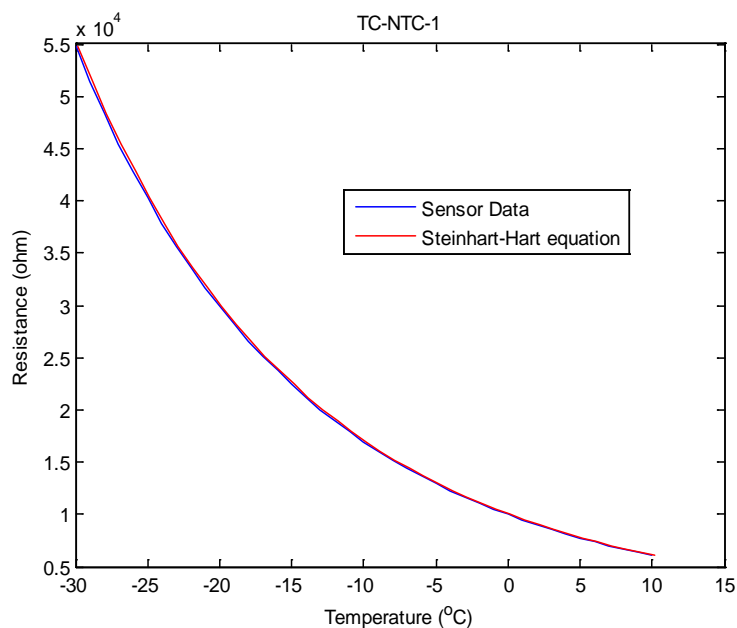


**Figure 2.3-6** Temperature-Resistance relationship of TC-NTC-1 thermistor.

## 2.4 Data loggers

### PT-104 data logger

All the Pt-100 sensors are connected to the PT-104 data logger (Figure 2.4-1). Each PT-104 unit has 4 temperature channels, so two units are used to register the eight signals. This device measures temperature from both Pt-100 and Pt-1000 sensors and it can also measure resistance and voltage. It offers both a high resolution (0.001 °C) and accuracy (0.01 °C), and support sensors in four-wire configuration [16].



**Figure 2.4-1** PT-104 data logger.

Both PT-104 units are connected to the computer through the serial port, and using the PicoLog data logging software one can record and display the measurements.

### ADC-24 Precision Data Logger

The four heat flow sensors are connected to an ADC-24 Precision Data Logger unit (Figure 2.4-2). This device supports true differential inputs as the heat flow sensors signals previously described. As it operates with 24-bit resolution, it is able to detect small signal changes, with an accuracy of 0.1%. It also offers a fast conversion time and galvanic insulation from the PC to eliminate noise. The ADC-24 is connected to the computer through an USB port, and the measurements can be displayed and recorded using the PicoLog data logging software [20].



**Figure 2.4-2** ADC-24 precision data logger.

## 2.5 Electric schema of the STIC

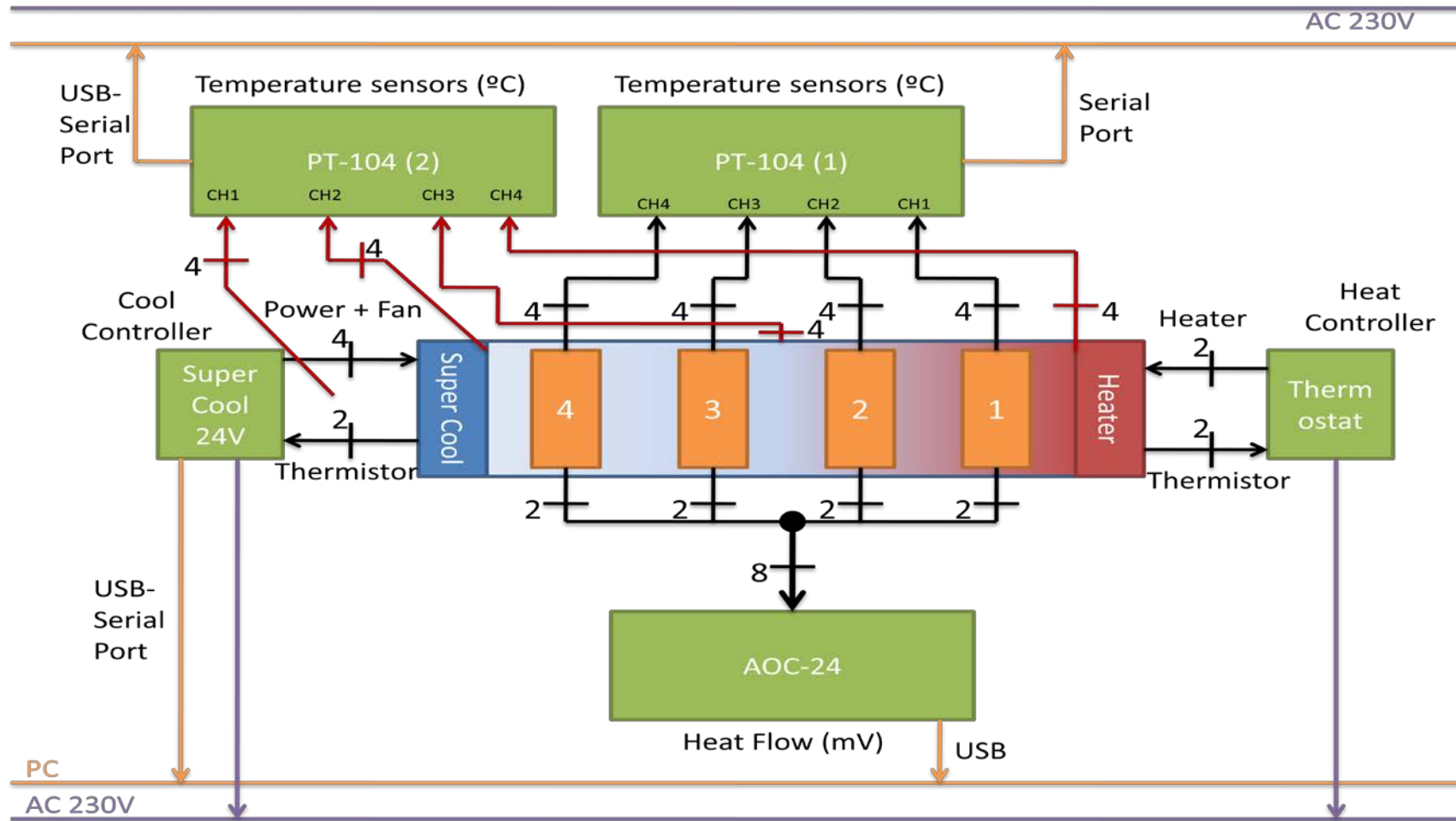


Figure 2.5-1 Electric schema of the STIC.



## 3. PID Controller in dSPACE Platform

In order to improve the control system of the STIC, a new control algorithm was developed using MATLAB Simulink and the control platform dSPACE. Before designing and implementing this new control system, the former PID control both in the heater and the TEC were implemented in dSPACE to have a reference to compare the dSPACE functionality versus the old PID control.

In this section, first the dSPACE platform and Simulink software are briefly described, and an explanation and description of all the electrical and electronic devices needed to implement the control is given. Finally, the control algorithm designed in Simulink is explained.

### 3.1 dSPACE and MATLAB Simulink

The dSPACE platform, developed by the company dSPACE, allows the user to run a control algorithm, designed either in MATLAB Simulink or in C-language, using a board installed on the PC and connected to an external connector panel.

In the current thesis, the board DS1104 is installed in a host PC, which is connected to an external connector panel through the board port. This panel has several inputs and outputs, such as digital-analog and analog-digital converters, digital inputs and outputs and a slave PWM generator.

The MATLAB Simulink software, developed by MathWorks, is a tool widely used in control theory and digital signal processing, as it is useful for modeling, simulating and analyzing multidomain dynamic systems. Its interface is a graphical block diagramming tool and it can interact with the rest of the MATLAB environment.

### 3.2 Electrical and electronic devices

The aim of this part of the thesis is to substitute both the old PID controllers in the heater and in the TEC, which were physically implemented in two external boxes, by new PID controllers designed in Simulink and executed by dSPACE. This change has two main advantages:

- The control algorithm would be transparent, so it would be possible to know exactly what is happening every moment. This was not the case with the previous controllers, as they were already programmed and implemented in closed boxes.

- It would be possible to apply and implement all the modifications needed to improve the control system, something that would have been impossible with the old controllers.

In order to achieve this, some electronic and electrical elements are needed to implement both the heater and the TEC controllers. The electric schema of the connections in the new controller system is given in Figure 3.2-1:

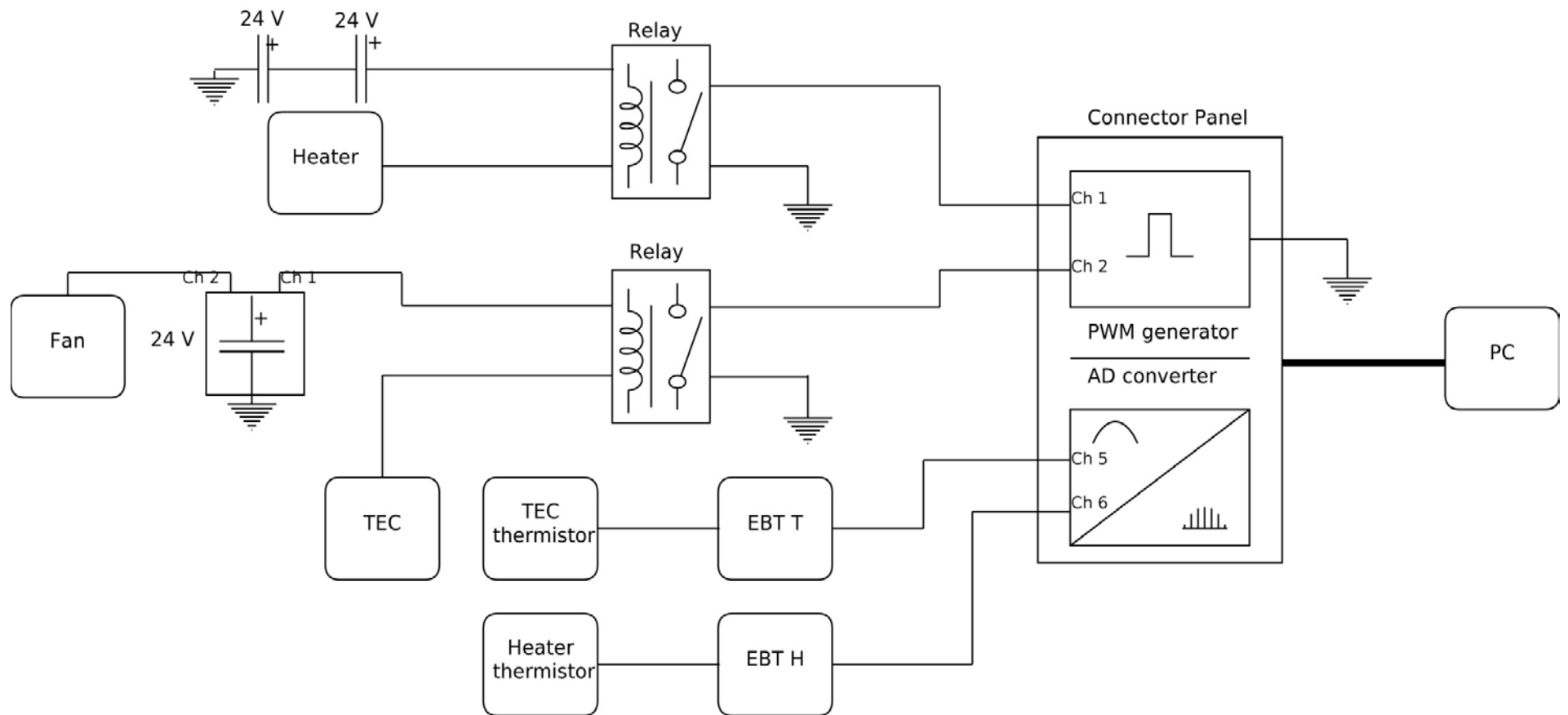


**Figure 3.2-1** Electric schema of the connections in the new controller system. Note: EBT X refers to the electronic board of the thermistor in the heater or TEC.

## Heater

In the former situation, the heater controller was made by regulating the duty cycle of a PWM generator, with a voltage of 48 V, and using a thermistor as a feedback signal. In the new scenario, the following procedure was used: through the algorithm control, the duty cycle is generated. This signal, as has been previously explained, will have a certain voltage value during a fraction of the period, and a null voltage during the rest of the period. This signal will come out of the dSPACE board on the computer by the connector panel (output channel 1 of the slave PWM generator).

This output has a certain voltage value when it is on (between 2.4 and 5 V), but it is smaller than the required 48 V. To solve that, the output PWM signal is connected to the input of a relay. A relay is an electrically controlled switch, in which a low electrical voltage can be used to turn on/off a current which is often – such as here – much higher than the control signal. When the input  $V_{in}$  is higher than a certain value  $V_{lim}$ , the output  $V_{out}$  has the value of the feed  $V_{feed}$ , and when the input is smaller, the output is null. The relays used are Crouzet solid state relays [21].

As the desired voltage in the heater is 48 V, the relay's feed input has to be also 48 V. It is achieved by connecting two power sources of 24 V in series with the relay.

As the input signal only has two values, when it is null the output will be null, and when it is the upper voltage the output will be 48 V. So, by using the relay, the heater will get a signal with the same duty cycle as the output of the controller, but with a voltage varying between both 0 and 48 V (Figure 3.2-2).

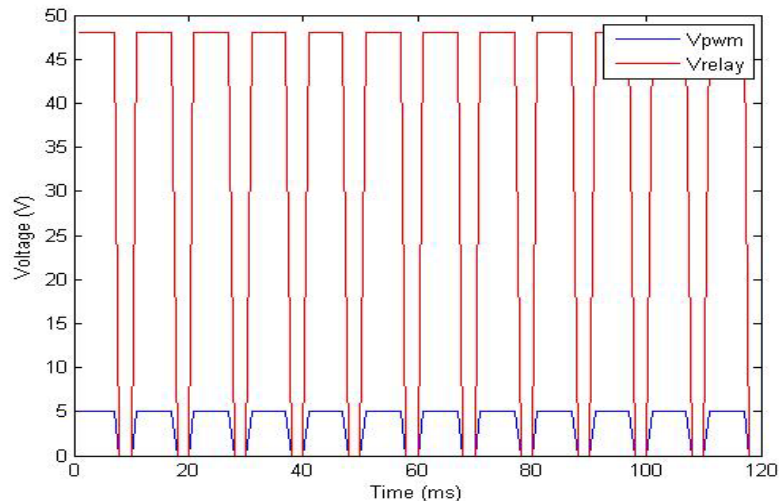


**Figure 3.2-2** Representation of  $V_{pwm}$  and  $V_{relay}$  for a duty cycle = 70%, and a frequency of 100 Hz.

Finally, a new temperature sensor was needed, as the characteristics of the former thermistor of the heater were unknown. The new thermistor was placed in the same position as the former thermistor, and was connected to an electronic board. This electronic board contains a circuit whose most important components are a Wheatstone bridge and a low power amplifier.

A Wheatstone bridge is an electrical circuit used to measure an unknown resistance value. The bridge is composed by four resistances, three that have identical known resistance values  $R$  and one that is the resistance to be measured  $R_x$ . It is connected as shown in Figure 3.2-3. The circuit is fed by a constant direct

voltage  $V_{in}$ , and by measuring the output voltage  $V_{out}$ , it is possible to know the value of the unknown resistance  $R_t$ .

In the current situation, the thermistor, which is a temperature varying resistor, is connected to the electronic board as one of the resistances of the bridge, whilst the other resistances are fixed and known. It is important to choose a thermistor whose resistance around the normal working temperature is close to the other three resistances, to get an accurate measurement of the temperature.

There were two different Wheatstone bridges available, one with fixed resistances of 5 kΩ and another with 10 kΩ resistances. The normal working temperature of the heater is in the range 35-60 °C. The temperature-resistance relationship of the two types of available thermistors is shown in the Table 3.2-1:

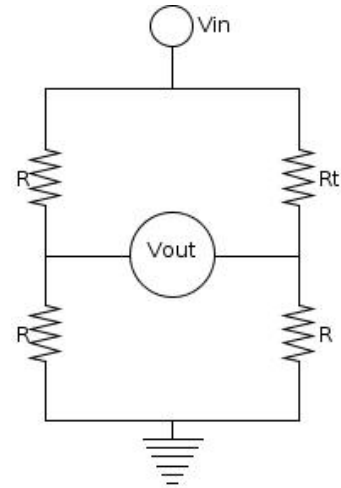


Figure 3.2-3 Wheatstone bridge configuration.

Temperature (°C)	ACC-003 (Ω)	ACC-004 (Ω)
-20	48 535	97 070
-10	27 665	55 330
0	16 325	32 650
10	9 950.0	19 900
20	6 245.0	12 490
25	5 000.0	10 000
30	4 028.5	8 057.0
40	2 666.3	5 327.0
50	1 801.5	3 603.0
60	1 244.0	2 488.0
70	876.0	1 752.0
80	627.5	1 255.0

Table 3.2-1 Relationship temperature-resistance for the thermistors ACC-003 and ACC-004 [12].

Around the working temperatures, the thermistor ACC-004 is close to 5 kΩ, so the final disposition of the Wheatstone bridge is: one thermistor ACC-004 ( $R_t$ ) connected with 3 resistances  $R$  of 5 kΩ and a feed voltage  $V_{in}$  of 2 V, whose output voltage  $V_{out}$  is sent to a low power amplifier.

The output of the amplifier is between ±10 V. The amplifier used, called INA 128, has a gain  $G$  defined as [22]:

$$G = 1 + \frac{50 \text{ k}\Omega}{R_a}$$

Where  $R_a$  (kΩ) is a resistance that has to be determined. It is known that the output of the Wheatstone bridge is:

$$V_{out} = V_{in} \left( \frac{1}{2} - \frac{R}{R + R_T} \right)$$

As the values of  $V_{in}$  and  $R$  are known:

$$V_{out} = 2 \left( \frac{1}{2} - \frac{5}{5 + R_T} \right)$$

With a resistance in the amplifier  $R_a = 1 \text{ k}\Omega$ , the gain is

$$G = 1 + \frac{50 \text{ k}\Omega}{1 \text{ k}\Omega} = 51$$

Dividing the output range of the amplifier by the gain, the range of the output voltage of the Wheatstone bridge that can be measured is obtained:

$$V_{out} = \frac{\pm 10}{51} = \pm 0.1961 \text{ V}$$

Solving the equation of the  $V_{out}$  for  $R_t$ , for those two values of  $V_{out}$ :

$$\pm 0.1961 = 2 \left( \frac{1}{2} - \frac{5}{5 + R_T} \right); \begin{cases} R_t = 3.36 \text{ k}\Omega \\ R_t = 7.44 \text{ k}\Omega \end{cases}$$

That means that the thermistor resistance  $R_t$  can be measured as long as its value belong to the interval [3.36 k $\Omega$ , 7.44 k $\Omega$ ], and thus, the range of measurable temperatures is 32.3-52.2  $^{\circ}\text{C}$  (values calculated applying linear interpolation to the relation temperature-resistance of the thermistors). The values of the thermistor and the different resistances are shown in the Table 3.2-2.

Element	Value
Thermistor $R_t$	ACC-004 (10 k $\Omega$ at 25 $^{\circ}\text{C}$ )
Wheatstone bridge fix resistances $R$	5 k $\Omega$
Amplifier resistance $R_a$	1 k $\Omega$

**Table 3.2-2** Resume of the elements used in the Heater side.

The Figure 3.2-4 shows the schematic electronic disposition of the Wheatstone bridge and the amplifier on the electronic board.

Finally, the output voltage of the amplifier  $V_t$  is connected to an analog-digital converter (the ADCch5) in the connection board.

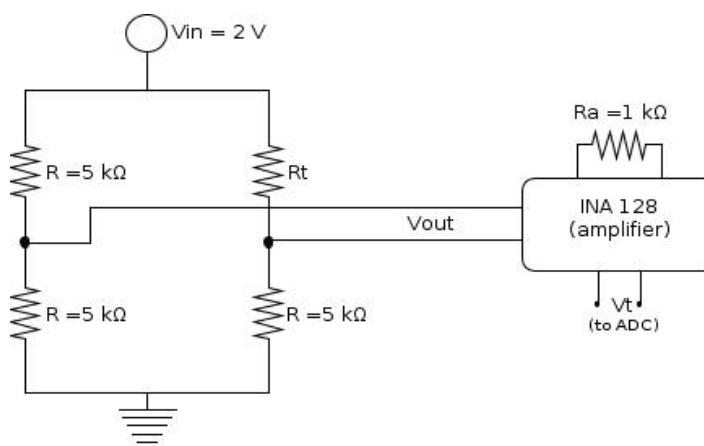


**Figure 3.2-4** Schema of the electronics on the electronic board of the Heater.

## TEC

The methodology followed to design the electronic and electrical control system for the TEC is the same as for the heater, so only the differences will be explained.

In the TEC, the output of the controller is also a duty cycle of a PWM signal which is sent to the PMW generator in the dSPACE board, which is the input of a second relay.

As the TEC works at 24 V, here a power source of this voltage is needed. Again, this power source feeds the relay, so the TEMs will see either 0 or 24 V during a fraction of the period of the PWM signal determined by the duty cycle. The fan of the TEC, necessary to avoid the overheating of the finned surface, also works at 24 V, so it is connected directly to a second output channel of the power source.

To select the thermistor and the resistance values, the same procedure as before was followed. As the normal working temperature of the TEC is supposed to be between 5-15 °C, the thermistor chosen is the ACC-003, which has a resistance close to 10 kΩ. And so, the fixed resistances in the Wheatstone bridge will be  $R = 10 \text{ k}\Omega$ .

With an amplifier resistance  $R_a$  of 500 Ω, the gain is:

$$G = 1 + \frac{50 \text{ k}\Omega}{0.5 \text{ k}\Omega} = 101$$

And the values of  $V_{out}$ :

$$V_{out} = \frac{\pm 10}{101} = \pm 0.099 \text{ V}$$

Therefore, the extreme values of  $R_t$  measurable are:

$$\pm 0.099 = 2 \left( \frac{1}{2} - \frac{10}{10 + R_T} \right); \begin{cases} R_t = 8.20 \text{ k}\Omega \\ R_t = 12.20 \text{ k}\Omega \end{cases}$$

And so, the range of measurable temperatures is between 6.5-14.7 °C.

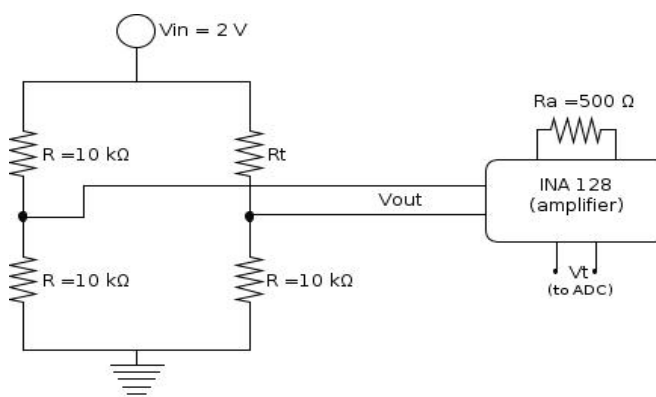
Table 3.2-3 gives the elements used:

Element	Value
Thermistor $R_t$	ACC-003 (5 kΩ at 25 °C)
Wheatstone bridge fix resistances $R$	10 kΩ
Amplifier resistance	500 Ω

Table 3.2-3 Resume of the elements used in the TEC side.

The output voltage of the amplifier is connected to an analog-digital converter (the ADCch6) in the connection board.

The Figure 3.2-5 shows the schematic electronic layout of the Wheatstone bridge and



the amplifier on the electronic board of the TEC thermistor.

Figure 3.2-5 Schema of the electronics on the electronic board of the TEC.

### 3.3 Control algorithm

The control algorithm has been implemented in Simulink, using both the standard control libraries of Simulink and the library *rtlib1104*, which provides a real-time interface for the DS1104 controller board.

The idea of the new controller is the same as for the former one: the error signal, calculated as the difference between the reference value and the sensor signal, is sent to a PID, whose output is the duty cycle of the PWM signal which is sent to the heater or to the TEC.

The whole Simulink algorithm is shown in the Figure 3.3-1.

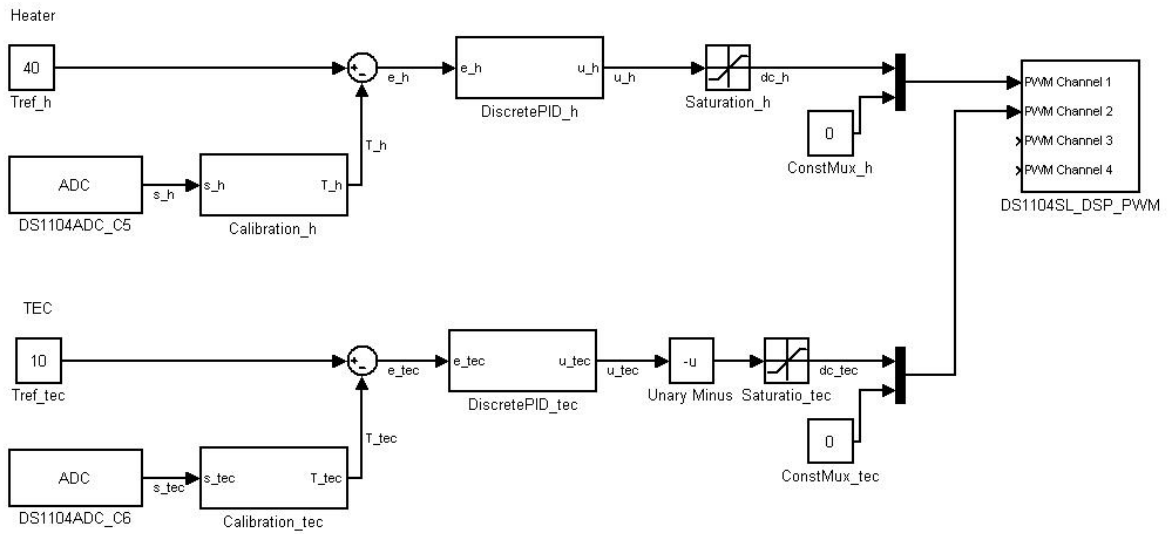


Figure 3.3-1 Control algorithm.

As can be seen, the algorithms for the heater and for the TEC are almost the same, as only one block is different. The algorithm works as follows. The blocks  $Tref_h$  and  $Tref_tec$  are the reference values of the heater and the TEC, respectively, i.e. the value that the system has to achieve. These values are the desired temperatures in the heater and in the TEC respectively. The blocs  $DS1104ADC_C5$  and  $DS1104ADC_C6$  are the signals from the thermistors, the first bloc from the heater sensor, and the second one from the TEC. Under each of these blocs, there is an analog-digital converter which transforms the continuous input signal, with a value between  $\pm 10$  V, into a discrete signal with a value between  $\pm 1$  V.

The voltage of the sensors is sent to a  $Calibration_x$  block, which transforms that voltage into its correspondent temperature. These blocks contain a mathematical expression which relates the voltage given by the sensor to the actual temperature. To find these expressions, the sensors have been calibrated. The calibration process is explained below.

At this point, the error signal is calculated as the reference temperature minus the temperature from the sensor, and sent to the  $DiscretePID_h$  bloc in the heater, and to the  $DiscretePID_tec$  in the TEC. The inside of these blocs is shown in Figure 3.3-2 and Figure 3.3-3:

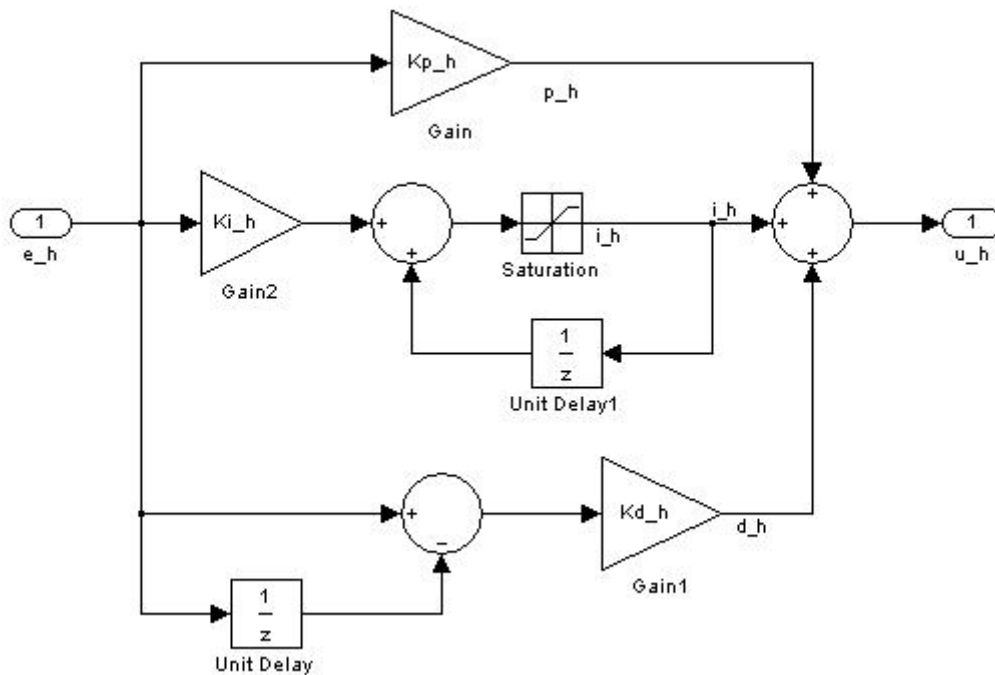


Figure 3.3-2 Heater PID controller.

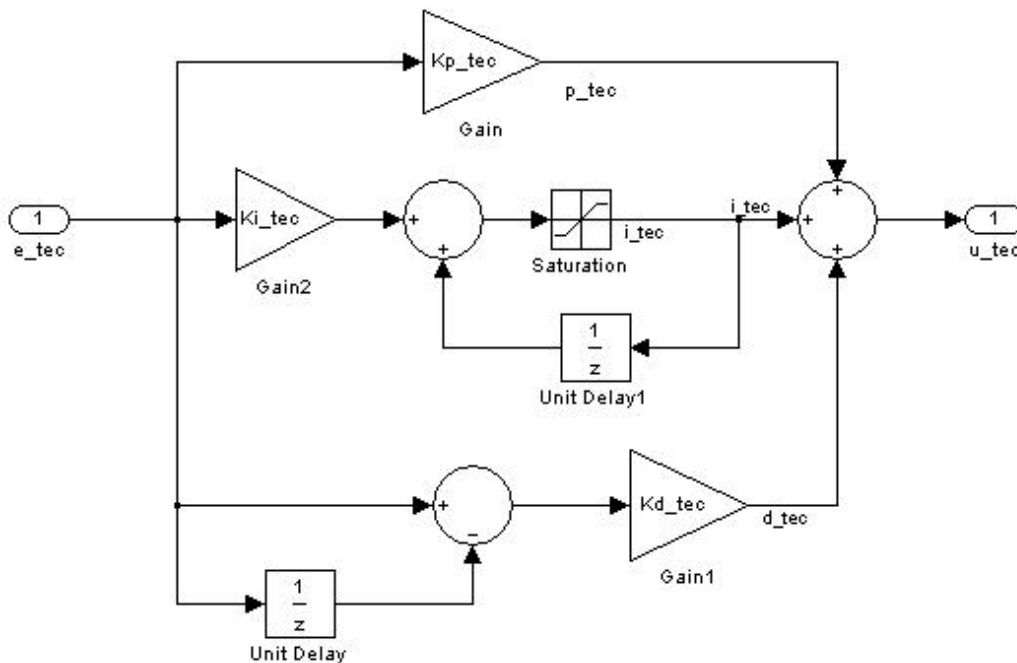


Figure 3.3-3 TEC PID controller.

The two blocks are identical, and they represent a typical discrete PID controller with integrator anti-windup. The general principle of the PID controller has been explained in section 1.1 TEC controller. To understand how the controller works, is important to keep in mind that the error is a signal at discrete times, which means that there is a succession of values corresponding to each sample time.

The current error is multiplied by  $K_p$  to get the proportional term. To generate the integral term, the current error is first multiplied by  $K_i$  and then

added to the sum of the error in the previous time step. That signal goes through a saturation block (Figure 3.3-4), which limits the integral term value between  $\pm 1$  (anti-windup). If there were no saturation block, the integral term could become so high that the controller would take extremely long time to react.

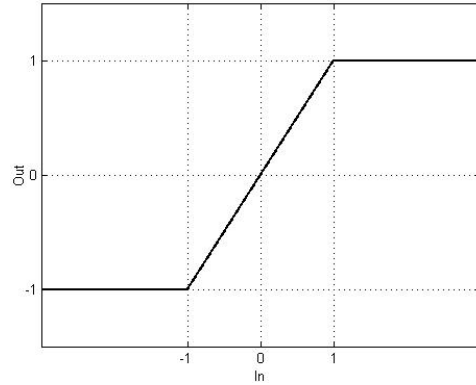


Figure 3.3-4 Anti-windup saturation.

Finally, to calculate the derivative term, the difference between the current error and the error in the previous step is multiplied by  $Kd$ . The addition of these three terms is the output of the PID controller, i.e. a duty cycle with a value between 0 and 1. The constants of the PIDs are introduced in dialog boxes, which appear when the *DiscretePID\_x* bloc is double-clicked, as shown in Figure 3.3-5 and Figure 3.3-6.

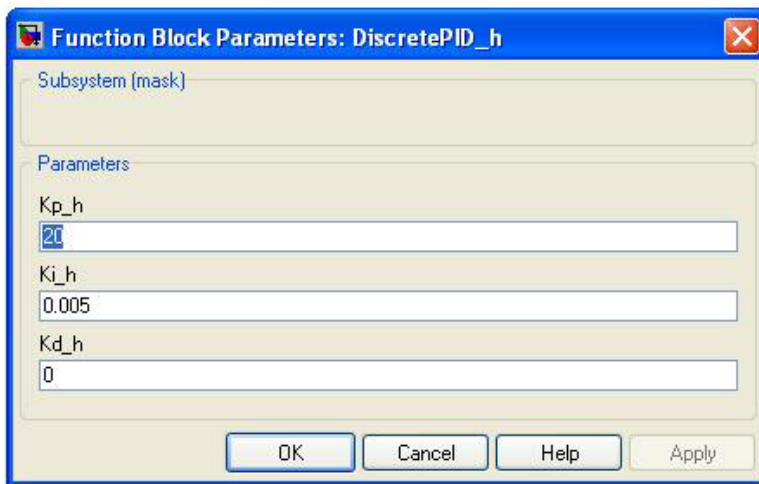


Figure 3.3-5 Heater PID parameters.

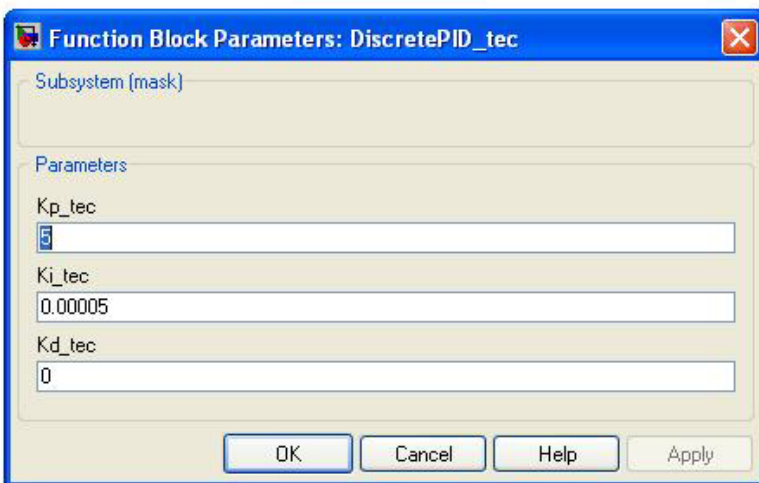


Figure 3.3-6 TEC PID parameters.

At this point, it is convenient to separate the heater controller and the TEC controller. The error has been defined as the reference minus the sensor signal, so if the sensor temperature is lower than the reference temperature, the error is positive. In the heater, it means that more heating power is needed. But as said before, the duty cycle has to be between 0 and 1 (0-100%). So the output of the *DiscretePID\_h* goes through the *Saturation\_h* bloc, which limits the output between 0 and 1. For example, as shown in Figure 3.3-7, if the input of the saturation is negative, the output is zero (the heater cannot cool); if the input is between 0 and 1, the output equals the input; and finally, if the input is higher than 1, the output is 1, as the duty cycle cannot be higher than 1 (100%).

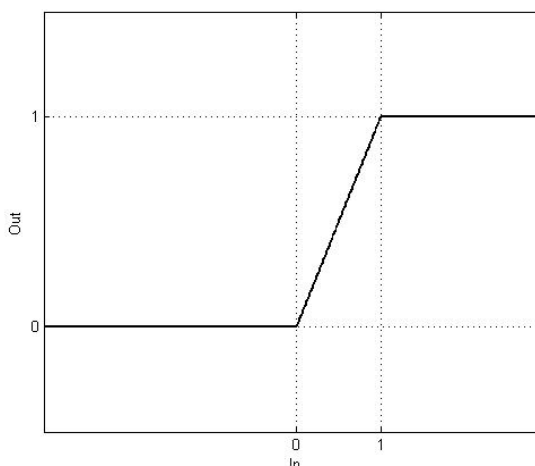


Figure 3.3-7 Duty cycle saturation.

On the other hand, the TEC in the STIC instrument is cooling (a TEC can also heat, but this is not used here). According to the definition of the error and the PID structure, the *DiscretePID\_tec* output is positive when heating is needed and negative when cooling is needed. But the duty cycle cannot be negative, so the bloc *Unary Minus* is used. This bloc multiplies the input by -1, so its output is positive when the TEC has to cool down. As was the case with the heater, the duty cycle has to be between 0 and 1, and the TEC in the STIC heats, so the block *Saturation\_tec*, which is identical to *Saturation\_h*, is used.

Each output signal of the saturations is sent to a multiplexer which is connected to a block constant (*ConstMux\_h* and *ConstMux\_tec*) whose value equals zero, and whose function is to activate the respective channel of the PWM block. The outputs of both multiplexers are connected to the block *DS1104SL\_DSP\_PWM*, the PWM generator. The heater is connected to the channel 1 of the block, and the TEC to channel 2. This block is connected by hardware to the PWM pins in the connector panel.

Both the heater PID and the TEC PID were tuned as a PI with the values shown in Figure 3.3-5 and 3.3-6, respectively.

### 3.4 Temperature sensor calibration

To calibrate a resistive temperature sensor means to find the relationship between the actual temperature that the sensor is measuring, and its resistance. In the present scenario, as the sensors are connected to the electronic boards which transform the resistance value into a voltage value, and are then connected to the ADC in the dSPACE board, the calibration will consist in find the relationship between the actual temperature the sensor has to measure and the output voltage of each ADC.

The process to find this relationship is simple. The idea is to place the sensors to calibrate together with an already calibrated sensor close together a constant temperature environment. In the present case a vacuum (Dewar) flask

together with warm or cold objects with high heat capacity. As the vacuum flask is highly insulated the temperature will change only slowly (be essentially constant) within the flask. The sensors that are to be calibrated are then connected to the dSPACE board through the electronic board, and a Simulink program is made to show the outputs of the ADCs as the same time as the precision thermometer gives the real temperature. Now, the vacuum flask will either slowly warm up or cool down towards the ambient temperature, so different temperature-voltage measurements can be made over, e.g., a day.

In the present calibration, the body used was water (in plastic bags), which was hot to calibrate the heater sensor and cold to calibrate the TEC sensor.

The results are shown in the Table 3.4-1:

Temperature (°C)	Hot sen (V)	Outside sen (V)	TEC sen(V)
49,23	0,64	1	1
48,32	0,56	1	1
47,14	0,47	1	1
46,21	0,38	1	1
45,21	0,28	1	1
44,31	0,2	1	1
35,87	-0,62	1	1
35,39	-0,67	1	1
34,84	-0,71	1	1
32,86	-1	0,955	1
23,26	-1	-0,15	1
11,83	-1	-1	0,82
11,29	-1	-1	0,66
10,26	-1	-1	0,09
9,52	-1	-1	-0,16
9,11	-1	-1	-0,36
8,55	-1	-1	-0,62
7,97	-1	-1	-0,82

**Table 3.4-1** Sensor calibration results.

Note that a value of 1 means that the temperature is higher than the highest value of the sensor working range, and a value of -1 means that the temperature is lower than the lowest value of the working range.

### Heater sensor

Plotting the values shown in the previous table where the heater sensor is active, the results in Figure 3.4-1 were obtained:

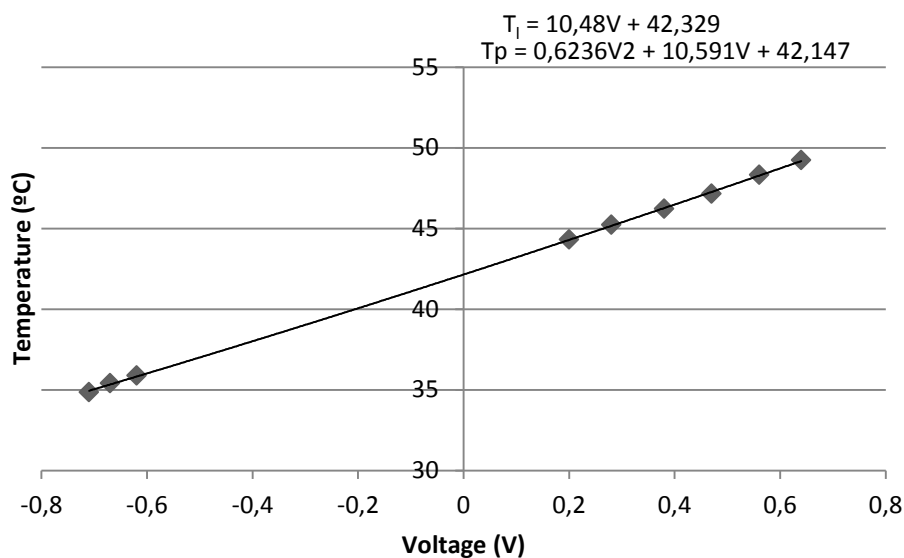


Figure 3.4-1 Heater sensor data.

The data was fitted using both a linear function and a second order polynomial function, whose expressions are given in Figure 5.4-1. In order to decide which one to use, the relative error between the two was calculated, as:

$$Error_i = \frac{T_{l,i} - T_{p,i}}{T_{p,i}}$$

Where  $i$  is each value of the voltage  $V$  used to calculate  $T_l$  and  $T_p$ . The results are shown in Figure 3.4-2:

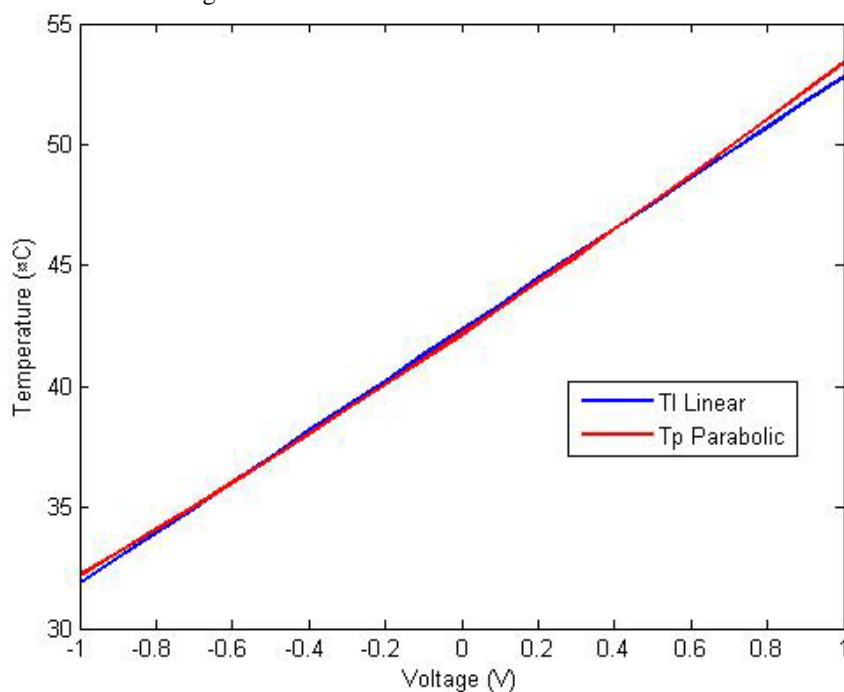


Figure 3.4-2 Linear fitted data vs Parabolic fitted data.

The results obtained with both equations are similar and quite small. The maximum relative error determined by using the linear is about 1% which is an acceptable error. Thus, the linear expression was used in the control algorithm.

Furthermore, as it is more important to keep a constant temperature than its exact value, it is enough with the linear approximation.

### TEC sensor

The fitted expression for the data obtained in the TEC sensor is shown in Figure 3.4-3:

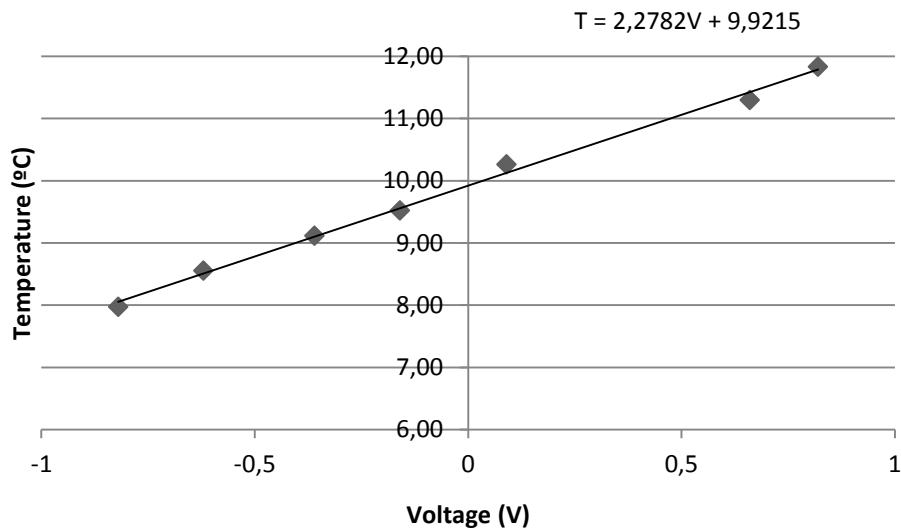


Figure 3.4-3 TEC sensor data.

As the linear equation fits the data well such an equation was used.

## 3.5 Results

In order to test that the designed and implemented controller works properly, some experiments were carried out. These experiments were made using an ampoule filled with 1 ml of water as a sample and an empty ampoule (filled with air) as a reference. As the heat capacity of each ampoules are considerably different (the sample's heat capacity is higher than the reference's heat capacity), the calorimeter is unbalanced, which drastically increase the effect of all disturbances, making it easier to quantify the controller's ability to keep the temperatures of the STIC constant.

The STIC present an initial transient behavior before reaching the steady-state when it is turned on, i.e., from when it is turned off (there is no temperature gradient along it, so all the components of the STIC are at ambient temperature) to its working state with the temperature gradient and each calorimeter at a different temperature. Figure 3.5-1 shows the transient behavior of different temperatures in the STIC. The nomenclature used is the following:

- Tch1: Temperature of the calorimeter 1.
- Tch2: Temperature of the calorimeter 2.
- Tch3: Temperature of the calorimeter 3.
- Tch4: Temperature of the calorimeter 4.
- Totec: Ambient temperature in the TEC side.

Ttec: Temperature of the aluminum plate Al2, which is close to the TEC.

To: Ambient temperature of the room.

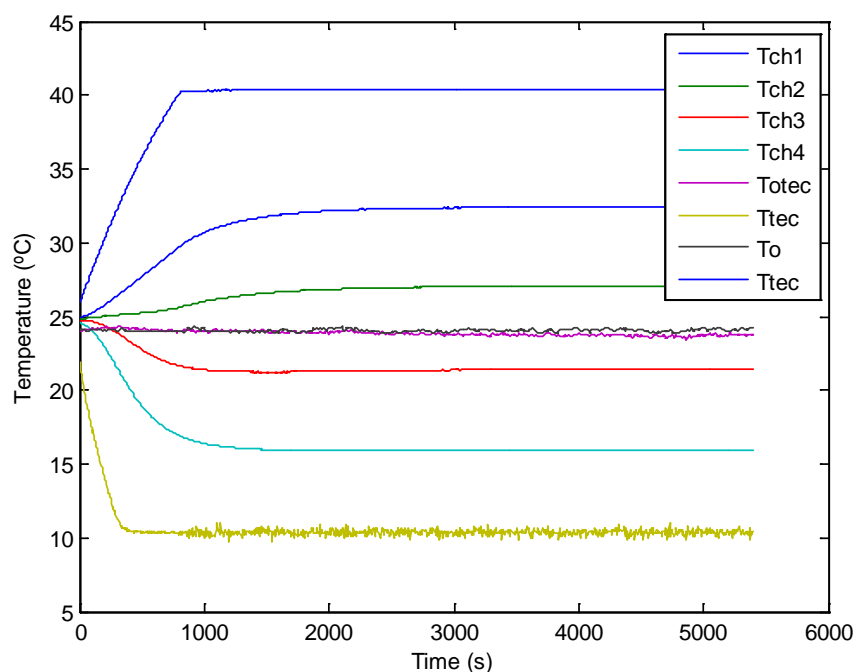
Th: Temperature of the Al4 plate, which is close to the heater.

Ch1: Voltage proportional to the thermal power of the sample in the calorimeter 1.

Ch2: Voltage proportional to the thermal power of the sample in the calorimeter 2.

Ch3: Voltage proportional to the thermal power of the sample in the calorimeter 3.

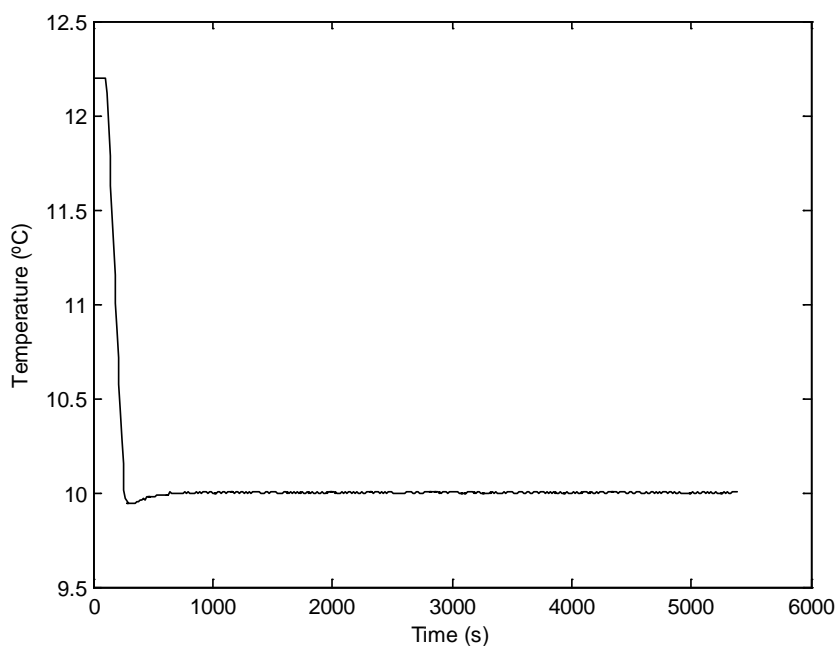
Ch4: Voltage proportional to the thermal power of the sample in the calorimeter 4.



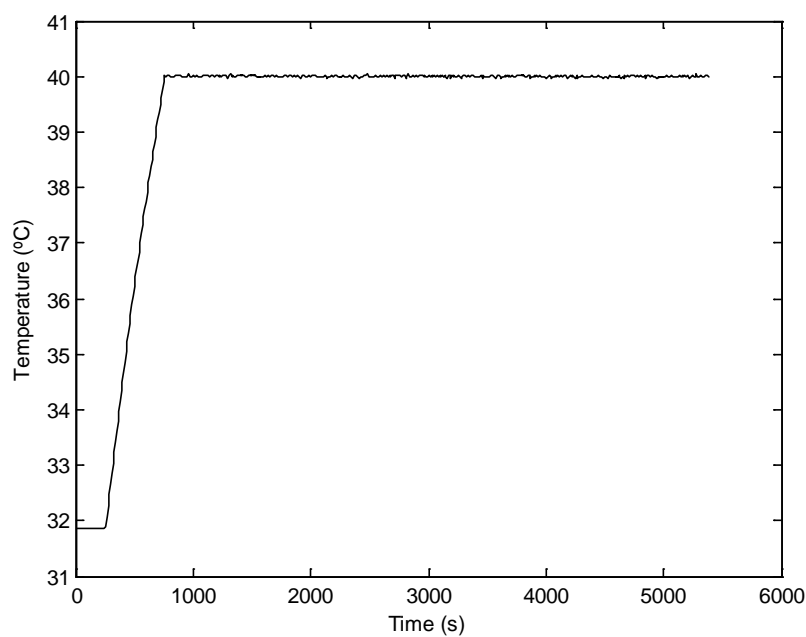
**Figure 3.5-1** Initial transient behavior of the temperatures in the STIC.

In this case, the TEC is set at 10 °C and the heater is set at 40 °C. In the image can be seen that it take about half an hour to reach stable temperatures (steady-state), and once it has been reached, the temperatures are stable. The four calorimeters then have temperatures of about 32.4, 27.0, 21.4 and 15.9 °C.

It is important to note that the signals Tc and Th are not the same signals used to control the TEC and the heater, respectively, but are different sensors placed in similar positions that the others. The signals from the sensors used in the control algorithm are shown in Figure 3.5-2 and Figure 3.5-3. Note that the constant value of both signals at the beginning appears because the temperatures are out of the working range of the sensors, so they give a constant value. Both temperatures are stable and close to the reference value, so the designed PID controller is working properly.



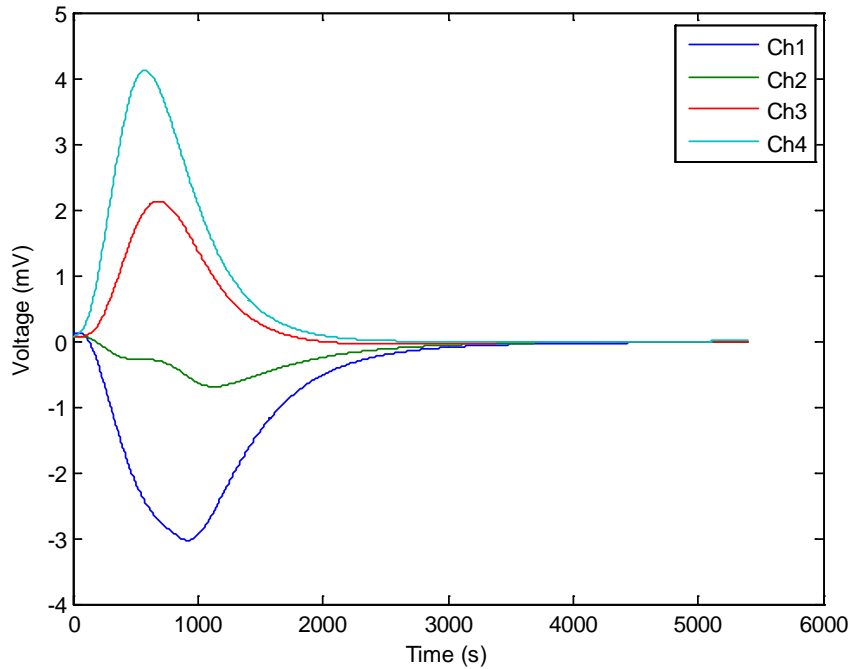
**Figure 3.5-2** *TEC temperature sensor signal  $T_{tec}$ .*



**Figure 3.5-3** *Heater temperature sensor signal  $T_h$ .*

Figure 3.5-4 shows the transient behavior for the calorimeter signals. Their stabilization time is longer than the stabilization times for the temperatures. If an experiment is to be done, it is necessary to wait at least one hour before starting the experiment (if turning on the STIC) to obtain correct results. The reason that the calorimeters take longer time to come to steady state is that they are extremely sensitive to changes in temperature, as their output signal in the absence of internal heat production (in the sample) is proportional to the rate of change of the temperature of the calorimeter. Even though the measured temperature looks constant it is still asymptotically approaching a final value and these small temperature changes are measured by the calorimeters. So an unbalanced calorimeter is a sensitive way of measuring temperature change; much more

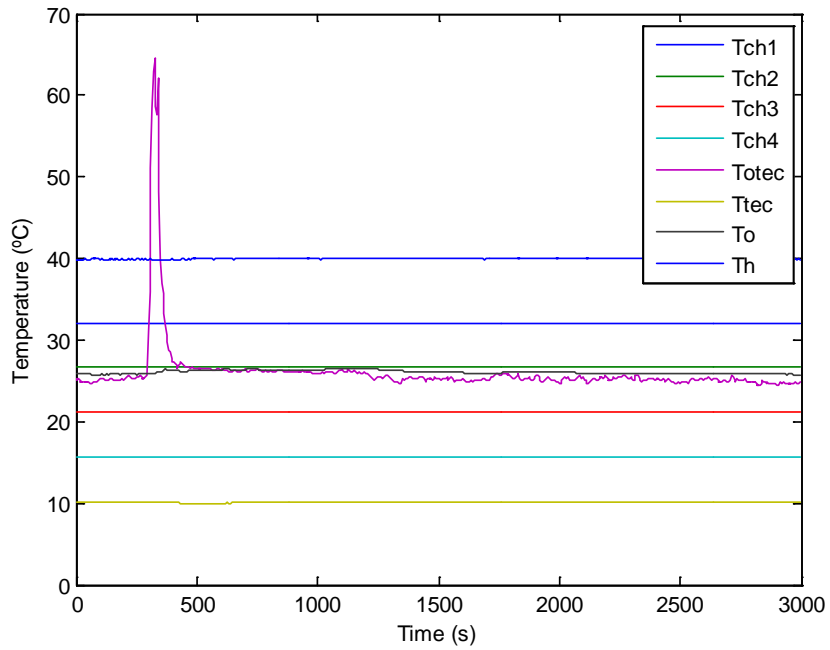
sensitive than if the temperature change was calculated from temperature measurements



**Figure 3.5-4** Initial transient behavior of the calorimeters signals in the STIC.

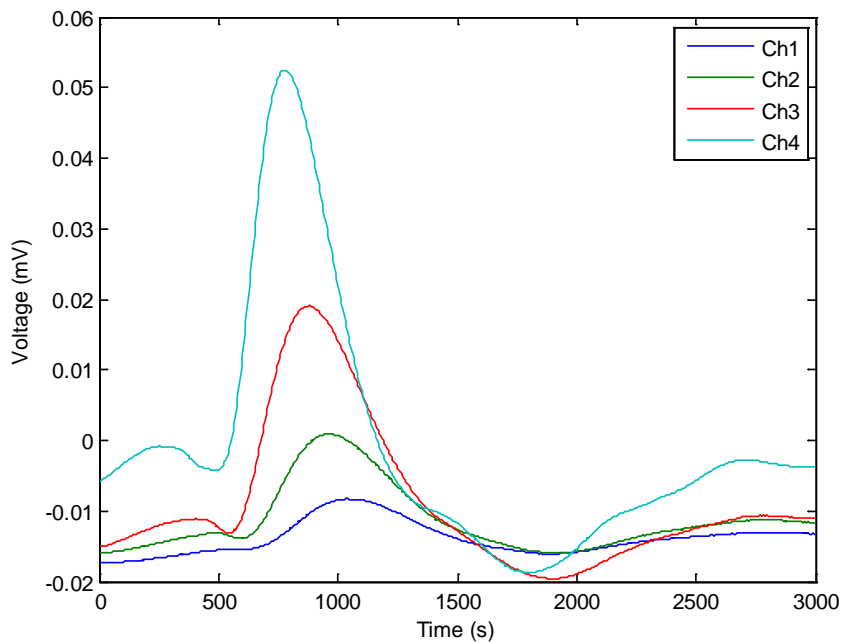
To illustrate how ambient temperature perturbations can affect the calorimeter signals, an experiment was carried out. It consisted on heating different parts of the STIC with a hot air gun (Bosch PHG 600, [23]) to increase the external temperatures in different parts of the instrument. The results showed that the perturbations only have effect when the hot air gun heated the external part of the TEC (the finned heat exchanger with the fan), which is the only component of the STIC not covered by insulation.

Figure 3.5-5 shows the temperatures before and after the heating of the gun, which was applied directly over the fan (and over the sensor giving the signal Totec). In this experiment the temperature perturbation was very high to show the temperature behavior of the STIC (the results of lower –more realistic– temperature perturbations will be seen in the calorimeter’s output, but are difficult to see in the internal temperature measurements). The air gun was on during 60 s.



**Figure 3.5-5** *Temperatures during the experiment.*

Figure 3.5-6 shows the reaction of the calorimeter signals to the perturbation.



**Figure 3.5-6** *Calorimeters' signals during the experiment.*

Each calorimeter's signal is proportional to the temperature difference between the sample and the reference. As the heat capacity of the sample is higher than the heat capacity of the reference, the sample reacts slower to temperature changes than the reference (the heat capacity is the amount of heat needed to increase the temperature one degree). When the perturbation is applied, the reference temperature therefore increases faster than the sample temperature, so the difference between them gets higher in value but negative. This is the explanation of the first decrease of the signals (around 450 s in Ch4). The

perturbation takes some time to propagate inside the STIC: it goes in by the TEC and then affects the calorimeters successively, with calorimeter 4 being the first to be affected and with the highest output from the perturbation, and with calorimeter 1 being the last to notice the perturbation and with a lower output than the others.

The TEC PID does not act immediately but it takes some time to react as its temperature sensor is placed inside the STIC (feed-back control). Its reaction to the perturbation is to give more cooling power as the temperature of its sensor is increasing. So the TEC increases the cooling power and both the sample and the reference of each calorimeter will cool down to the temperature they had before the perturbation. Again, the reference reacts quicker, so the difference between them increases and so does the signal. Then the PID stops cooling (around 800 s in Ch4) until it reaches the steady-state again (it overcools at the beginning), so both ampoules heat up and the difference between them decreases (and oscillates slightly) until it achieves the steady-state again. Note that each calorimeter is essentially isothermal during these events, so the changes in the sample and reference temperatures are insignificant compared to the actual temperature of the calorimeters. An experiment at, for example, 20 °C, will be disturbed by external temperature perturbations even if the temperatures of the sample will only change insignificantly.

To illustrate the propagation of the perturbation inside the TEC, the same experiment was repeated but with a higher heating power. Figure 3.5-7 shows the external temperature at the external part of the TEC (the finned heat exchanger with the fan), and the temperature of each calorimeter, being calorimeter 1 in the second row of the image and calorimeter 4 in the fifth row. In this figure, it is clearly appreciable that the first calorimeter to notice the perturbation is the closest to the TEC, and also that the perturbation effect decreases with the distance to the TEC.

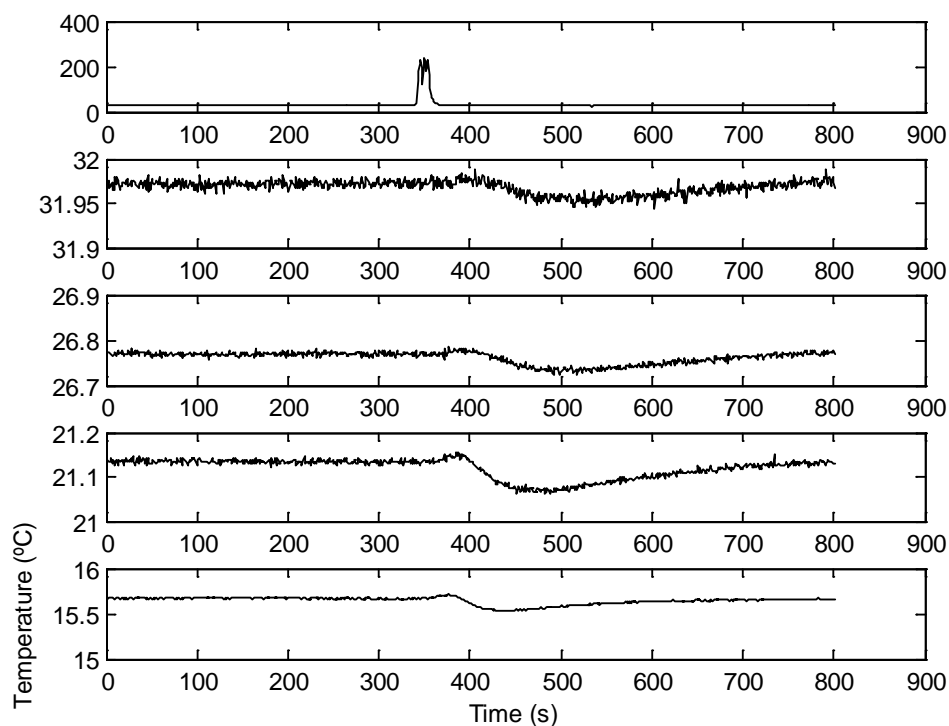


**Figure 3.5-7** *Totec, Tch1, Tch2, Tch3 and Tch4 during the experiment.*

## 4. Simulation Model

In order to study and understand the STIC instrument and its controllers, a simulation model was developed.

### 4.1 Model

The simulation model used in the present thesis is written in MATLAB and is a one-dimensional model of the STIC based on the node-connections modeling method solved by explicit forward differences. The whole STIC (with the TEC and the heater) is divided in different nodes along its length. Each node represents a physical part of the STIC and has its own heat capacity  $C$  (J/K). The different nodes are connected by thermal conductances  $k$  (W/K·m) or by thermal resistances  $R$  (K·m/W). As  $R=1/k$  these two representations are equivalent; both are used as it is sometimes easier to use  $k$  and sometimes easier to use  $R$ .

During this project the simulation model was built and all parameters were given realistic values that were either calculated or taken from manufacturers. The TEC has been modeled in some detail to get a more accurate model.

#### Nodes

The final model of the STIC consists of 198 nodes. They can be grouped according of where they are placed. So, the TEC is divided in 7 different nodes, the tube in 174 nodes, the heater in 2 nodes, each calorimeter in 3 nodes, the ambient in 2 nodes and finally 1 node which represents the thermistor placed next to the TEC.

In the Table 4.1-1 the distribution of nodes is shown:

Group	Node	Description
Ambient	A	Ambient in the TEC side
TEC	F	External part of the finned part of the TEC
	B	Part of the finned part of the TEC in contact with the hot side of the thermocouple
	H	Hot side of the thermocouple TEC
	C	Cold side of the thermocouple TEC
	D	Aluminum plate in contact with the cold side of the thermocouples Al 2
	E	Copper plate between D and G Cu 2
	G	Aluminum plate in contact with the tube of the calorimeter Al 1
Tube	1-31	2 mm slices of rectangular tube
	32	2 mm slice to which calorimeter 4 is attached
	33-68	2 mm slices of rectangular tube
	69	2 mm slice to which calorimeter 3 is attached
	70-105	2 mm slices of rectangular tube
	106	2 mm slice to which calorimeter 2 is attached

	107-142	2 mm slices of rectangular tube
	143	2 mm slice to which calorimeter 1 is attached
	144-174	2 mm slices of rectangular tube
Calorimeter	nHS	Heat sink of the calorimeter n (n=1,2,3,4)
	nA	Sample of the calorimeter n (n=1,2,3,4)
	nB	Reference of the calorimeter n (n=1,2,3,4)
Heater	V	Heated plates at warm side
	W	Heated side external insulation
Ambient	O	Ambient in the heated side
Sensor	S	TEC thermistor, connected with D

**Table 4.1-1** Nodes in the simulation model.

The heat capacity of an object is the amount of heat needed to increase its temperature one degree. To calculate the heat capacity of each node, the following equations have been used [5]:

$$C = c \cdot m = c \cdot \rho \cdot V$$

Where:

$C$ : Heat capacity of the node (J/K)

$c$ : Specific heat capacity of the material (J/K·kg)

$m$ : Mass of the physical element represented by the node (kg)

$\rho$ : Density of the material (kg/m<sup>3</sup>)

$V$ : Volume of the physical element represented by the node (m<sup>3</sup>)

The values of  $c$  and  $\rho$  for the different materials are given in an annex. The sample consist on 1 ml of water, and the reference an empty ampoule.

### Connections

The connections between the nodes are defined as thermal conductances or thermal resistances. A thermal conductance can be defined as the amount of heat that will flow through a one-dimensional object when it is exposed to a temperature difference of one degree. To calculate most thermal conductances, the following equation of thermal conductance is used [5]:

$$k = \lambda \frac{A}{L}$$

Here:

$k$ : thermal conduction conductance of the connection (W/K)

$\lambda$ : thermal conductivity of the material (W/K·m)

$A$ : Area perpendicular to the heat flow (m<sup>2</sup>)

$L$ : Distance between nodes (m).

With this expression, the following connections were calculated:  $RDE$  (thermal resistance from node D to node E) and  $RGE$  (thermal resistance from node G to node E) in the TEC group, all the connections in the tube, the calorimeters and the heater, and the connection between the sensor and the node D  $kDS$ .

To calculate the connection between the external surface of the insulation at the heater side and the ambient, the convection conductance equation is used [5]:

$$k_h = h \cdot A$$

Where:

$k_h$ : Convection conductance with the ambient (W/K).  
 $h$ : Convection coefficient of the ambient air (W/m<sup>2</sup>K).  
 $A$ : Area in contact with the ambient (m<sup>2</sup>).

With this expression, the connection  $kWO$  has been calculated.

Finally, to calculate the connections between the different nodes of the TEC, the equations shown in the paper *Thermoelectric air-cooling module for electronic devices* by Chang et al.[24] have been used. These equations calculate spreading resistances, constriction resistances and conductance and convective resistance in finned bodies. The spreading resistance appears when the area of two bodies in contact are different, and so the heat flow has to expand or contract, decreasing the conductivity of the junction. The constriction resistance arises in non-ideal thermal interfaces because contact is made at discrete spots as defined by the surface roughness and contact pressure.

Figure 4.1-1 from reference [24] shows the TEC-heat sink assembly. In this case, the heat source is the Al 2 plate or node D. The next resistances can thus be defined as shown in Table 4.1-2:

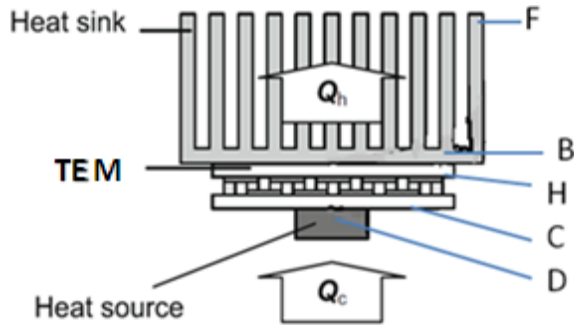


Figure 4.1-1 Set TEC-Heat sink.

Resistance	Description
$R_{csp}$	Spreading resistance between D and C
$R_{bsp}$	Spreading resistance between H and B
$R_{cons}$	Constrict resistance between H and B
$R_b$	Conduction resistance between B and F
$R_{conv}$	Convective resistance between F and A

Table 4.1-2 Different types of resistances presents in the simulation model.

In Figure 4.1-2 (also from reference [24]) the geometrical parameters of the TEC, the heat source and the heat sink are shown:

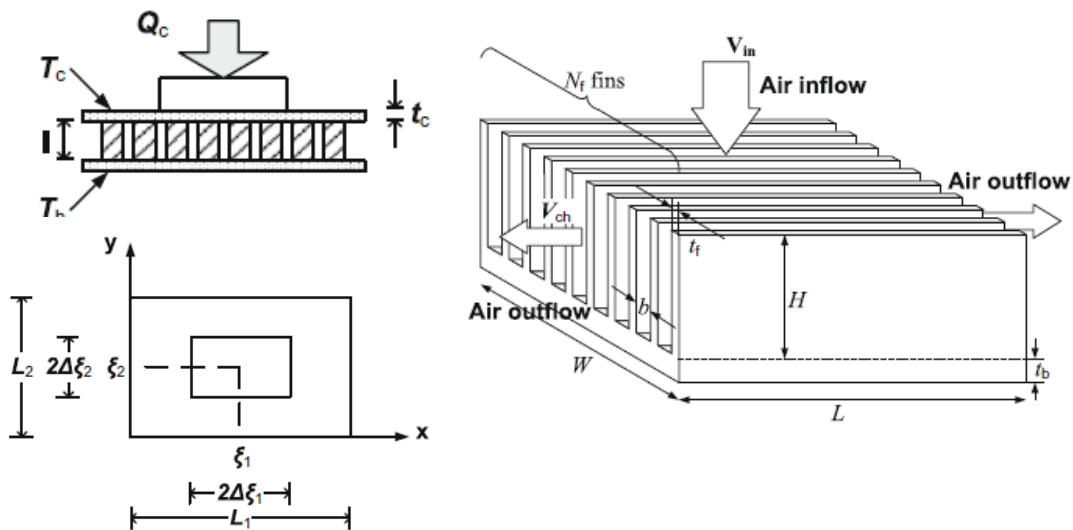


Figure 4.1-2 Geometrical parameters of the TEC, the heat source and the heat sink.

It is important to note that  $L_1, L_2$  are the dimensions of the four TEMs placed together, while  $\xi_1, \xi_2$  correspond to the heat source, specifically to the Al 1 plate or node D. So in this case, the heat source is larger than the TEMs.

The expressions used to calculate the resistances are shown below. The different values of the physical parameters, such as  $h$  and  $\lambda$  are given in an annex.

For the heat sink:

$$A_b = L \cdot W$$

$$R_b = \frac{t_b}{k_b A_b}$$

$$\eta_f = \frac{\tanh(H\sqrt{2h/t_f k_b})}{H\sqrt{2h/t_f k_b}}$$

$$R_{conv} = \frac{1}{hN_f 2LH\eta_f + h(N_f - 1)bL}$$

Being:

$A_b$ : Area of the heat sink ( $m^2$ )

$k_b$ : Thermal conductivity of the aluminum ( $W/K \cdot m$ )

$h$ : Convection coefficient with the ambient air ( $W/K \cdot m^2$ )

$N_f$ : Number of fins in the heat sink

$\eta_f$ : Fin efficiency.

$W, t_b, H, t_f, L, b$ : Geometrical values of the heat sink as showed in the Figure 4.1-2.

For the spreading and constrict resistances calculations are made in three steps. The first calculations:

$$B_i = \frac{SI + k}{k_c t_c} L_i^2$$

$$\bar{\xi}_i = \frac{\xi_i}{L_i}$$

$$\Delta \bar{\xi}_i = \frac{\Delta \xi_i}{L_i}$$

$$i = 1, 2$$

Here:

$S$ : Seebeck coefficient of the TEMs (calculated in section 1.1 TEC)(V/K)

$I$ : Current trough the TEMs (A).

$k$ : Thermal conductance of the TEMs (calculated in section 1.1 TEC)(W/K)

$k_c$ : Thermal conductivity of the ceramic plates ( $W/K \cdot m$ )

$t_c$ : Width of the ceramic plates (m)

$\Delta \xi_i, \xi_i, L_i$ : Dimensions of the TEMs and the heat source (m).

Intermediate calculations:

$$p_i = \frac{L_i}{L_{i+(-1)^{i-1}}} \sqrt{B_{i+(-1)^{i-1}} \left( 1.5 - \left[ \frac{\sinh(2\sqrt{B_{i+(-1)^{i-1}}})}{2\sqrt{B_{i+(-1)^{i-1}}}} + 1 \right] \right)^{-1}}$$

$$K_i = \frac{2 \sinh(p_i \Delta \bar{\xi}_i) \cosh(p_i (1 - \bar{\xi}_i))}{\sinh(p_i)}$$

$$\phi_{i \max} = K_i \cosh(p_i \bar{\xi}_i) - \cosh(p_i \Delta \bar{\xi}_i) + 1$$

$$\bar{\phi}_i = \frac{K_i}{p_i} \sinh(p_i) - \frac{1}{p_i} 2 \cos(p_i (1 - \bar{\xi}_i)) \sinh(p_i \Delta \bar{\xi}_i)$$

$$i = 1,2$$

Final calculations:

$$R_{csp} = \frac{(\phi_{1max}\phi_{2max} - \bar{\phi}_1\bar{\phi}_2)L_1L_2}{4\Delta\xi_1\Delta\xi_2(\alpha I + k)}$$

$$A_{TEM} = L_1L_2$$

$$\lambda = \frac{\pi^{3/2}}{\sqrt{A_b}} + \frac{1}{\sqrt{A_{TEM}}}$$

$$R_{bsp} = \frac{\sqrt{A_b} - \sqrt{A_{TEM}}}{k_b\sqrt{\pi A_b A_{TEM}}} \cdot \frac{\lambda k_b A_b R_{conv} + \tanh(\lambda t_b)}{1 + \lambda k_b A_b R_{conv} \cdot \tanh(\lambda t_b)}$$

$$R_{cons} = \left( \frac{1}{2k_b\sqrt{A_{TEM}}} \left( 1 - \sqrt{\frac{A_{TEM}}{A_b}} \right)^{3/2} - \frac{\sqrt{A_b} - \sqrt{A_{TEM}}}{k_b\sqrt{\pi A_b A_{TEM}}} \right) \cdot \frac{\lambda k_b A_b R_{conv} + \tanh(\lambda t_b)}{1 + \lambda k_b A_b R_{conv} \cdot \tanh(\lambda t_b)}$$

In the simulation model, these resistances are calculated by the MATLAB function `chang_eq` which has as inputs the Seebeck coefficient  $S$ , the current  $I$  and the thermal conductance  $k$  (which is previously calculated):

$$[R_{csp}, R_{bsp}, R_{cons}, R_{conv}, R_b] = \text{chang\_eq}(\alpha, k, I);$$

### Thermoelectric Module properties

The Seebeck coefficient  $\alpha$ , the thermal conductance  $k$  and the electric resistance of the TEMs are calculated by a MATLAB function `prop_BiTe`, using the equations, considerations and values given in section 1.1:

$$[\alpha, r, k, HC] = \text{prop\_BiTe}();$$

The current through each TEM is calculated as the ratio between the voltage given by the power source and the resistance the current flows through (twice the resistance of each TEM, as there are two TEM connected in series.).

$$I = 24 / (2 * r);$$

### Methodology

The goal of the simulation model is to calculate the temperature of each node as a function of time and under certain external conditions. To reach that goal, first the physical properties of the STIC are needed. Those properties are the heat capacities and the thermal conductances explained above. The next step is to define the initial state of the system, that is: to assign a numerical value to each node temperature at time zero. It is also needed to specify the duration of the simulation and the time step that should be used in the simulation. The time step is the time difference between two calculated values in the simulation. For example, with a time step of one second, the program will calculate the temperature values for every second of the simulation, but with a time step of one millisecond the program will calculate the temperature of every millisecond. So, if simulating one hour, in the first case the program would give 3600 values of each output parameter, while in the second case it would give 3600000 values. However, a too large time constant will make the simulation unstable, as it will move too much

heat in each time step. In the present simulations a time step of 1 ms was used. The reason that such a small time step (and consequently a rather long simulation time) has to be used is that there are many components in the STIC-model that have high heat conductances and low heat capacities.

Once the properties, initial temperatures and time settings had been introduced, the program starts its cyclical part. Starting with the initial values, the program calculates first the heat flows between the nodes, and then, using these values, calculates the new temperature of each node. These two steps are repeated until the program gets to the end time of the simulation.

### Heat flow

There are three different types of heat flows involved in the system: those in the TEC, the heat created by the heater and internal heat flows generated by temperature differences between nodes.

The heat flows generated by the TEC, called  $\Phi_C$  on the cold side and  $\Phi_H$  on the hot side, are calculated using the expressions presented in section 2.1:

$$\begin{aligned}\Phi_C &= 2 \cdot \left( 2SIT_C - \frac{1}{2}R_e I^2 \right) \cdot f - K(T_H - T_C) \\ W_e &= 2 \cdot (2SI(T_H - T_C) + R_e I^2) \cdot f \\ \Phi_H &= \Phi_C + W_e\end{aligned}$$

Note that a new parameter  $f$  has been added to the first two equations. This parameter, as has been explained in the section 2.1, is the output of the PID controller of the TEC and represents the duty cycle of the PWM-generated current. This parameter is calculated by a MATLAB function `PID_TEC`, which the temperature of the sensor (node S) and the time step as inputs.

$$f = \text{PID\_TEC}(TS, dt);$$

The heat generated by the heater, produced in node V with a rate  $qV$ , is also controlled by a PID controller that regulates a PWM-generator. The heat is the maximum power that the heater can give multiplied by the duty cycle given by the function `PID_heater`.

$$qV = (\text{PID\_heater}(TV, dt) * 48)^{2/57};$$

The remaining heat flows are calculated by the basic heat transfer equation:

$$\Phi_{ij} = k_{ij} \Delta T_{ij} = \frac{\Delta T_{ij}}{R_{ij}}$$

Here:

$\Phi_{ij}$ : Heat flow between node  $i$  and node  $j$  (W)

$k_{ij}$ : Conductive or convective thermal conductance (W/K)

$R_{ij}$ : Conductive thermal resistance (K/W)

$\Delta T_{ij}$ : Temperature difference between node  $i$  and node  $j$  (K or °C).

### Temperatures

To calculate the temperatures in each node, the following expression is used:

$$T_i^{t+1} = T_i^t + \frac{\sum_j \Phi_{ij}}{C_i} dt$$

Here:

$T_i^{t+1}$ : Temperature of node  $i$  at time  $t+1$  (°C)

$T_i^t$ : Temperature of node  $i$  at time  $t$  ( $^{\circ}\text{C}$ )

$\sum_j \Phi_{ij}$ : The sum of all the heat flows that enter the node  $i$  (+) minus all the heat flows that leave the node  $i$  (-) (W).

$C_i$ : Heat capacity of node  $i$  (J/K)

$dt$ : Time step of the simulation (s).

### PID controllers

The PID controllers are implemented in two MATLAB functions. They work in the same way as the controllers implemented in Simulink and were explained above. Both functions have the duty cycle as output, and their temperature sensor value and the time step as inputs.

```
function P=PID_heater(T,dt)
```

```
function P=PID_TEC(T,dt)
```

The complete code of the simulation model can be found in an annex.

## 4.2 Test and validation

In order to validate the simulation model, a simulation was run and the results were compared to the results described in section 3.5. A total of 10000 s were simulated. To be able to compare the results, the same conditions as shown in figure 3.5-5 were reproduced. So the simulation was run with an ambient temperature of  $25^{\circ}\text{C}$  and a perturbation of  $60^{\circ}\text{C}$  was applied during 60 s. Figure 4.2-1 shows the simulated initial transient behavior of the temperatures in the STIC.

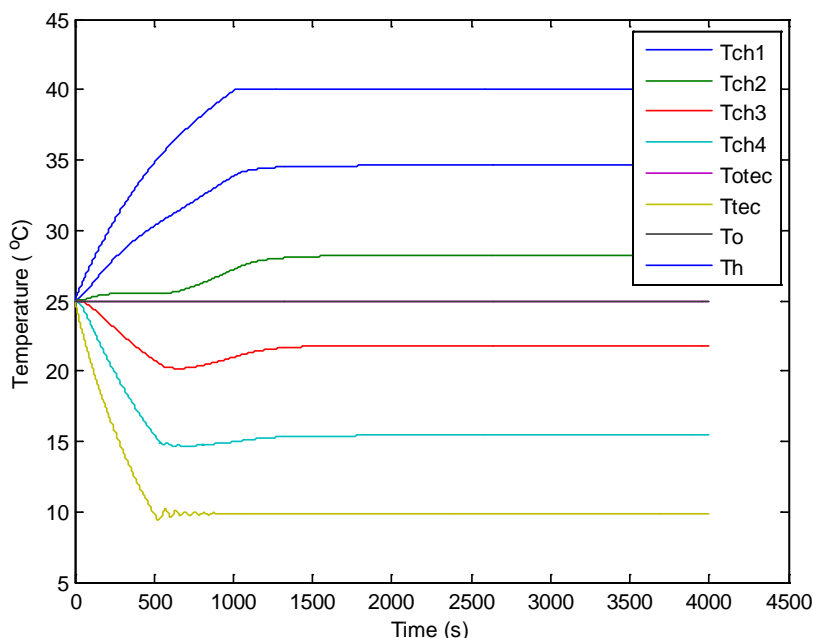


**Figure 4.2-1** STIC temperatures' simulated initial transient behavior.

Compared to Figure 3.5-1, the simulated results are qualitatively similar to the real results, but with some differences. It takes approximately half an hour to get to the steady state, as it happens in the real system. The simulated temperature trajectories from the beginning to the steady state are also similar to the real ones. However, simulated temperatures  $Tch3$  and  $Tch4$  have an undershoot that does not appear in the real system. Simulated TEC temperature  $T_{tec}$  presents small

oscillations around its steady-state value that do not appear in the real system. It is also observed that the heater and the TEC in the real system reach their steady-state value quicker than in the simulation.

Figure 4.2-2 shows the simulated initial transient behavior of the calorimeters:

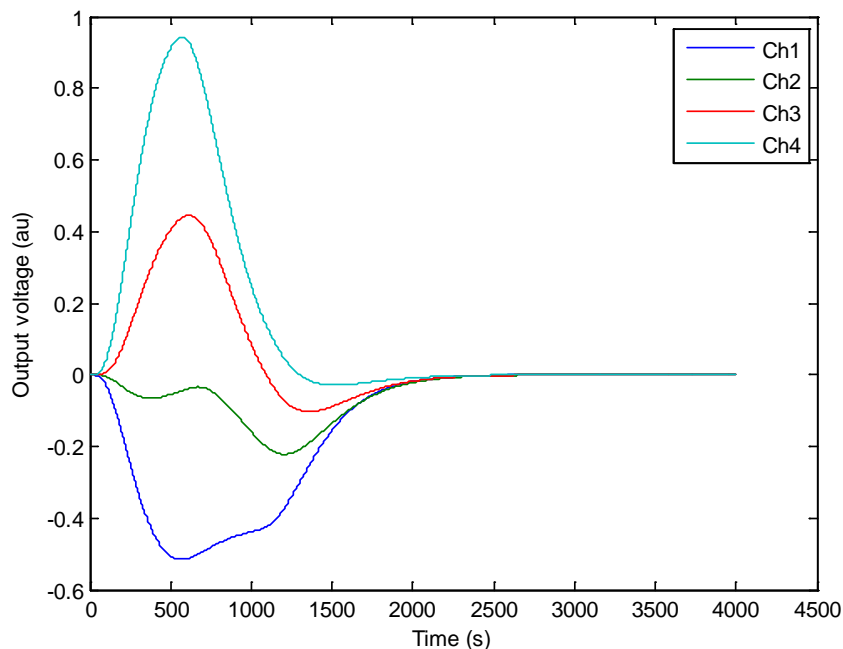


**Figure 4.2-2** Calorimeters' simulated initial transient behavior.

Compared to figure 3.5-4, the simulated calorimeters' signals and the real signals agree to some extent, but the simulated response is faster than the real one, as it takes about 2500 s to the simulated calorimeters to reach the steady state, while the real ones took 4500 s. The simulated signal trajectories of Ch3 and Ch4 are similar to the real ones, but simulated Ch1 and Ch2 are significantly different. It is not possible to compare the amplitudes, because the simulation gives the output of the calorimeters as the difference between the sample temperature and the reference temperature, but the calorimeters' output is a voltage proportional to the temperature difference. Thus the y-axis in figure 4.2-2 is a voltage with arbitrary units.

Figure 4.2-3 shows the simulated temperatures during the perturbation application, and figure 4.2-4 shows the simulated reaction of the calorimeters to the perturbation. This reaction is different of the real one, shown in Figure 3.5-6. In the simulation, when the perturbation happens, the calorimeters' signals get lower as the reference temperature increases faster than the sample temperature. When the controller reacts to the perturbation, then it starts cooling, but it overcools (the higher peak), so the signals go quickly up and then down slowly until they reach the steady state again. Comparing the real system and the simulation, the controller reacts faster in the real system, as the first undershoot is smaller in the real system (although it is not possible to compare the amplitude values, qualitatively this is clear).

In conclusion, there are some significant differences between the real system and the results of the simulation. The simulation model does therefore not fully mirror the real system. To further understand the behavior of the STIC and its controllers it would be of interest to improve the model in the future. However, note that the model as it is presented here is solely based on the physical

principles and calculated parameters by which the instrument is believed to work. No attempts have been made to improve the model by changing the model parameters.

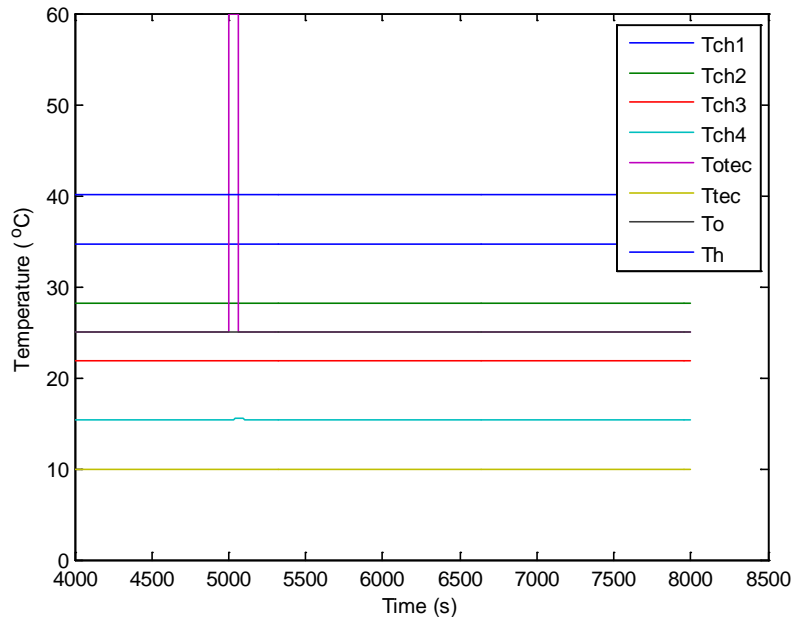


Figure 4.2-3 Simulated temperatures.

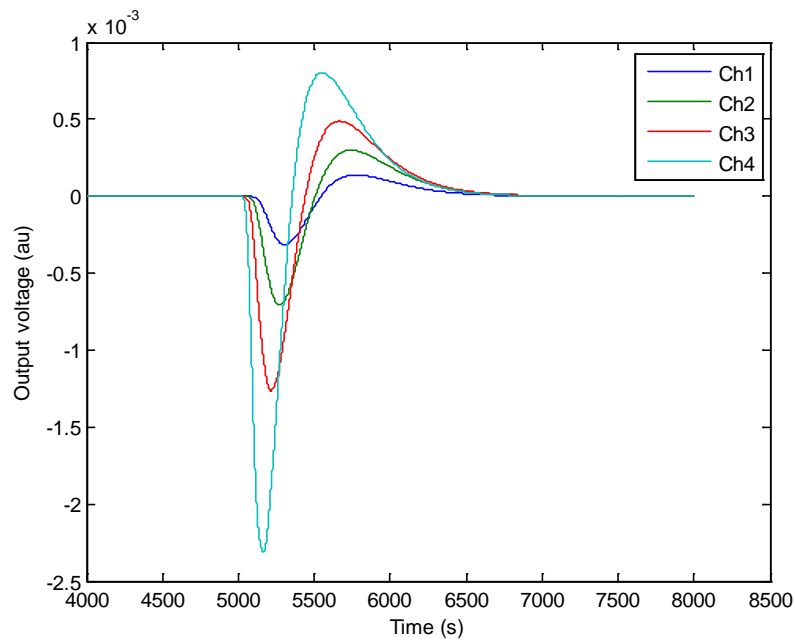


Figure 4.2-4 Simulated calorimeters' signals.



## 5. Control System Improvement

In the current section, a new control algorithm is proposed, and the result obtained with it will be discussed. Its goal is to decrease the effect of external temperature perturbations in the calorimeter signals.

### 5.1 Feed forward control

Until now, all the control algorithms used were in a feedback configuration: the variable to control is measured and compared with the reference value to calculate the error, which should go towards zero. So first the control action is done, and afterwards the result of this action is compared to the reference [25]. In such control algorithms, the effect of an external perturbation is only noticed after it has affected the control signal. Once this signal is perturbed, the error changes and the PID reacts to compensate it. This kind of control is not good in this application, where a high precision in the measurements is wanted, a precision that increases as the effects of external perturbations decrease.

In order to get a faster and better control, feed forward algorithms can be used. In feed forward control one measures the source of the perturbation, in this case the outside temperature in the TEC side, and use this signal to react to changes before they have disturbed the instrument. By feed forward, the controller reaction is faster, as it does not have to wait until the set-point control signal gets modified [26]. One possible feed forward algorithm will be presented here. To use it, a third sensor has to be used to measure the external temperature (the temperature at which the TEC deposits the heat).

#### Outside sensor

The process to choose the outside sensor is the same as that followed with the heater and the TEC sensors. The normal working temperature range of this sensor is the room temperature, usually between 21-25 °C. According to the Table 5.1-1, the best sensor is one thermistor  $R_t$  ACC-003 (5 k $\Omega$  at 25 °C) connected with 3 resistances  $R$  of 5 k $\Omega$  in the Wheatstone bridge and with an amplifier resistance  $R_a$  of 1 k $\Omega$  which gives a working range approximately between 17 °C and 35 °C. Those values are resumed in the Table 5.1-1:

Element	Value
Thermistor $R_t$	ACC-003 (5 k $\Omega$ at 25 °C)
Wheatstone bridge fix resistances $R$	5 k $\Omega$
Amplifier resistance $R_a$	1 k $\Omega$

**Table 5.1-1** Resume of the elements used in the Outside.

The chosen sensor has been calibrated as the other two sensors. The result of the calibration is shown in Figure 5.1-1:

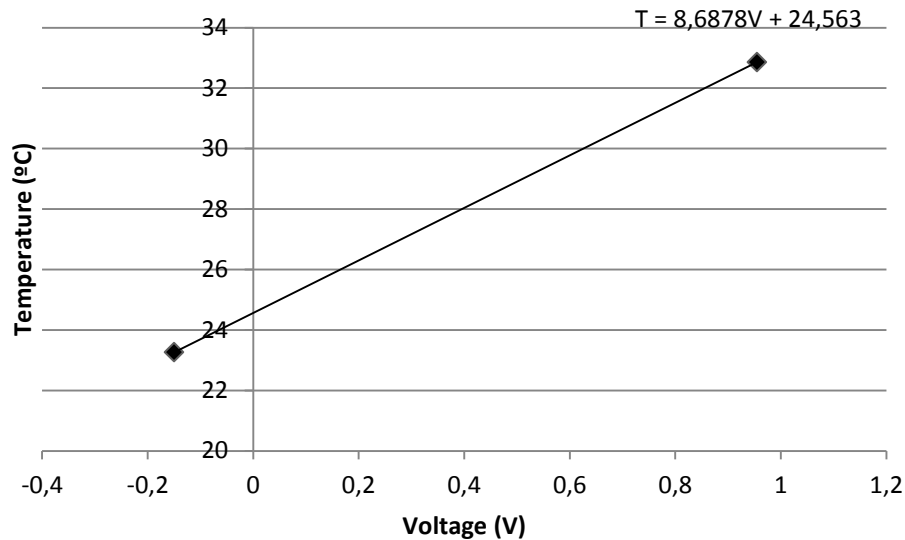


Figure 5.1-1 Outside sensor data.

The sensor is located over the protection grid of the fan of the TEC.

## 5.2 Relationship between ambient temperature and TEC duty cycle

It is important to know the relation between the changes in the ambient (external) temperature and the cooling power needed in the TEC, in order to avoid the noise effect caused by those changes. In the present project, the ambient is the air in the laboratory, which is not perfectly constant even if an air cooling system is. Also, changes in the outdoor temperature, opening of doors etc., can give temperature variations that propagate into the STIC instrument and disturb the calorimeter signals. To reduce the effect of such variations, the controller, through the outside sensor, has to notice the ambient temperature changes and then modify the duty cycle to compensate those changes.

The thermal power of the TEC can be considered as proportional to the difference between the ambient temperature  $T_{amb}$  and the desired cold temperature in the TEC  $T_{TEC}$ . So, if more cooling is wanted, more power is needed, and then a higher duty cycle  $DC$  has to be used.

$$DC \propto T_{amb} - T_{TEC}$$

To find the relationship between the ambient temperature and the duty cycle, the procedure described below has been followed. Keeping the ambient temperature constant, the desired cold temperature  $T_{TEC}$  (the reference temperature in the control algorithm) was changed to different values, and then the duty cycle was determined for each of these values. Then, a new value  $T_{dif}$  is calculated as the original reference temperature in the TEC,  $T_0$  (in this case a set-point of  $T_0 = 10$  was used) minus the actual temperature  $T_{TEC}$ .

$$T_{dif} = T_0 - T_{TEC} = 10 - T_{TEC}$$

By this operation, the relation between the duty cycle and the reference temperature change in the TEC is known. Assuming that the duty cycle is proportional to the temperature difference, and knowing the duty cycle  $DC_0$  for  $T_0$  then:

$$\Delta DC = DC - DC_0 = (T_{amb} - T_{TEC}) - (T_{amb} - T_0) = T_0 - T_{TEC} = T_{dif}$$

In the Table 5.2-1 the data obtained is shown:

$T_{TEC}$ (°C)	$T_{dif}$ (°C)	DC
12	-2	0,31
11	-1	0,37
10	0	0,42
9	1	0,48
8	2	0,53

**Table 5.2-1** Values of  $T_{TEC}$ ,  $T_{dif}$  and DC obtained.

The linear equation that fits the data is shown in Figure 5.2-1:

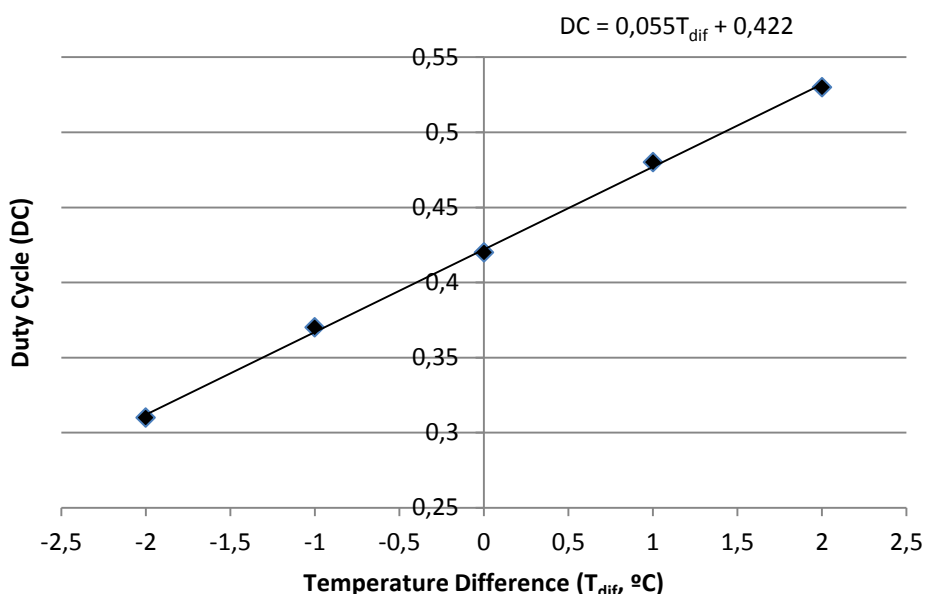


**Figure 5.2-2** Fitted data Temperature difference versus Duty cycle.

### 5.3 Feed forward control algorithm

From the data of the Table 5.3-1, it is known that when the ambient temperature is constant at the value fixed by the cooling system (10 °C in the present case), the duty cycle given by the PID controller is 0.42. As has been previously explained, when the ambient temperature changes without a feed forward controller, this change flows into the instrument and affects both the TEC sensor and the calorimeter signals, actuating then the PID controller to compensate the change. As this propagation takes some time, when the controller reacts the calorimeter signal has already been affected. In the new algorithm, an outside sensor is used to measure the ambient temperature. This temperature is compared with reference temperature (the mean ambient temperature), giving a temperature difference. From the equation in Figure 5.2-1, multiplying this temperature difference by a constant  $ff$  equal to 0.055, and then adding the output of the PID controller (which is around 0.42), the corrected duty cycle is generated.

In this algorithm there is no time delay due to the temperature propagation as the outside sensor is directly in contact with the ambient air at high air velocity, and the temperature difference is compensated with the feed forward part instead of with the PID controller. The implemented algorithm of the new controller is shown in Figure 5.3-1:

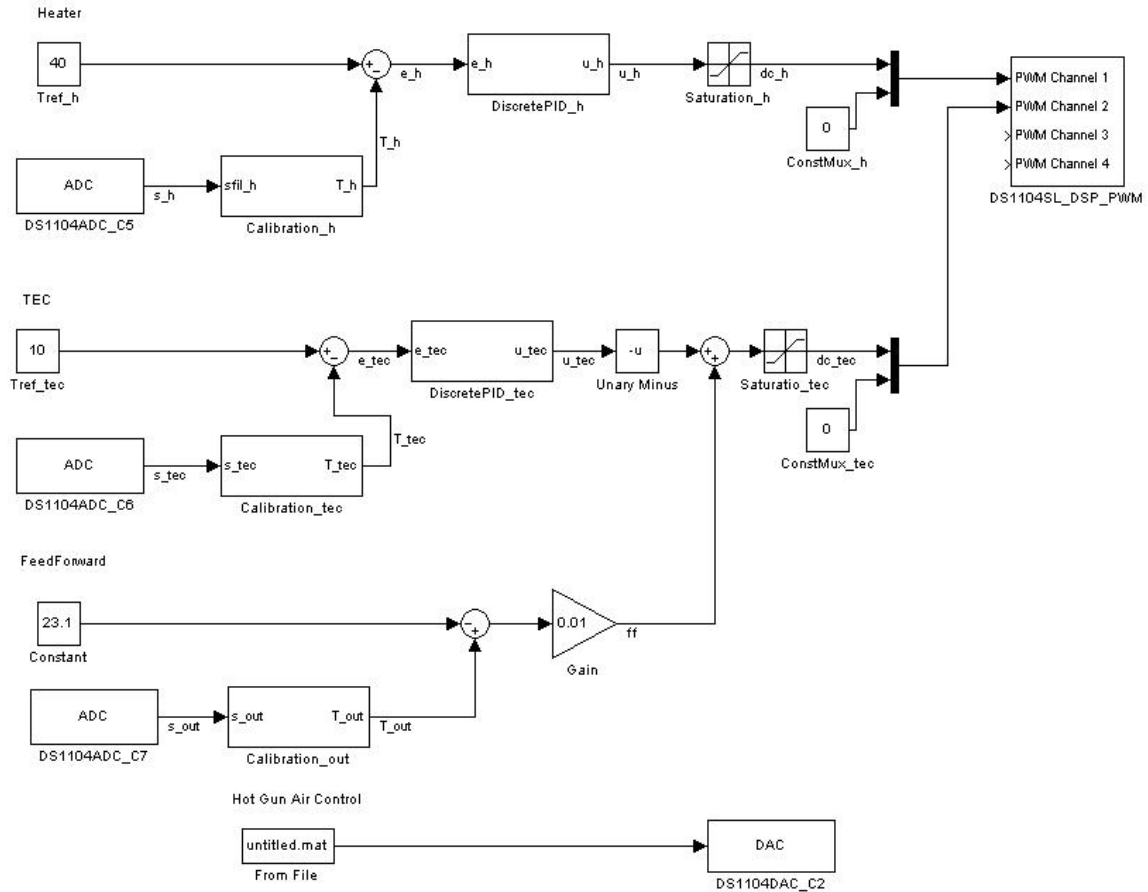


Figure 5.3-1 Feed forward algorithm (shown with  $ff = 0.01$ ).

It is possible that the theoretical value  $ff = 0.055$  is not the optimal value for the real system. To find the optimum value, i.e., to tune the feed forward controller, a new experiment was done. But before, to check if the proposed algorithm has any effect, a simulation was carried out.

### 5.4 Feed Forward simulation

In order to check the usefulness of the proposed feed forward algorithm, a simulation was carried out. The feed forward was implemented in the MATLAB function `PID_TEC(T, dt)`, by adding the ambient temperature in the TEC side  $T_A$  as input, and adding the feed forward output to the PI output to get the total duty cycle:

$$f = \text{PID\_TEC}(T_S, T_A, dt);$$

To compare the results obtained for different values of  $ff$ , a experiment was defined. To make it similar to the real experiment, the ambient temperature was defined as 23 °C. The experiment consisted in apply five steps changing the ambient temperature to 26 °C during eight minutes, with eight minutes between

each step with the ambient temperature as 23 °C again. Figure 5.4-1 shows this temperature steps and the temperatures in the instrument (in this scale the effect of the temperature disturbance cannot be seen).

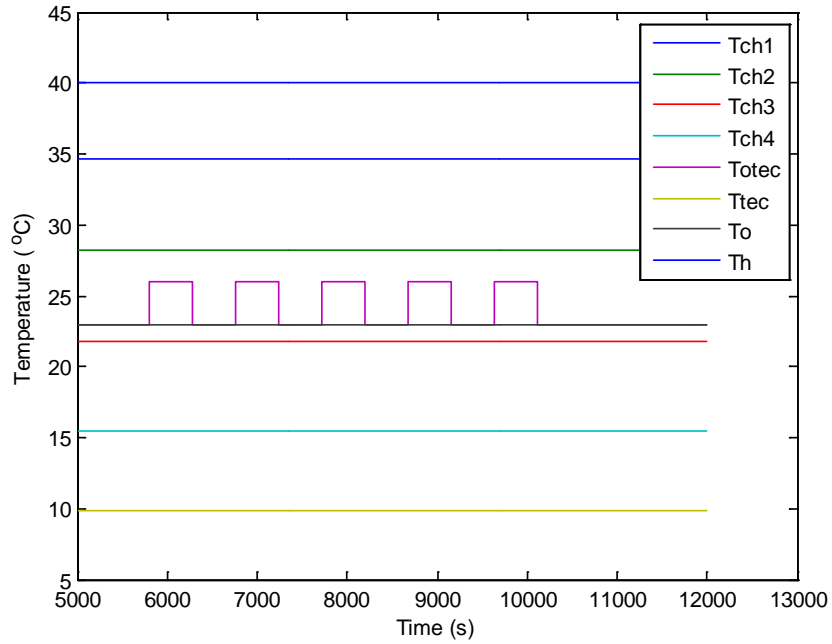


**Figure 5.4-1** Ambient temperature steps.

To compare the results, only the signal of the 4<sup>th</sup> calorimeter (the closest to the TEC) will be taken into account. Figure 5.4-2 shows the calorimeter signal for  $ff = 0$ .

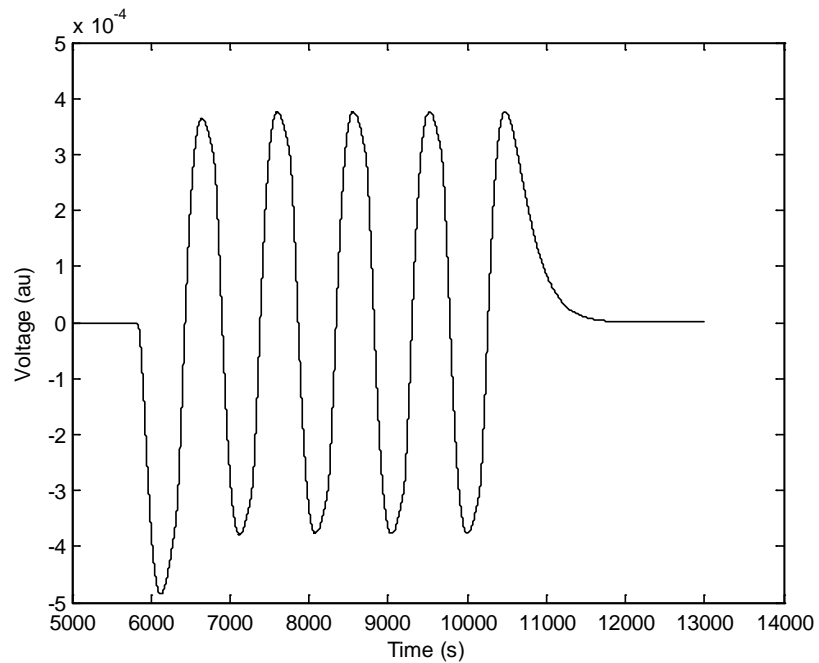


**Figure 5.4-2** Ch4 calorimeter signal for  $ff = 0$ .

The same simulation was carried out with different values of  $ff$ : -0.01, 0.001, 0.005, 0.0075, 0.01, 0.02, 0.05. Figure 5.4-3 shows the signal from the 4<sup>th</sup> calorimeter for each value of  $ff$ .

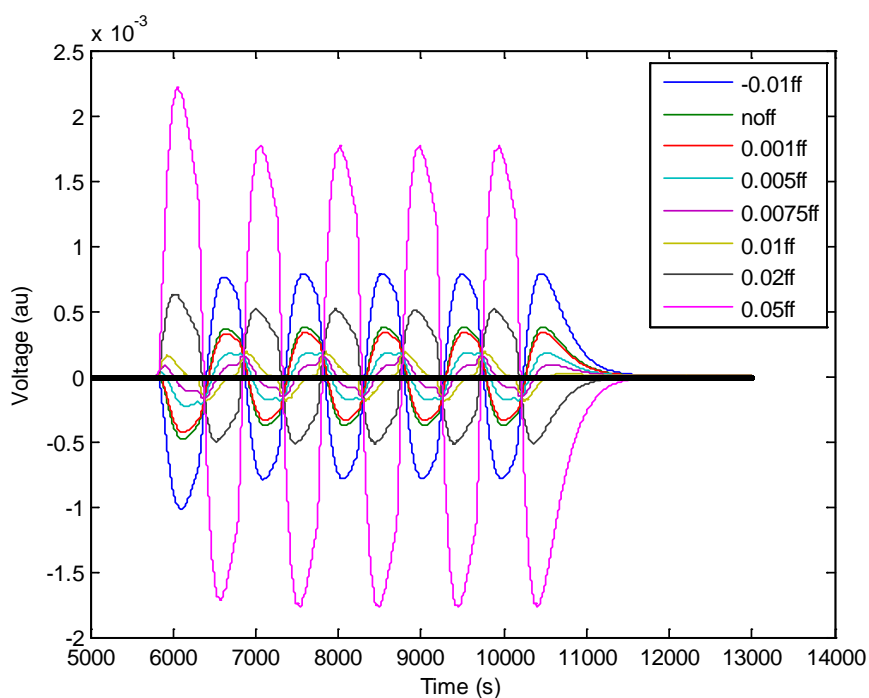


**Figure 5.4-3** *Ch4 calorimeter signal for different values of  $ff$ .*

There are some values of  $ff$  that decrease the effect of the perturbation, i.e., that made the amplitude of the oscillations lower. It is interesting to note that for values of  $ff$  from 0.0075 to 0.05, when the controller reacts to the perturbation, it overcools (the higher the  $ff$  value, the higher the overcooling); that is why those signals start going up, as both the sample and the reference cool down, but the reference is quicker so the difference between both temperatures gets greater. On the other hand, for  $ff$  equal to 0.001, the effect of the feed forward is so small that it is almost the same as without feed forward. With the negative value the effect of the perturbation is clearly worse than without feed forward.

As it is difficult to appreciate in Figure 5.4-3, to quantify the improvement the amplitude of the oscillations was measured (the first peak, which is higher in each signal, was not taken into account). Figure 5.4-4 shows the relationship  $ff$  value-amplitude. According to this figure, there is a  $ff$  value of minimum amplitude around 0.075. The improvement obtained with  $ff = 0.075$  over no feed forward is about 55%. It is not so important to find this value for the simulation, as it would most probably be slightly different in the real system, but this result shows that the real system should also have an optimal value of  $ff$  that reduces the effect of room temperature perturbations in the calorimeter signals.

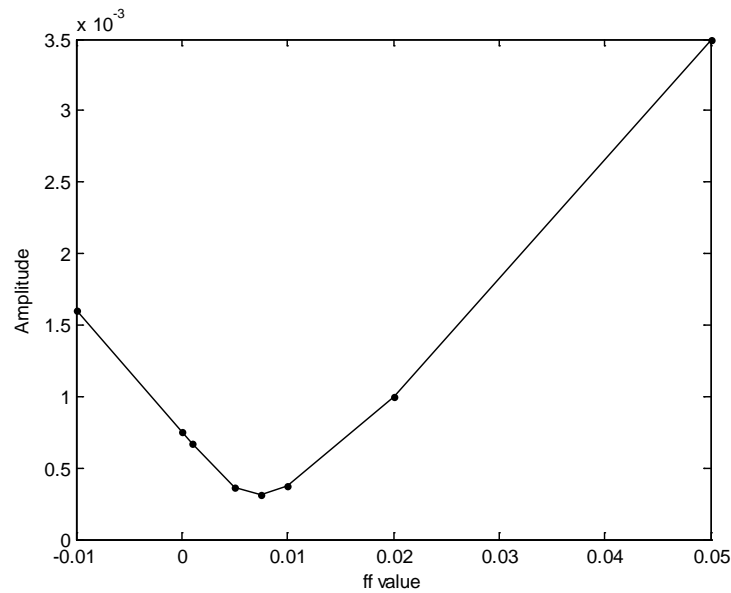


Figure 5.4-4 Relationship  $ff$  value-Amplitude of the oscillations.

## 5.5 Feed forward tuning experiment

To tune the feed forward constant  $ff$ , an experiment was carried out. This experiment consisted of reproducing the experiment that was previously simulated. So a perturbation to the room temperature was applied using different values of  $ff$  in the feed forward algorithm and then the effect of the perturbation in the calorimeters signals were compared, with the aim of finding the optimal constant.

As the perturbation has to be as similar as possible in each experiment, the hot air gun was connected to a relay controlled by the dSPACE. The experiment consisted in a sequence of five steps of eight minutes with the hot air gun producing heat, separated by eight minutes in which the hot air gun was off. Before and after the steps, one additional hour of data was saved in order to let the signals reach steady-state both at the start and after the perturbations. The hot air gun was fixed about 1 m from the fan of the TEC and so that it pointed towards a point slightly below the center of the fan. It was set to its minimum power. This arrangement gave temperature increases of 2-3 °C. This experiment was made with different values of the feed forward coefficient  $ff$ , including  $ff = 0$  to have a reference to compare the other results. As in the simulation, only the signal from the fourth calorimeter – which is the closest to the TEC – was considered. Figure 5.5-1 shows the output from the (unbalanced) calorimeter for  $ff = 0$ . The experiment was repeated another 19 times with different values of the  $ff$  constant (for  $ff = 0.015$ ,  $0.0175$  and  $0.02$  the experiment was repeated three times). Some of these results are shown in Figure 5.5-2 and Figure 5.5-3. All the experiments gave the same general results, with an increasing trend during the oscillations, and thus changing peak values. This made it more difficult to measure the amplitude than in the simulated case, where the amplitude was constant and without the increasing trend.

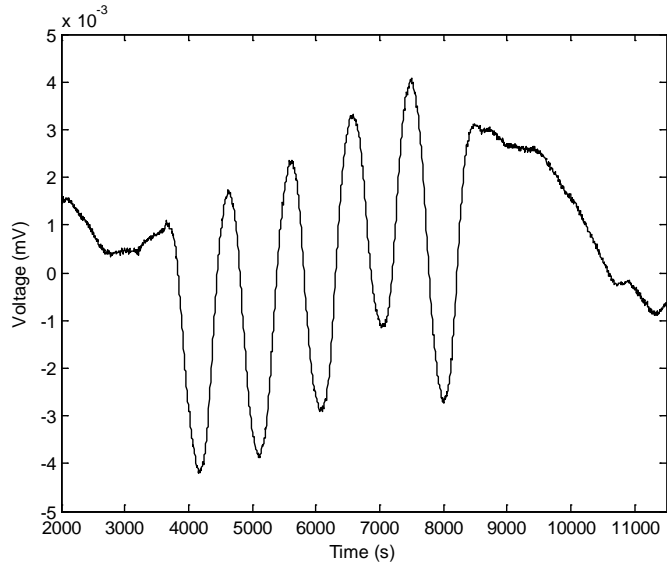


Figure 5.5-1 Calorimeter signal without feed forward during the experiment.

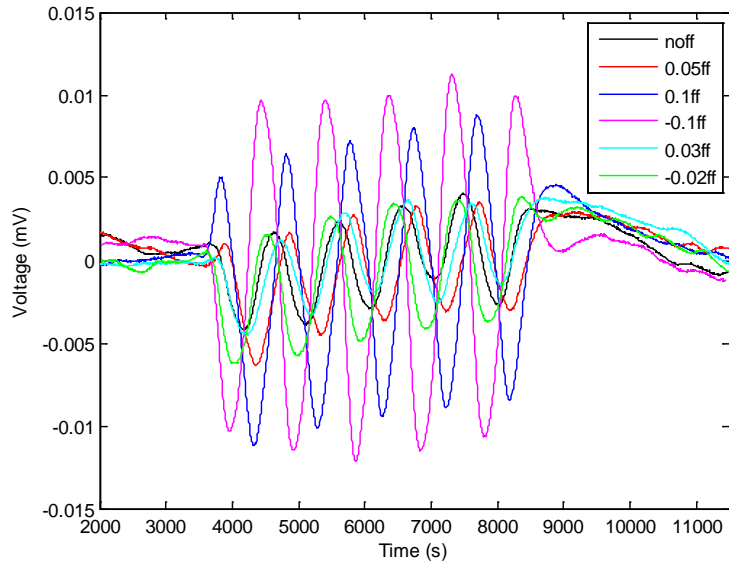


Figure 5.5-2 Calorimeter signal for different values of  $ff$ .

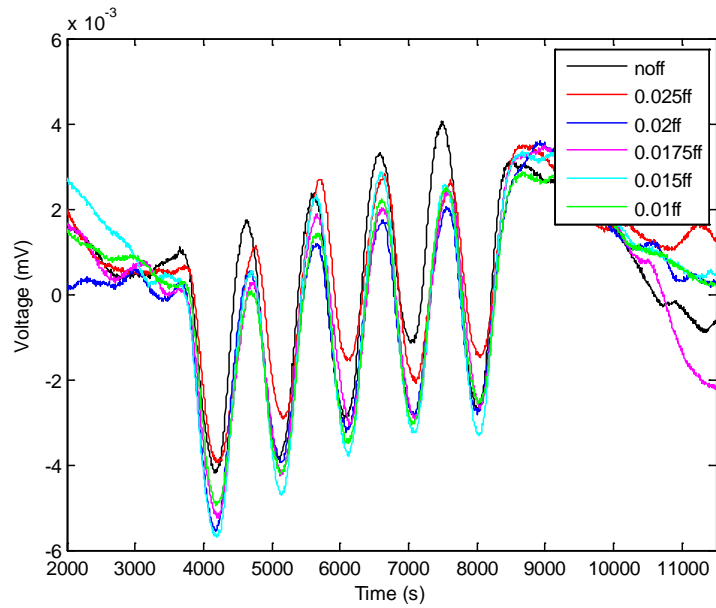


Figure 5.5-3 Calorimeter signal for different values of  $ff$ .

To be able to compare the amplitudes, a new value  $Amp$  was proposed. This value is the mean of the difference between each one of the first three higher peaks minus the second and the third lower peaks. If we call the maximum values  $H1$ ,  $H2$  and  $H3$  (the first, second and third green symbols in Figure 5.5-4) and the minimum values  $L1$  and  $L2$  (the same with the red symbols), the value  $Amp$  is:

$$Amp = \frac{(H1 - L1) + (H2 - L2) + (H2 - L1) + (H3 - L2)}{4}$$

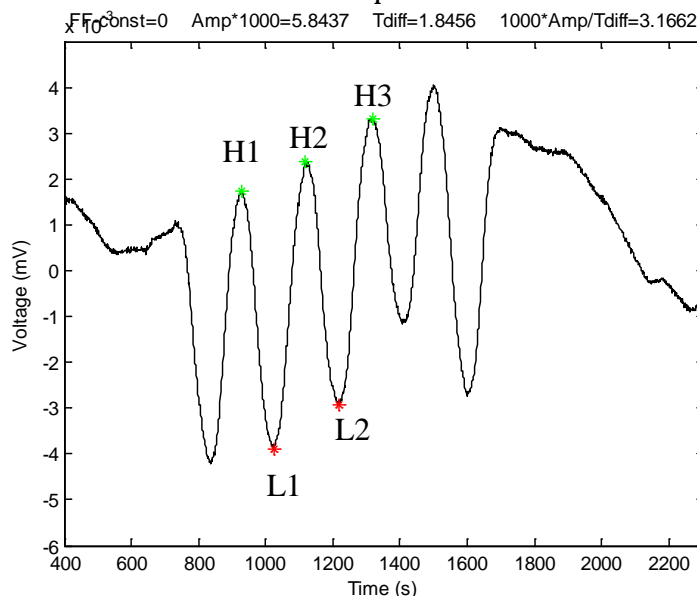
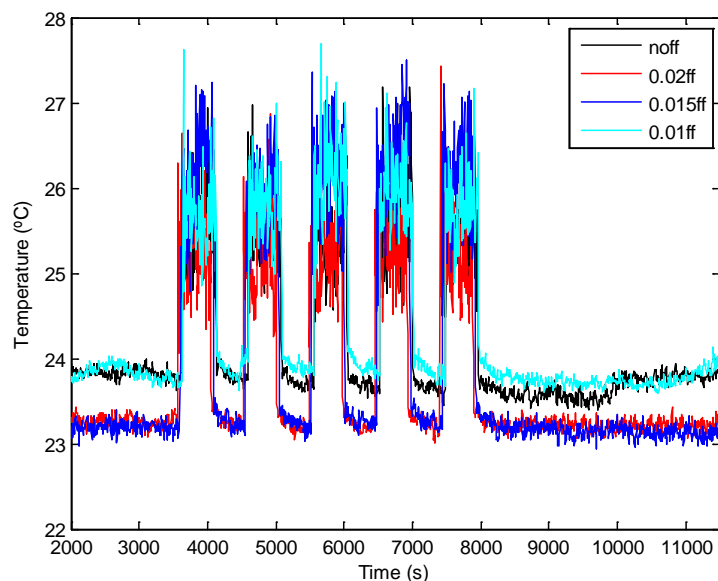


Figure 5.5-4 Calculated values for  $ff=0$ .

Contrary to the simulation, in the experiment the room temperature is not constant during the experiment and it is not the same in each experiment, as shown in Figure 5.5-5, where the room temperature in the TEC side (where the perturbation is applied) are plotted for some experiments. It is also seen that when the perturbation happens (the hot air gun is on), the step temperature is also quite noisy. It is thought that the amplitude of the temperature step is related with the amplitude of the oscillations in the calorimeter signal. To be able to compare the different experiments, a temperature difference  $T_{diff}$  was calculated as the mean of all the values higher than 24.5 °C (perturbation) minus the mean of all the values lower than 24.5 °C (original room temperature).



**Figure 5.5-5** Room temperature for different experiments.

Then, a normalized value  $U$  was calculated:

$$U = \frac{Amp}{T_{diff}}$$

Using this number  $U$  the results of each experiment can be compared. The lower the  $U$ -value is, the better the control is. Figure 5.5-6 shows the relation  $ff$  value- $1000 \cdot U$ . The shape is similar to the shape obtained in the simulation (Figure 5.4-4). It can be seen that there is a range of values of  $ff$ , between 0 and 0.04, which reduces the effect of the perturbation in the calorimeter signal compared with the no feed forward situation. It also seems that there exists a minimum optimal value of  $ff$  even if the scatter in the data is quite high..

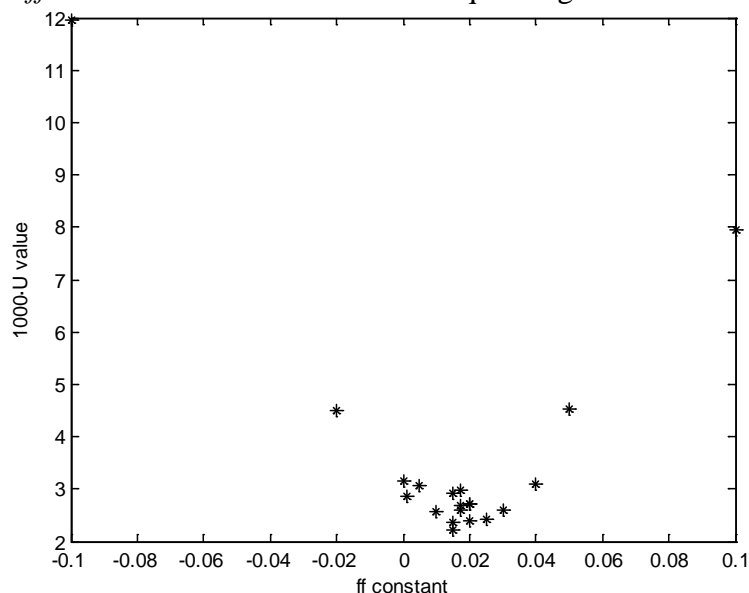


**Figure 5.5-6** Relationship  $ff$  constant-  $1000 \cdot U$ .

This optimal value is hard to find, but it seems to be placed between 0.015 and 0.02. The improvement obtained with one of these values respect no feed forward is about 25%. Around these values, several experiments have been done

with the same  $ff$ , but there is some variability in the results, as can be better seen in Figure 5.5-7.

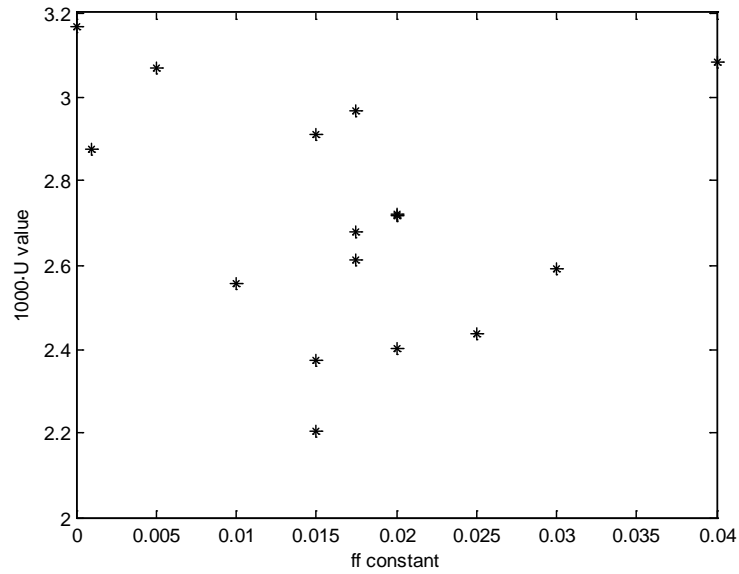


**Figure 5.5-7** A close-up of the relationship  $ff$  constant-  $1000 \cdot U$ .

As an example, the results for the three experiments with  $ff = 0.02$  are shown in Figure 5.5-8 and 5.5-9. Figure 5.5-10 shows the relationship between  $Amp$  and  $T_{diff}$  for each of these three experiments. As thought, the higher the temperature difference, the higher the amplitude of the oscillations. But this relation is not linear, so it difficult to decide which one of these three values is the best one. The same happens with the experiments for  $ff = 0.015$  and  $0.0175$ .

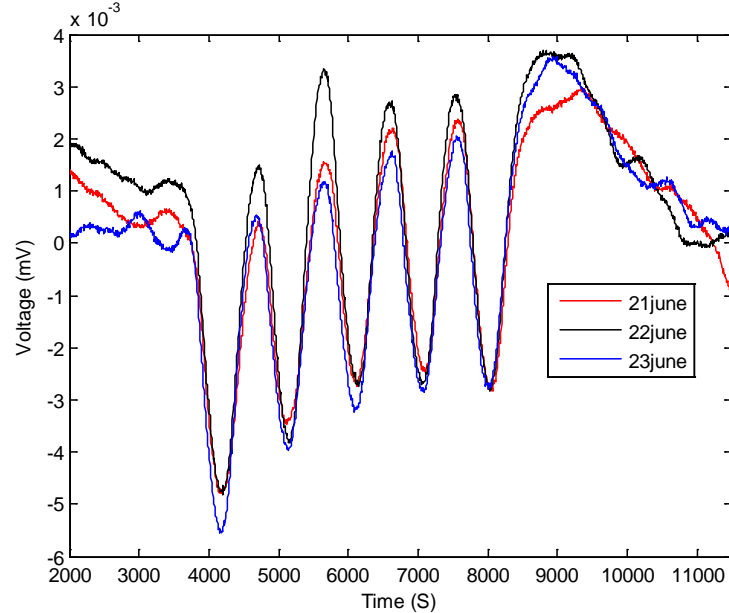


**Figure 5.5-8** Calorimeter signals for  $ff = 0.02$  in different experiments.

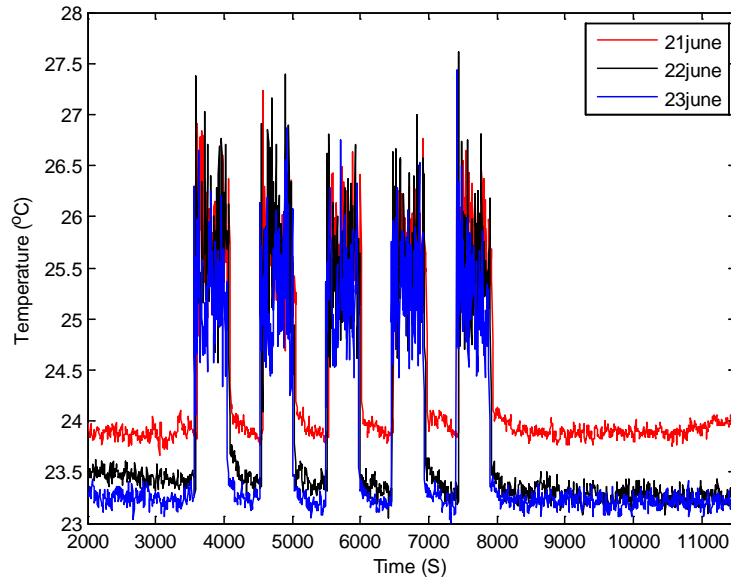


**Figure 5.5-9** Room temperature during different experiments for  $ff = 0.02$ .

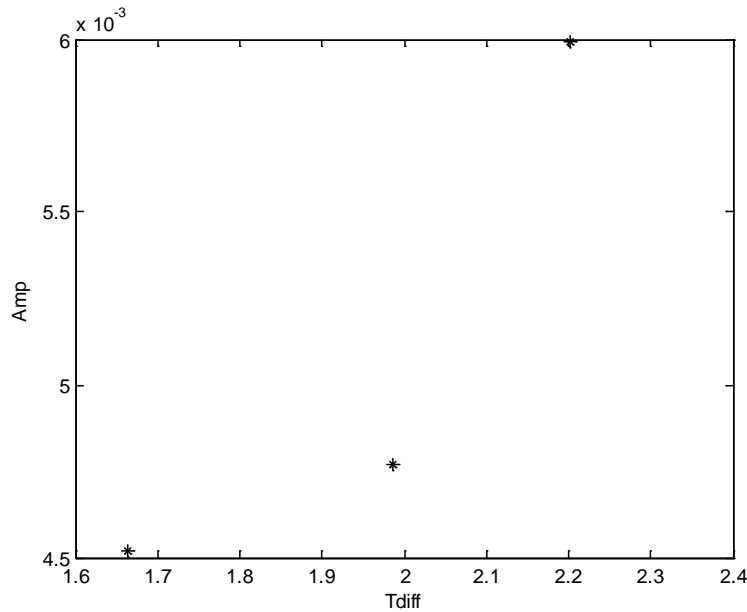


**Figure 5.5-10** Relationship  $T_{diff}$ -Amp.

It is also interesting to look at the controller parameters and compare how they react for different values of  $ff$ . Figure 5.5-11 shows the data from the TEC sensor  $T_{tec}$  (used by the TEC PID controller) without feed forward ( $ff = 0$ , the corresponding ambient temperature change is seen in Figure 5.5-5). It is difficult to appreciate the effect of the perturbations in  $T_{tec}$ , which means that the PID controller works rather well controlling the temperature (however, the disturbance to the sensitive calorimeter signal is still significant). Figure 5.5-12 shows the data from the Outside sensor  $T_{out}$  (used in the feed forward controller), the integral part of the PID  $i_{tec}$  and the output of the feed forward  $ff_{output}$  (which is zero as  $ff = 0$ ). The  $T_{out}$  y-axis value has been rescaled to allow a better plot.

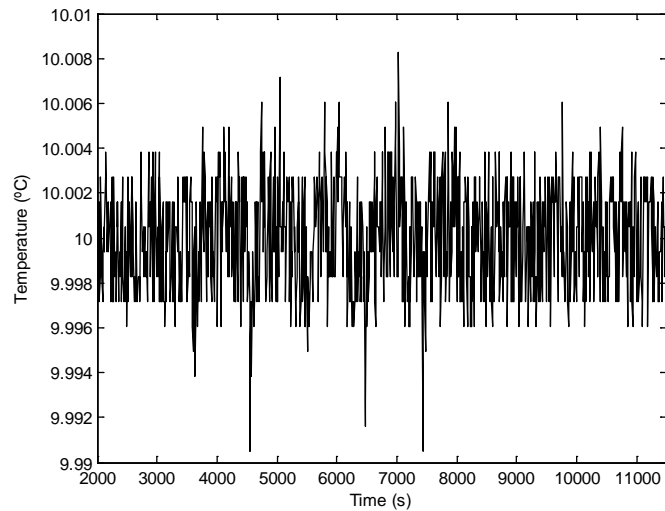


Figure 5.5-11  $T_{tec}$  temperature for  $ff = 0$ .

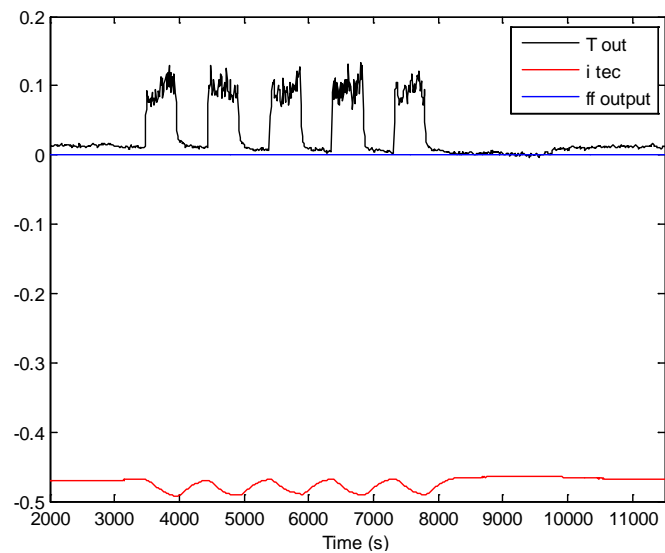
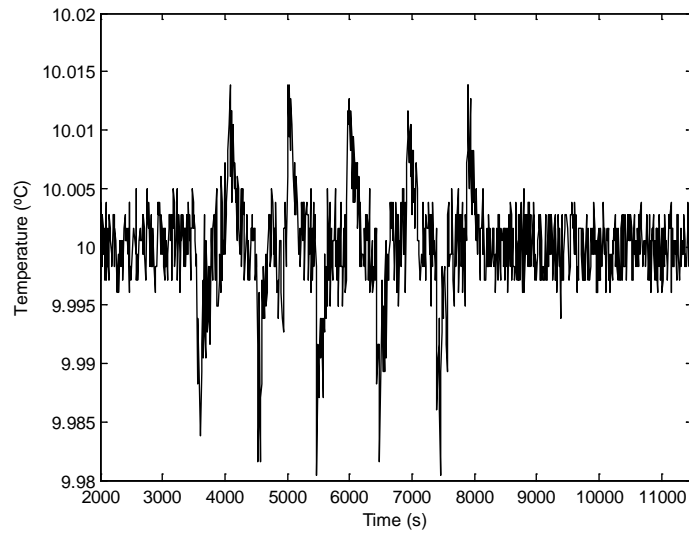


Figure 5.5-12  $T_{out}$ ,  $i_{tec}$  and  $ff_{output}$  for  $ff = 0$ .

In this case, when the perturbation happens, the integral part takes care of it by increasing the cooling power (the  $i_{tec}$  gets higher in value but negative), and when the perturbation ends, it returns to its steady state value.

Figures 5.5-13 and 5.5-14 show the same results with  $ff = 0.05$ , one of the worst values. In the first figure one can appreciate the influence of the perturbations: when the perturbation starts, the temperature goes down fast because the feed forward constant is too high and the system overreacts. That can also be seen in the second figure: as the perturbation begins, the feed forward reacts immediately, which means that the algorithm is working properly. However, as the controller is overcooling, the integral part tries to compensate part of this overcool, and this is why  $i_{tec}$  decreases.



**Figure 5.5-13**  $T_{tec}$  temperature for  $ff = 0.05$ .

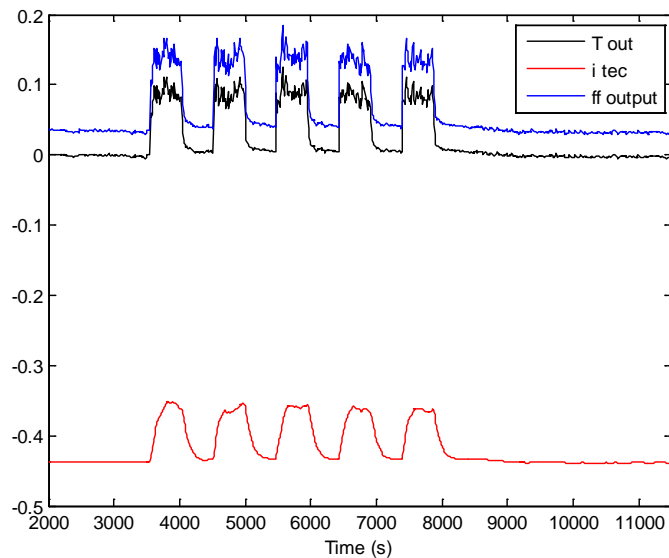


**Figure 5.5-14**  $T_{out}$ ,  $i_{tec}$  and  $ff_{output}$  for  $ff = 0.05$ .

Figures 5.5-15 and 5.5-16 show the same results with  $ff = 0.02$ , one of the best values. In this situation, one can also see the perturbation effects in  $T_{tec}$ , but here the temperature decreases less than with  $ff = 0.05$ . As shown in the second figure, the controller reacts in a similar way as with  $ff = 0.05$ , but now the feed forward output is lower, so there is a lower overcooling and the integral part has to compensate less. The ideal situation would be that the feed forward fully compensates for the effect of the perturbation, so that the integral part does not have to do anything and the PID does not even notice the perturbation.

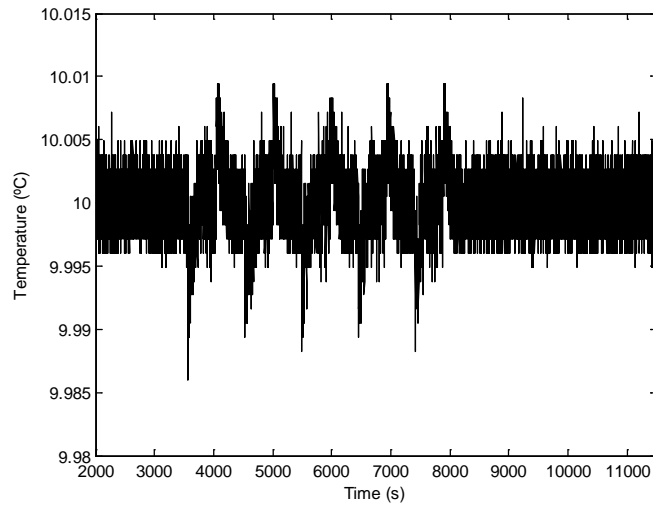


**Figure 5.5-15**  $T_{tec}$  temperature for  $ff = 0.02$ .

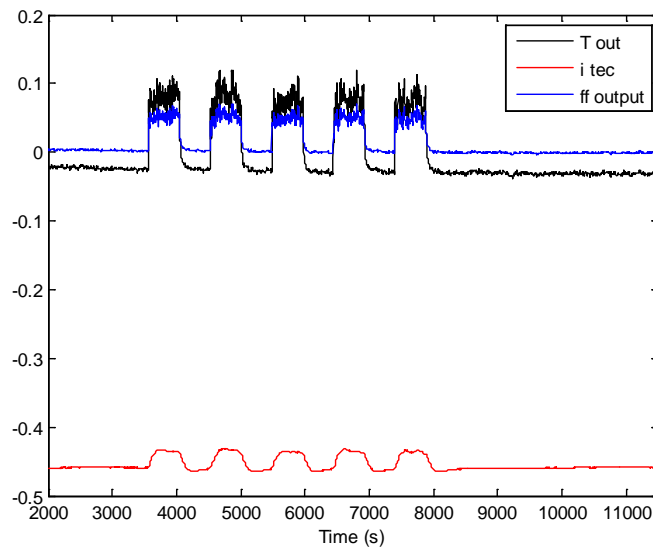


**Figure 5.5-16**  $T_{out}$ ,  $i_{tec}$  and  $ff_{output}$  for  $ff = 0.02$ .

In conclusion, for positive values of  $ff$  lower than 0.04, the effect of external perturbations in the calorimeter signal is reduced compared to the scenario without feed forward, and the maximal reduction happens with a value of  $ff$  between 0.015 and 0.02. However, in order to find the optimal value, the experiment needs to be run in an environment with a more constant temperature and the perturbations should be made in a way that could make the temperature steps more constant.



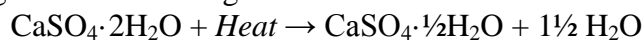
## 6. Gypsum plaster setting experiment

To give an example of an application of the STIC, an experiment with the setting of gypsum (plaster of Paris) was carried out. This experiment illustrates the usefulness of such an instrument as the STIC. In the sections below gypsum plaster will be briefly presented. The experimental procedure will be explained and the results will be commented.

### 6.1 Description of gypsum plaster

The term plaster refers to a building material used for coating walls and ceilings. There are different kind of plasters, such as gypsum plaster, lime plaster and cement plaster. Gypsum plaster, also known as plaster of Paris, is made from calcium sulfate hemihydrate ( $\text{CaSO}_4 \cdot \frac{1}{2}\text{H}_2\text{O}$ ) that reacts with water to produce calcium sulfate dihydrate ( $\text{CaSO}_4 \cdot 2\text{H}_2\text{O}$ ), a soft sulfate mineral.

Calcium sulfate hemihydrate is produced by heating gypsum minerals to about 150 °C, which gives the following reaction:



where the products are gypsum plaster ( $\text{CaSO}_4 \cdot \frac{1}{2}\text{H}_2\text{O}$ ) and steam ( $1\frac{1}{2} \text{H}_2\text{O}$ ). As happens with mortar or cement, gypsum plaster starts as a dry powder which is mixed with water to form a gypsum paste which liberates heat and hardens (hydrates). The setting of plaster starts about 10 minutes after mixing with water and is complete in about 45 minutes.

Plaster, unlike mortar and cement, remains quite soft after setting and can be easily manipulated with metal tools. This property made gypsum plaster useful in several fields, such as architecture, art and medicine [27, 28].

### 6.2 Experimental procedure

The experiment consisted on measuring the heat liberated in the setting process of the gypsum plaster at the following four temperatures: 32.4, 27.0, 21.4 and 15.9 °C. The samples used in the experiment were a mix of calcium sulfate hemihydrate with water, and the references were 1 g of water. In the samples, the ratio water/binder was 0.6 to ensure constant reaction conditions [28].

As was explained in section 1.1, the heat capacities of the sample and the reference should be similar to decrease the noise. The specific heat capacity of the water is  $c_w = 4.2 \text{ J/g} \cdot \text{K}$ . So the heat capacity of the reference  $C_R$  is:

$$C_R = 1 \text{ g} \cdot 4.2 \frac{\text{J}}{\text{gK}} = 4.2 \frac{\text{J}}{\text{K}}$$

The composition of the sample is calcium sulfate hemihydrate, which has a specific heat capacity of about  $c_{gp} = 0.8 \text{ J/g} \cdot \text{K}$ , and water, with the 0.6 ratio. So the specific heat capacity of the sample  $c_s$  is:

$$c_s = \frac{0.6 \text{ g} \cdot 4.2 \frac{\text{J}}{\text{gK}} + 1 \text{ g} \cdot 0.8 \frac{\text{J}}{\text{gK}}}{1.6 \text{ g}} = 2.08 \frac{\text{J}}{\text{gK}}$$

As both heat capacities must be equal, the mass of each sample  $m_s$  is found as:

$$C_R = C_S = m_s \cdot c_s \Rightarrow m_s = \frac{C_R}{c_s} = \frac{4.2 \frac{\text{J}}{\text{K}}}{2.08 \frac{\text{J}}{\text{gK}}} \approx 2 \text{ g}$$

In conclusion, each sample has to contain 2 g of the mix gypsum plaster-water to have a similar heat capacity as the reference. This calculation is quite approximate as the heat capacity of the sample will change during the reaction, but will give a good balancing of the calorimeters.

To carry out the experiment, the following procedure was used: first, the STIC was run with the references but without the samples. Once it reached the steady state, the samples were prepared by mixing 1 part of plaster with 0.6 parts of water, and filling each ampoule with about 2 g of the mix. Finally, the samples were placed in the STIC. It is important to do the mixing-filling process quickly, as it only takes 10 min for the mix to start setting. The STIC was controlled with the PID + feed forward algorithm with a constant  $ff = 0.015$ . Table 6.2-1 shows the actual mix mass of each sample in each calorimeter:

Calorimeter	Sample mass (g)
1	2.03
2	2.03
3	2.04
4	2.06

**Table 6.2-1** Mass of each sample.

### 6.3 Results and discussion

Figure 6.3-1 shows the thermal power of the four samples (the calorimeter measures a voltage (mV) which is proportional to the thermal power (W) as explained in section 1.1) as a function of time. Generally the higher the temperature of the sample is, the higher the thermal power of the sample and the faster the hydration happens. This can be seen in Figure 6.3-1, except for that the two samples at the two higher temperatures give rather similar results (possibly this is caused by that the reaction mechanism actually changes at the higher temperatures. Figure 6.3-2 shows the heat in millijoules in each sample as a function of time. This heat is the heat produced in the sample, and is calculated as:

$$Q(t) = \int_0^t P dt$$

here:

$P$ : thermal power of the sample (W).

$Q$ : heat produced in the sample (J).

$t$ : time (s).

The total heat transferred in each sample is approximately the same at the end of the experiment when the reaction has come to an end, but the rate at which the heat is produced (the thermal power) is different at different temperature, as is seen in Figure 6.3-1.

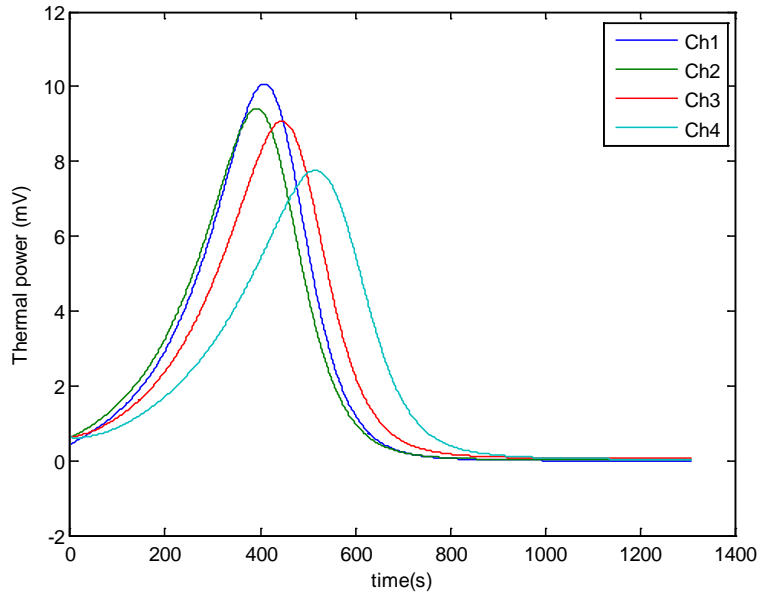


**Figure 6.3-1** Thermal power as function of time at 32.4, 27.0, 21.4 and 15.9 °C (Ch1-4).

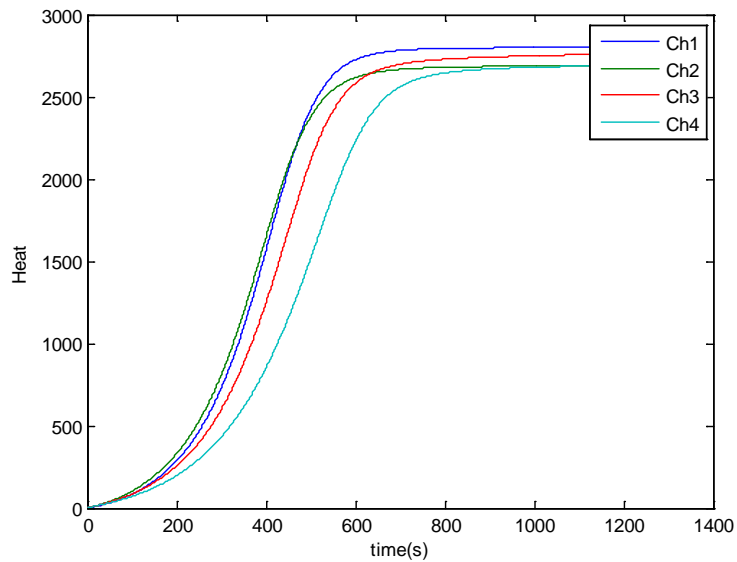


**Figure 6.3-2** Heat (mJ) as function of time (the integrals of the signals in Figure (6.3-1)).

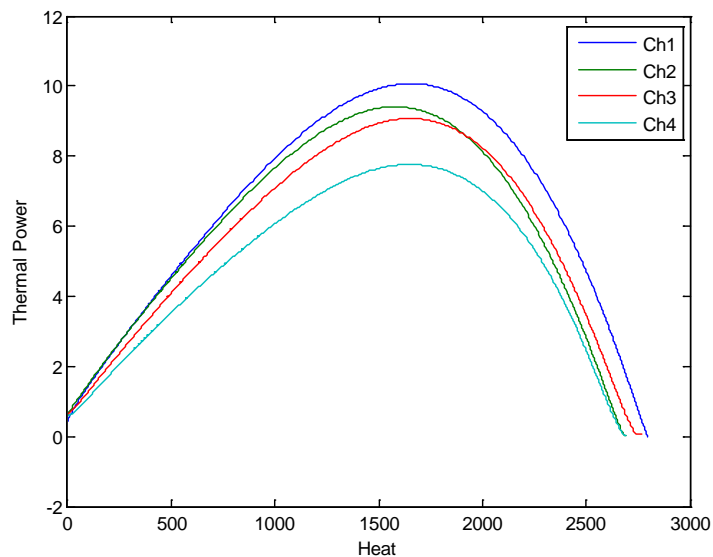


**Figure 6.3-3** Thermal power as function of heat(a combination of Figures 6.3-1 and 6.3-2).

Figure 6.3-3 shows the thermal power as function of heat. This figure is actually the most interesting of the three figures above as it shows how the reaction rate (thermal power) is a function of the extent of reaction (heat). It can be used to calculate for example the activation energy necessary to start the setting process at different temperatures. This is done as follows. The thermal power  $P$  (W) is proportional to the reaction rate  $dm/dt$  (g/s):

$$P = \Delta h \frac{dm}{dt}$$

Here,  $\Delta h$  (J/g) is the enthalpy of the process (the heat produced by the process per gram that has reacted). In a similar way is the heat  $Q$  (J) produced proportional to the mass that has reacted:

$$Q = \Delta h \cdot (m_0 - m_t)$$

Here,  $m_0$  (g) is the initial mass (for example of the calcium sulfate hemihydrates in the described experiment) and  $m_t$  (g) is the mass remaining at time  $t$ . The proportionality constant is the same in this equation as in the previous equation.

In the science of kinetics one is often interested in finding relations between the rate of a process and the remaining amount of material. With a single calorimetric measurement one will measure both these parameters (assuming that one knows the initial mass of the reactant):

$$\frac{dm}{dt} = \frac{P}{\Delta h}$$

$$m_t = m_0 - \frac{Q}{\Delta h}$$

The enthalpy can be calculated from the heat produced when all material has reacted.

The above discussion refers to a calorimetric measurement at one temperature. Often it is of interest to also evaluate how the temperature influences the reaction. This is usually done by using the Arrhenius equation with an activation energy  $E_a$  (J/mol) that quantifies the temperature dependence:

$$\frac{dn}{dt} = A \cdot \exp\left(-\frac{E_a}{RT}\right)$$

Here,  $A$  is a constant,  $R$  is the gas constant (8.314 J/k mol) and  $T$  (K) is the temperature. Using measurements at different temperatures – such as the measurements presented above – it is possible to evaluate  $E_a$  by taking thermal powers at different temperatures, but at the same produced heat (the same extent of reaction).

In conclusion, one run with the STIC calorimeter will generate data that can give both the kinetics of the process and its temperature dependence. In this way the STIC is a complete instrument for generating kinetics data.

## 7. References

1. en.wikipedia.org. *Calorimetry*. Available from: <http://en.wikipedia.org/wiki/Calorimetry>.
2. *Ice calorimeter developed by Lavoisier and Laplace*. 2010; Available from: <http://www.nature.com/scitable/content/ice-calorimeter-developed-by-lavoisier-and-laplace-14898943>.
3. Wadsö, L., *Introduction to Isothermal Calorimetry*: Lund University, Sweden.
4. Instrumentation, S. *The history of Setaram* Available from: <http://www.setaram.com/History.htm>.
5. Çengel, Y.A., *Heat and Mass Transfer, a Practical Approach* 3rd ed 2006: McGraw Hill
6. L Wadsö, Y.S., S Johansson, *Biological applications of a new isothermal calorimeter that simultaneously measures at four temperatures*. J. Thermal Anal. Calorimetry, 2011. **104**: p. 119-126.
7. Technologies, L. *DA-075-24-02-00-00*,. Available from: <http://lairdtech.thomasnet.com/item/thermoelectric-assemblies/rcool-series-direct-to-air-thermoelectric-assembly/da-075-24-02-00-00?>
8. Microsystems, T. *Thermoelectrics Coolers Basics*. Available from: [http://www.tec-microsystems.com/EN/Downloads\\_files/Thermoelectric%20Coolers%20Basics.pdf](http://www.tec-microsystems.com/EN/Downloads_files/Thermoelectric%20Coolers%20Basics.pdf).
9. Abramzon, B., *Numerical Optimization of the Thermoelectric Cooling Devices*. Journal of Electronic Packaging 2007. **129**: p. 339.
10. Igor Bejenari, V.K., *Thermoelectric properties of the bismuth telluride nanowires in the constant-relaxation-time approximation*. 2008.
11. Technologies, L. *Programmable PID Controller*. Available from: <http://lairdtech.thomasnet.com/item/all-categories/temperature-controllers/pn-4324?plpver=10&catid=100&prodid=3001273&origin=keyword>.
12. Electronics, R. *Precision Thermistors (Accu-Curve)*. Available from: <http://www.rtie.com/category-s/93.htm>.
13. ELECTROLUBE. *Non-Silicone Heat Transfer Compound*. 2003; Available from: <http://www.electrolube.com/products/tds/HTC.pdf>.
14. Duckworth, H.E., *Electricity and Magnetism* 1960.
15. en.wikipedia.org. *Resistance thermometer* Available from: [http://en.wikipedia.org/wiki/Resistance\\_thermometer](http://en.wikipedia.org/wiki/Resistance_thermometer).
16. Technology, P. *PT100 Platinum Resistance Thermometers* Available from: <http://www.picotech.com/applications/pt100.html>.
17. en.wikipedia.org. *Thermistor* Available from: <http://en.wikipedia.org/wiki/Thermistor>.
18. en.wikipedia.org. *Steinhart–Hart equation*. Available from: [http://en.wikipedia.org/wiki/Steinhart%E2%80%93Hart\\_equation](http://en.wikipedia.org/wiki/Steinhart%E2%80%93Hart_equation).
19. Technology, L. *TC-NTC-1 Thermistor Specification* Available from: <http://www.lairdtech.com/SearchResults.aspx>.

20. Technology, P. *PT-104 Platinum Resistance Data Logger* Available from: <http://www.picotech.com/pt100.html>.
21. Elfa. *Solid state relay single phase 3...32 VDC, 84134870*. Available from: [https://www.elfa.se/elfa3~eu\\_en/elfa/init.do?item=37-450-23&toc=0](https://www.elfa.se/elfa3~eu_en/elfa/init.do?item=37-450-23&toc=0).
22. Burr-Brown. *Precision Low Power INSTRUMENTATION AMPLIFIERS INA128 & INA129*. 1996; Available from: <http://www.alldatasheet.com/datasheet-pdf/pdf/56687/BURR-BROWN/INA128UA.html>.
23. Bosch. *PHG 600*. Available from: <http://www.bosch-do-it.co.uk/boptocs2-uk/DIY/Tools/GB/en/hw/Hot+Air+Guns/95243/PHG+600-3/7714/3165140288347/index.htm>.
24. Yu-Wei Chang, C.-C.C., Ming-Tsun Ke, Sih-Li Chen, *Thermoelectric air-cooling module for electronic devices*. Applied Thermal Engineering 2009. **29**: p. 2731.
25. Karl Johan Åström, R.M.M., *Feedback Systems, An Introduction for Scientists and Engineers* 2008: Princeton.
26. J.L. Guzmán, T.H., *Simple tuning rules for feedforward compensators*. Journal of Process Control, 2011. **21**: p. 92.
27. en.wikipedia.org. *Plaster*. Available from: [http://en.wikipedia.org/wiki/Plaster#Gypsum\\_plaster\\_.28plaster\\_of\\_Paris.29](http://en.wikipedia.org/wiki/Plaster#Gypsum_plaster_.28plaster_of_Paris.29).
28. A.J.Lewry, J.W., *The setting of gypsum plaster. Part III The effect of additives and impurities*. Journal of Materials Science, 1994. **29**.

## 8. Software

Software used to control and operate the STIC:

- *SC\_Interface 1.1.22* Former software to control the TEC, supplied by the TEC manufacturer.
- *Picolog Recorder*. Software used to record the signals from the eight Pt-100 temperature sensors through the two PT-104 data loggers and the four signals from the calorimeters through the ADC-24 Precision Data Logger.
- *dSPACE ControlDesk*. Platform used to record and visualize the data from the new controller implemented in Simulink and loaded in the dSPACE board.
- *Simulink*. Software used to design and implement the new control algorithm, connected to the STIC through the dSPACE board.

Software used through the project:

- *Matlab 7.5 (R2007a)*.
- *SolidWorks 2011*
- *Microsoft Office Excel 2007*.
- *Microsoft Office Power Point 2007*.



## **9. Annexes**



## 9.1 Material's properties

Material	Density $\rho$ (kg/m <sup>3</sup> )	Thermal conductivity $\lambda$ (W/K·m)	Specific heat capacity $c$ (J/K·kg)	Seebeck coefficient $\alpha$ ( $\mu$ V/K)	Electrical resistivity $\rho$ ( $\Omega \cdot m$ )
Aluminum (Al)	2770	177	875	-	-
Aluminum oxide (Al <sub>2</sub> O <sub>3</sub> )	3900	30	800		
n-doped Bismuth Telluride (Bi <sub>2</sub> Te <sub>3</sub> )	7850	1.5	-	-238	$1.2 \cdot 10^{-5}$
p-doped Bismuth Telluride (Bi <sub>2</sub> Te <sub>3</sub> )	7850	1.5	-	165	$0.53 \cdot 10^{-5}$
Copper (Cu)	8933	401	385	-	-
Electrolube	2040	0.9	-	-	-
Epoxy	1400	0.87	935	-	-
Extruded Polystyrene Foam XPS	30	0.037	1400	-	-
Glass	-	-	750	-	-
Rubber	-	-	2010	-	-
Silicon (Si)	2330	148	700	-	-
Water (H <sub>2</sub> O)			4200		

\*In the table only appear the values used during the current project

\*\*[5, 10, 13]



## 9.2 Simulation model

### Main program:

```

%Simulation model of STIC
%
%   A is area (m2)
%   C is heat capacity of part of instrument (J/K)
%   cv is volumetric heat capacity (J/m3K)
%   k is the thermal conductance between two parts of the
instrument (W/K)
%   L is length(m)
%   q is heat flow (W)
%   t is time (s)
%   T is temperature (oC)
%   V is volume (m3)
%   lambda is thermal conductivity (W/Km)
%
%The external temperature is T0
%
%The instrument is modelled as consisting of the following parts:
%   A   Ambient in the TEC side
%   F   External part of the finned part of the TEC
%   B   Part of the finned part of the TEC in contact with the hot
side of the
%   thermocouple
%   H   Hot side of the thermocouple TEC
%   C   Cold side of the thermocouple TEC
%   D   Aluminum plate in contact with the cold side of the
thermocouples
%   E   Copper plate between D and G
%   G   Aluminum plate in contact with the tube of the calorimeter
%   V   Heated plate(s) at warm side
%   W   Heated side external
%   O   Ambient in the eated side
%   S   TEC thermistor
%   1HS, 1A, 1B      Calorimeter 1
%   2HS, 2A, 2B      Calorimeter 2
%   3HS, 3A, 3B      Calorimeter 3
%   4HS, 4A, 4B      Calorimeter 4
%   1-31      2 mm slices of rectangular tube
%   32        2 mm slice to which calorimeter 4 is attached
%   33-68     2 mm slices of rectangular tube
%   69        2 mm slice to which calorimeter 3 is attached
%   70-105    2 mm slices of rectangular tube
%   106       2 mm slice to which calorimeter 2 is attached
%   107-142   2 mm slices of rectangular tube
%   143       2 mm slice to which calorimeter 1 is attached
%   144-174   2 mm slices of rectangular tube
%
%The heat loss from A is modelled by  $q_{A0}=k_{A0}*(T_A-T_0)$  where  $k_A$ 
(W/K) is a
%convective heat transfer coefficient
%
%Lars Wadsö 23 feb 2012

%% Clear all
ok=input('clear will be executed (ctrl^c to exit before this is
done)');
clear all

```

## Temperature Control of a Scientific Instrument

---

```
close all
tpause=1000; %only used for testing

%% Material properties
cv_Al=2.42e6; %volumetric heat capacity of Aluminum
lambda_Al=177;%thermal condcutivity of Aluminum
lambda_Cu=401;%thermal condcutivity of Copper

%% Geometry etc
    %% Tube slices
    A=2*(135e-3*2e-3+110e-3*5e-3);%Cross area od the aluminum in
the gradient tube
    L=2e-3;%Length of each slide
    V=L*A;%Volume of each slide

%% Heat capacities
CF=2088.303;%Heat capacity of node F
CB=552.615;%Heat capacity of node B
CH=21.88;%Heat capacity of node H
CC=21.88;%Heat capacity of node C
CD=159.967;%Heat capacity of node D
CE=613.94;%Heat capacity of node E
CG=666.53;%Heat capacity of node G
Cslice=cv_Al*V;%Heat capacity of each slice
C=ones(1,174)*Cslice;
C4HS=95.1;C3HS=95.1;C2HS=95.1;C1HS=95.1;%Heat capacity of each
heat sink
C4A=11.85;C3A=11.85;C2A=11.85;C1A=11.85;%Heat capacity of each
sample
C4B=7.69;C3B=7.69;C2B=7.69;C1B=7.69;%Heat capacity of node of each
reference
CS=0.57; %Heat capacity of the TEC sensor
CV=1333.06;%Heat capacity of node H
CW=97.02;%Heat capacity of node W

%% Temperatures (initial)
Ti=23;
TA=Ti;TF=Ti;TB=Ti;TH=Ti;
TC=Ti;TD=Ti;TE=Ti;TG=Ti;
T(1:174)=Ti;
TV=Ti;TW=Ti;TO=Ti;
TS=Ti;
T4HS=Ti;T4A=Ti;T4B=Ti;
T3HS=Ti;T3A=Ti;T3B=Ti;
T2HS=Ti;T2A=Ti;T2B=Ti;
T1HS=Ti;T1A=Ti;T1B=Ti;

%% Thermoelectric Module properties
[alpha,r,kHC]=prop_BiTe();%Bismuth telluride properties
I=24/(2*r);%Intensity trough each branch of the TEC

%% Thermal conductances
[Rcsp,Rhsp,Rcons,Rconv,Rb]=chang_eq(alpha,kHC,I);
%Rcsp: spreading resistance between D and C
%Rhsp: spreading resistance between H and B
%Rcons: Constrict resistance between H and B
%Rconv: Convective resistance between A and F
%RB: conduction resistance between B and F
RDE=2.5641e-4;%Thermal resistance between D and E
REG=4.2222e-3;%Thermal resistance between E and G
kslice=lambda_Al*A/L;%Thermal Conductance of each slice
```

```

k=[kslice*2 ones(1,173)*kslice kslice*2];
kCu=lambda_Cu*2e-3*50e-3/30e-3;%Thermal conductance of the copper
connections
k4H32=kCu;k3H69=kCu;k2H106=kCu;k1H143=kCu;
kTCP=1.5*1e-3*1e-3/1.7e-3*31*2*1.3; %1.3 is approx other heat
flows
k4HS4A=kTCP;k3HS3A=kTCP;k2HS2A=kTCP;k1HS1A=kTCP;%Thermal
conductance between heat sink and sample
k4HS4B=kTCP;k3HS3B=kTCP;k2HS2B=kTCP;k1HS1B=kTCP;%Thermal
conductance between heat sink and reference
kDS=.02; %Thermal conductance between D and S
kVW=0.034;%Thermal conductance between V and W
kWO=15*(.215^2);%Convective Conductance between W and O

%% Simulation parameters
t=0;%Initial time
dt=0.01;%Time step
tend=15000;%Final time
toutinterval=1;
tnextout=dt;
nout=0;
n=0;
N=floor(tend/toutinterval); %number of outputs
tout=zeros(N,1); %output time
Uout=zeros(N,4); %signals from the four calorimeters
Tout=zeros(N,10); %temperatures of the eight sensors
qout=zeros(N,4); %PID output

%% Simulation
while t<tend
    t=t+dt;
    n=n+1;
    %% Ambient temperature
    if (t>5000)&&(t<5060) %perturbation legth
        TA=26; %perturbation amplitude
    else
        TA=23;
    end

    %% Calculate heat flows
    f=PID_TEC(TS,TA,dt); %TEC duty cycle, with feed forward
    qC=2*(2*alpha*I*f*(TC+273.15)-0.5*(I*f)^2*(2*r))-kHC*(TH-
TC);%TEC cooling power
    We=2*(2*alpha*I*f*(TH-TC)+(I*f)^2*(2*r));%Electric power
    applied to the TEC
    qH=qC+We;%Heat in the TEC hot side
    qF_A=(TF-TA)/Rconv;%Heat flow between F and A
    qB_F=(TB-TF)/Rb;%Heat flow between B and F
    qH_B=(TH-TB)/(-Rcons+Rhsp);%Heat flow between H and B
    qD_C=(TD-TC)/Rcsp;%Heat flow between D and C
    qE_D=(TE-TD)/RDE;%Heat flow between E and D
    qG_E=(TG-TE)/REG;%Heat flow between G and E
    q=k.*([TG T]-[T TV]);%Heat flow between each slice
    q4H32=k4H32*(T(32)-T4HS);q4H4B=k4HS4B*(T4HS-
T4B);q4H4A=k4HS4A*(T4HS-T4A);%Heat flow between copper conductance
    q3H69=k3H69*(T(69)-T3HS);q3H3B=k3HS3B*(T3HS-
T3B);q3H3A=k3HS3A*(T3HS-T3A);%and heat sink, heat sink and sample
    q2H106=k2H106*(T(106)-T2HS);q2H2B=k2HS2B*(T2HS-
T2B);q2H2A=k2HS2A*(T2HS-T2A);%and heat sink and reference.
    q1H143=k1H143*(T(143)-T1HS);q1H1B=k1HS1B*(T1HS-
T1B);q1H1A=k1HS1A*(T1HS-T1A);%

```

```

qV=(PID_heater(TV,dt)*48)^2/57;%Heat power in the Heater;
qV_W=kVW*(TV-TW);%Heat flow between V and W
qD_S=kDS*(TD-TS);%Heat flow between D and S
qF_O=kWO*(TW-TO);%Heat flow between W and O

%% Calculate new temperatures
TF=TF+(-qF_A+qB_F)/CF*dt;%New temperature in F
TB=TB+(-qB_F+qH_B)/CB*dt;%New temperature in B
TH=TH+(qH-qH_B)/CH*dt;%New temperature in H
TC=TC+(-qC+qD_C)/CC*dt;%New temperature in C
TD=TD+(-qD_C+qE_D-qD_S)/CD*dt;%New temperature in D
TE=TE+(-qE_D+qG_E)/CE*dt;%New temperature in E
TG=TG+(-qG_E-q(1))/CG*dt;%New temperature in G
T=T+(q(1:end-1)-q(2:end))./C*dt;%New temperature in each slice
T(32)=T(32)-q4H32/C4HS*dt;%New temperature in node 32 (Cal4)
T(69)=T(69)-q3H69/C3HS*dt;%New temperature in node 69 (Cal3)
T(106)=T(106)-q2H106/C2HS*dt;%New temperature in node 106
(Cal2)
T(143)=T(143)-q1H143/C1HS*dt;%New temperature in node 169
(Cal1)
T4HS=T4HS+(q4H32-q4H4A-
q4H4B)/C4HS*dt;T4B=T4B+q4H4B/C4B*dt;T4A=T4A+q4H4A/C4A*dt;%Temperat
ures in each heat
T3HS=T3HS+(q3H69-q3H3A-
q3H3B)/C3HS*dt;T3B=T3B+q3H3B/C3B*dt;T3A=T3A+q3H3A/C3A*dt;%sink,
samples and
T2HS=T2HS+(q2H106-q2H2A-
q2H2B)/C2HS*dt;T2B=T2B+q2H2B/C2B*dt;T2A=T2A+q2H2A/C2A*dt;%referenc
es
T1HS=T1HS+(q1H143-q1H1A-
q1H1B)/C1HS*dt;T1B=T1B+q1H1B/C1B*dt;T1A=T1A+q1H1A/C1A*dt;
TV=TV+(q(end)+qV-qV_W)/CV*dt;%New temperature in V
TW=TW+(qV_W-qF_O)/CW*dt;%New temperature in W
TS=TS+qD_S/CS*dt;%New temperature in S

%% Output
if tnextout>toutinterval
    nout=nout+1;
    tnextout=dt;
    tout(nout)=t;%Time output vector
    Uout(nout,1:4)=[T1A-T1B T2A-T2B T3A-T3B T4A-T4B];%Output
calorimeters signals
    Tout(nout,1:8)=[T(143) T(106) T(69) T(32) TA TD TO
TV];%Output temperatures
else
    tnextout=tnextout+dt;
end
end

%% Output
figure(1);clf
plot(tout,Uout);%Calorimeter sognals figure
xlabel('Time (s)');
ylabel('Output voltage (au)');
legend('Ch1','Ch2','Ch3','Ch4');

figure(2);clf
plot(tout,Tout(:,1:8));%Temperatures figure
xlabel('Time (s)');
ylabel('Temperature ( ^oC)');

```

```
legend('Tch1','Tch2','Tch3','Tch4','Totec','Ttec','To','Th');
```

## Functions

```
function [alpha,r,K]=prop_BiTe()
n=4;%number of modules
N=161;%num of thermocouples
k=1.5;%thermal conductivity (W/mK)
alpha_n=-238e-6;%Seebeck coef of n-doped BiTe (V/K)
alpha_p=165e-6;%Seebeck coef of p-doped BiTe (V/K)
ro_n=1.2e-5;%Electrical conductivity of n-doped BiTe(ohms*m)
ro_p=0.53e-5;%Electrical conductivity of p-doped BiTe(ohms*m)
A=(0.0012)^2;%Area of the pellets (m2)
L=0.0014;%Lenght of the pellets (m)
```

```
alpha=N*(alpha_p+abs(alpha_n));
r=N*L*(ro_p+ro_n)/A;
K=n*2*N*A*k/L;
```

```
function [Rcsp,Rbsp,Rcons,Rconv,Rb]=chang_eq(alpha,k,I)
%Aluminum Plate (heater)
DE=[110e-3 30e-3];%Dimensions of the heat source (m)
E=[80e-3 20e-3];%Dimensions of the heat source (m)
kc=35.3;%Thermal conductivity of the ceramic plates (W/Km)
```

```
%TEMs
L=[160e-3 40e-3];%Dimensions of the TEMs (m)
tc=1e-3;%Width of the ceramic plates (m)
l=1.4e-3;%High of the Bismuth Teluride pins (m)
Atec=L(1)*L(2);%Area of the TEMs (m2)
```

```
%Heat sink
Ab=0.152*0.3;%Area of the heat sink (m2)
tb=0.01;%Heat sink with (m)
kb=177;%Thermal conductivity of the aluminum (W/Km)
Nf=48;%Number of fins in the heat sink
h=100;%Convection coefficient with the ambient air (W/Km2)
Lf=0.3;%Lenght of the heat sink (m)
H=0.022;%Lenght of the fins (m)
tf=0.002;%Width of the fins (m)
b=0.0012;%Separation between fins (m)
```

```
%Fin calculations
ef=tanh(H*sqrt(2*h/(kb*tf)))/(H*sqrt(2*h/(kb*tf)));%Fin
efficiency.
Rconv=1/(h*Nf*2*Lf*H*ef+h*(Nf-1)*b*Lf);%Convective resistance
between A-F
Rb=tb/(kb*Ab);%conduction resistance between B-F
```

```
%intermediate calculations
nf=2;
for n=1:1:nf
B(n)=((alpha*I+k)/(tc*kc))*L(n).^2;
Eb(n)=E(n)/L(n);
DEb(n)=DE(n)/L(n);
end
```

```
for n=1:1:2
```

```

p(n)=(L(n)/L(n+(-1)^(n-1)))*sqrt(B(n+(-1)^(n-1))*(1.5-
((sinh(2*sqrt(B(n+...
(-1)^(n-1))))/(2*sqrt(B(n+(-1)^(n-1))))+1))^(n-1));
K(n)=2*sinh(p(n)*DEb(n))*cosh(p(n)*(1-Eb(n)))/sinh(p(n));
fimax(n)=K(n)*cosh(p(n)*Eb(n))-cosh(p(n)*DEb(n))+1;
fib(n)=(K(n)/p(n))*sinh(p(n))-(2/(p(n))*cos(p(n)*(1-Eb(n)))...
*sinh(p(n)*DEb(n)));
end

lambda=pi^(3/2)/sqrt(Ab)+1/sqrt(Atec);

%results
Rcsp=(fimax(1)*fimax(2)-
fib(1)*fib(2))*L(1)*L(2)/(4*DE(1)*DE(2))*...
(alpha*I+k);%Rcsp: spreading resistance between D and C
Rbsp=((sqrt(Ab)-
sqrt(Atec))/(kb*sqrt(pi*Ab*Atec)))*((lambda*kb*Rconv*Ab+...
tanh(lambda*tb))/(1+lambda*kb*Ab*Rconv*tanh(lambda*tb)));
%Rhsp: spreading resistance between H and B
Rcons=(inv(2*kb*sqrt(Atec))*(1-sqrt(Atec/Ab))^(3/2)-((sqrt(Ab)-...
sqrt(Atec))/(kb*sqrt(pi*Ab*Atec)))*(lambda*kb*Ab*Rconv+...
tanh(lambda*tb))/(1+lambda*kb*Ab*Rconv*tanh(lambda*tb)));
%Rcons: Constrict resistance between H and B

function P=PID_heater(T,dt)
persistent Eint Eold
if nargin==1
    Eint=0;
end
param=[40 5 0.005 0];%[Tset kP kI kD]
s=size(param);
if isempty(Eint)||length(Eint)~=s(1);Eint=zeros(s(1),1);end
if isempty(Eold)||length(Eold)~=s(1);Eold=zeros(s(1),1);end
Tset=param(1);%Reference temperature
kP=param(2);%Proportional constant
kI=param(3);%Integral constant
kD=param(4);%Derivative constant
E=Tset-T;%Error
P1=kP*E;%Proportional term
Eint=Eint+E*dt*kI;%Integral term
P2=Eint;%Integral term update
if abs(P2)>1
    P2=sign(P2)*1;%Integral anti-windup
end
P3=kD*(E-Eold)/dt;%Derivative term
Eold=E;%Derivative term update
P=P1+P2+P3;%PID output
if P>1%Output saturation between 0 and 1
    P=1;
elseif P<0
    P=0;
else
    P=P;
end
end

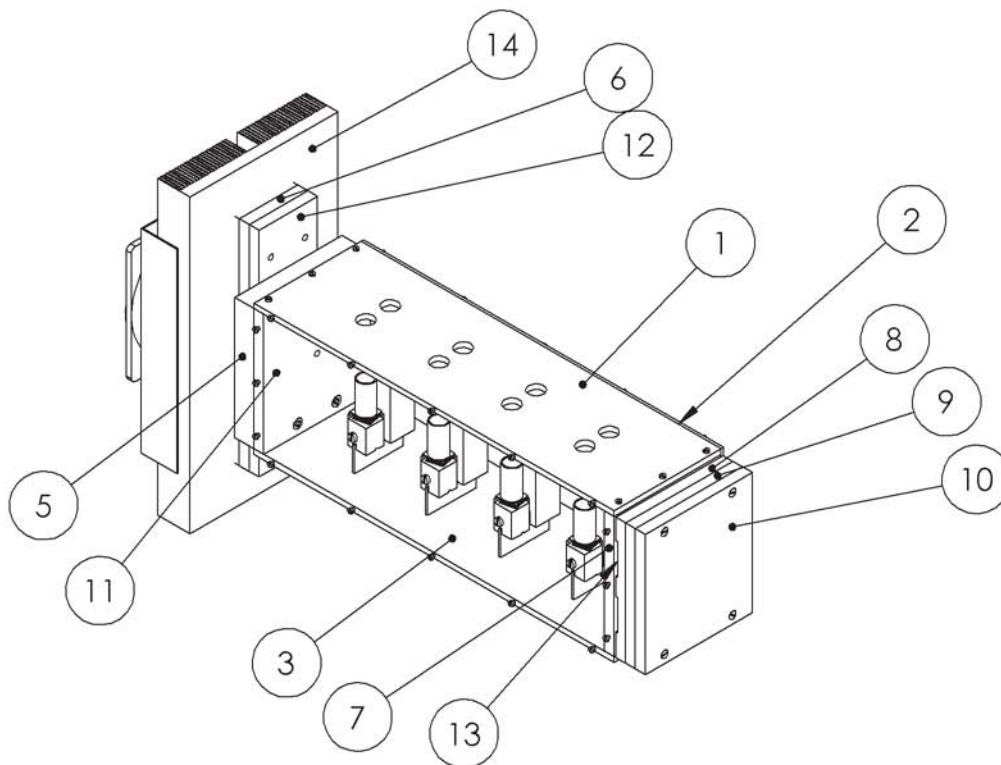
function P=PID_TEC(T,To,dt)
persistent Eint Eold
if nargin==1

```

```
Eint=0;
end
param=[10 5 0.005 0 0.05];%[Tset kP kI kD ff]
s=size(param);
if isempty(Eint)||length(Eint)~=s(1);Eint=zeros(s(1),1);end
if isempty(Eold)||length(Eold)~=s(1);Eold=zeros(s(1),1);end
Tset=param(1);%Reference temperature
kP=param(2);%Proportional constant
kI=param(3);%Integral constant
kD=param(4);%Derivative constant
ff=param(5);%Feed forward constant
E=Tset-T;%Error
P1=kP*E;%Proportional term
Eint=Eint+E*dt*kI;%Integral term
P2=Eint;%Integral term update
if abs(P2)>1
    P2=sign(P2)*1;%Integral anti-windup
end
P3=kD*(E-Eold)/dt;%Derivative term
Eold=E;%Derivative term update
P=P1+P2+P3;%PID output
P=-P;
Pf=ff*(To-23);%Feed forward term
P=P+Pf;%Total duty cycle output
if P>1%Output saturation between 0 and 1
    P=1;
elseif P<0
    P=0;
else
    P=P;
end
end
end
```



### **9.3 STIC drawings**



Number	Name	Quantity	Num Drawing
1	Cover	1	2
2	Lateral	2	3
3	Base	1	4
4	Calorimeter	4	5
5	Aluminum plate 1	1	12
6	Aluminum plate 2	1	13
7	Aluminum plate 3	1	14
8	Aluminum plate 4	1	15
9	Aluminum plate 5	1	16
10	Aluminum plate 6	1	17
11	Copper plate 1	1	18
12	Copper plate 2	1	19
13	Heater	1	20
14	TEC	1	21

**Licencia educacional de SolidWorks**  
**Sólo para uso académico**



**LUNDS UNIVERSITET**  
 Lunds Tekniska Högskola

MATERIAL:

NUMBER OF PIECES: 1

AUTHOR: ALBERT PLA RUIZ

DATE: May 2012

PROJECT: Temperature Control of a Scientific Instrument

TITLE:

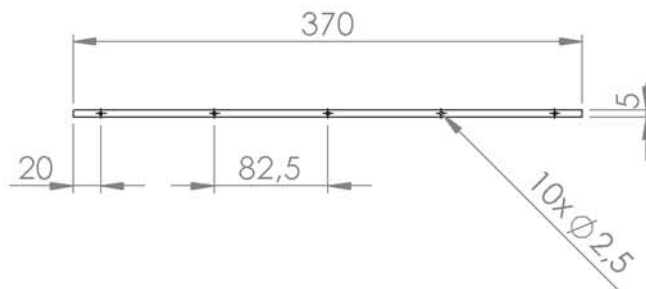
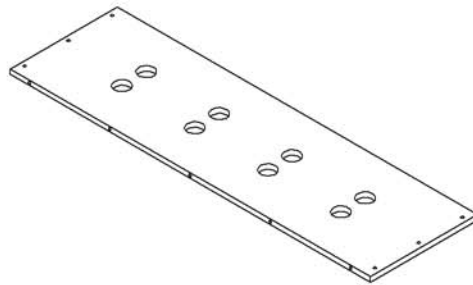
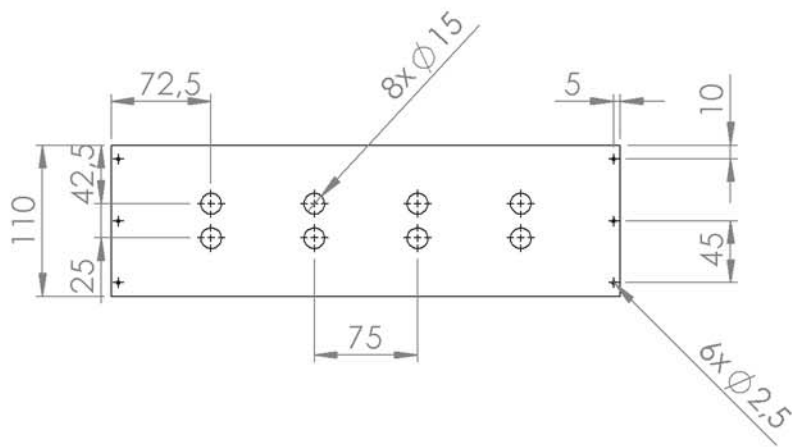
**STIC without insulation**

NUMBER OF DRAWING:

**1/36**

A4

SCALE 1:5



**Licencia educacional de SolidWorks**  
**Sólo para uso académico**

\*All distances in mm



**LUNDS UNIVERSITET**  
 Lunds Tekniska Högskola

MATERIAL: Aluminum

NUMBER OF PIECES: 1

AUTHOR: ALBERT PLA RUIZ

DATE: May 2012

PROJECT: Temperature Control of a Scientific Instrument

TITLE:

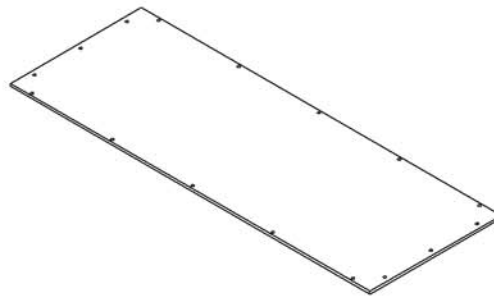
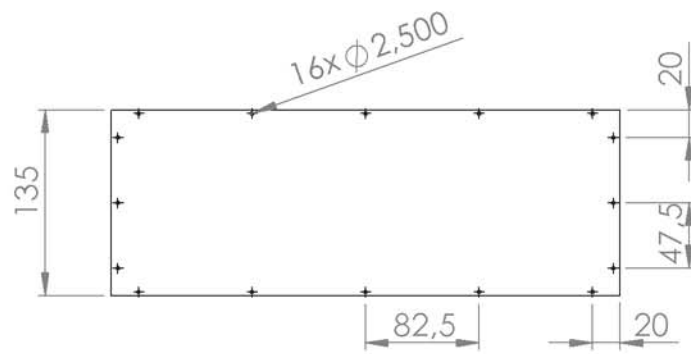
**Cover**

NUMBER OF DRAWING:

**2/36**

A4

SCALE 1:5



**Licencia educacional de SolidWorks**  
**Sólo para uso académico**

*\*All distances in mm*



**LUNDS UNIVERSITET**  
 Lunds Tekniska Högskola

MATERIAL: Aluminum

NUMBER OF PIECES: 2

AUTHOR: ALBERT PLA RUIZ

DATE: May 2012

PROJECT: Temperature Control of a Scientific Instrument

TITLE:

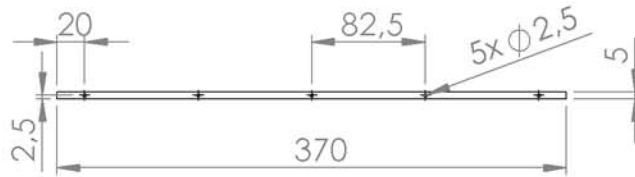
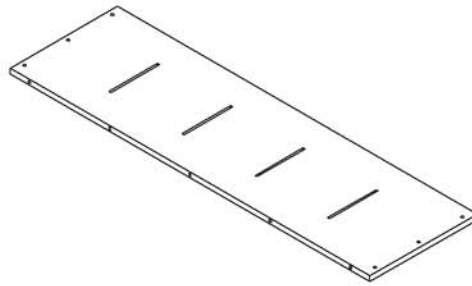
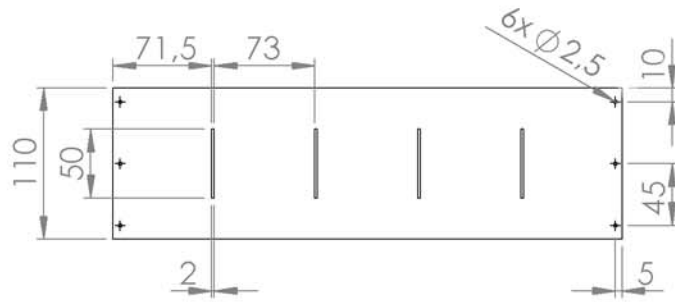
**Lateral**

NUMBER OF DRAWING:

**3/36**

A4

SCALE 1:5



**Licencia educacional de SolidWorks**  
**Sólo para uso académico**

*\*All distances in mm*

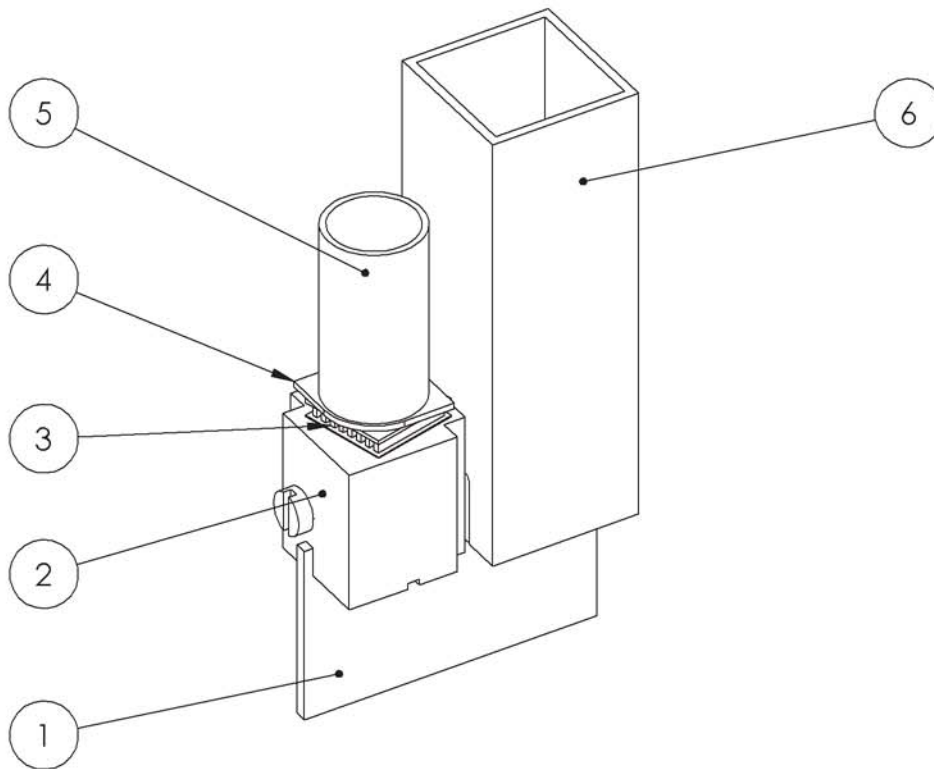


**LUNDS UNIVERSITET**  
 Lunds Tekniska Högskola

MATERIAL: Aluminum

NUMBER OF PIECES: 1

AUTHOR: ALBERT PLA RUIZ	DATE: May 2012
PROJECT: Temperature Control of a Scientific Instrument	
TITLE: <b>Base</b>	
NUMBER OF DRAWING: <b>4/36</b>	A4
	SCALE 1:5



Number	Name	Quantity	Num Drawing
1	Copper conductor	4	6
2	Heat sink	8	7
3	Heat flow sensor	8	8
4	Ampoule holder support	8	9
5	Ampoule holder	8	10
6	Square holder	8	11

**Licencia educacional de SolidWorks**  
**Sólo para uso académico**



**LUNDS UNIVERSITET**  
 Lunds Tekniska Högskola

MATERIAL:

NUMBER OF PIECES: 4

AUTHOR: ALBERT PLA RUIZ

DATE: May 2012

PROJECT: Temperature Control of a Scientific Instrument

TITLE:

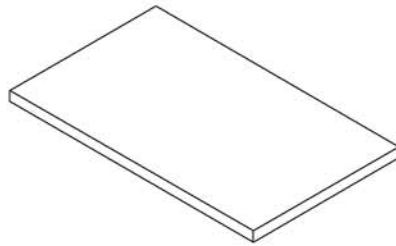
**Calorimeter**

NUMBER OF DRAWING:

**5/36**

**A4**

SCALE 1:1



**Licencia educacional de SolidWorks**  
**Sólo para uso académico**

*\*All distances in mm*

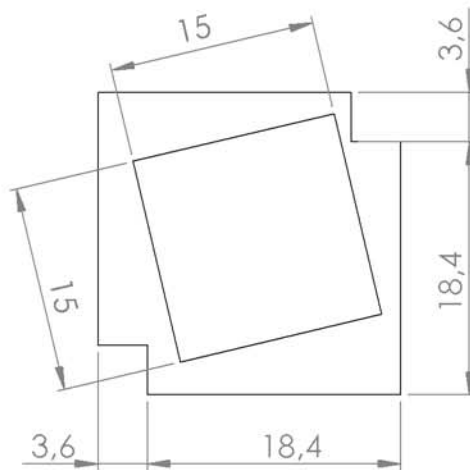
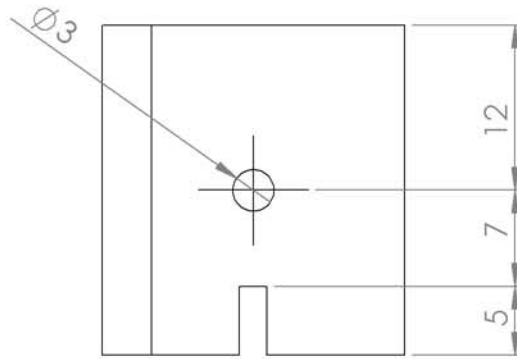
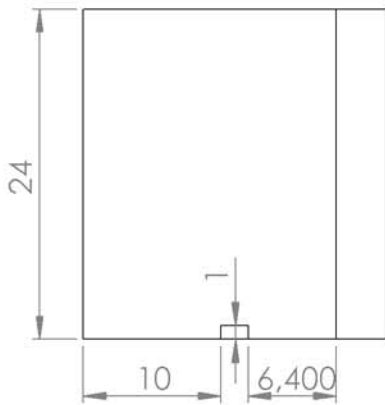
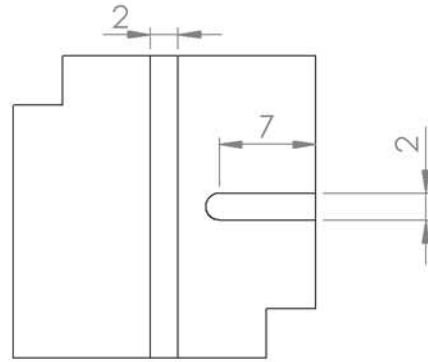
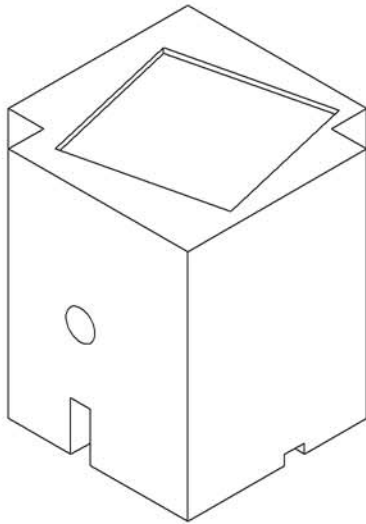


**LUNDS UNIVERSITET**  
 Lunds Tekniska Högskola

MATERIAL: Copper

NUMBER OF PIECES: 4

AUTHOR: ALBERT PLA RUIZ	DATE: May 2012
PROJECT: Temperature Control of a Scientific Instrument	
TITLE: <b>Copper conductor</b>	
NUMBER OF DRAWING:	6/36
	A4
	SCALE 1:1



**Licencia educacional de SolidWorks**  
**Sólo para uso académico**

\*All distances in mm



**LUNDS UNIVERSITET**  
 Lunds Tekniska Högskola

MATERIAL: Aluminum

NUMBER OF PIECES: 8

AUTHOR: ALBERT PLA RUIZ

DATE: May 2012

PROJECT: Temperature Control of a Scientific Instrument

TITLE:

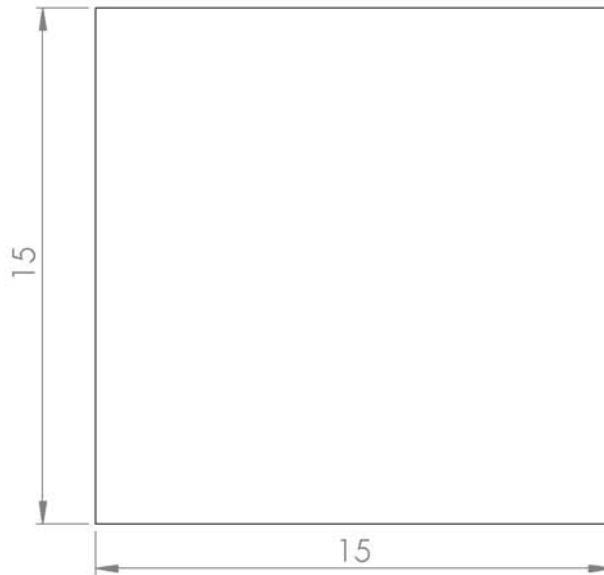
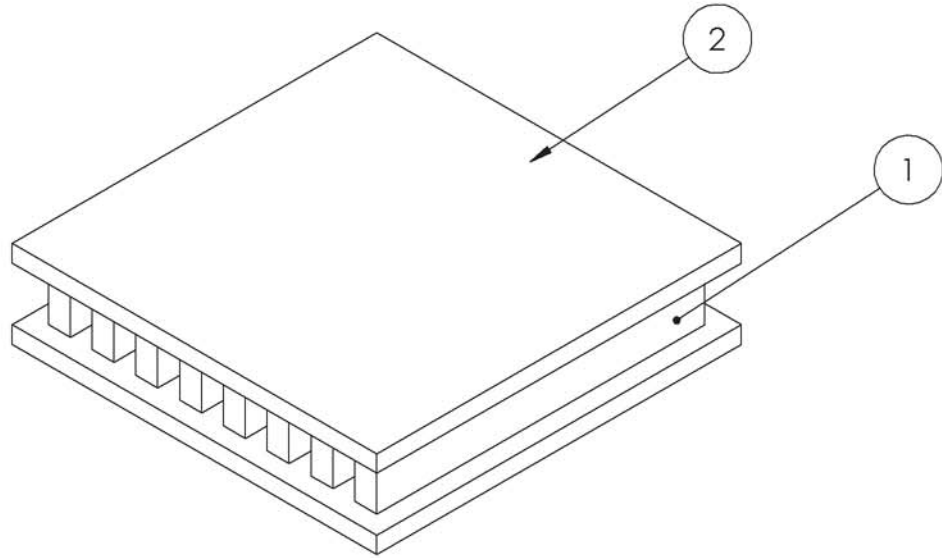
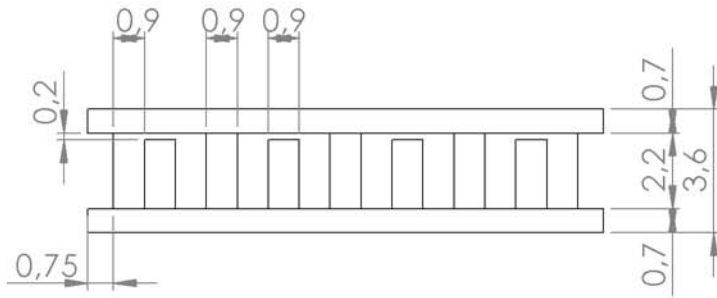
**Heat Sink**

NUMBER OF DRAWING:

**7/36**

A4

SCALE 2:1



Licencia educacional de SolidWorks  
Sólo para uso académico

\*All distances in mm

AUTHOR: ALBERT PLA RUIZ

DATE: May 2012

PROJECT: Temperature Control of a Scientific Instrument

TITLE:

Heat Flow Sensor



LUNDS UNIVERSITET  
Lunds Tekniska Högskola

MATERIAL: 1 - Bismuth telluride  
2 - Aluminum oxide

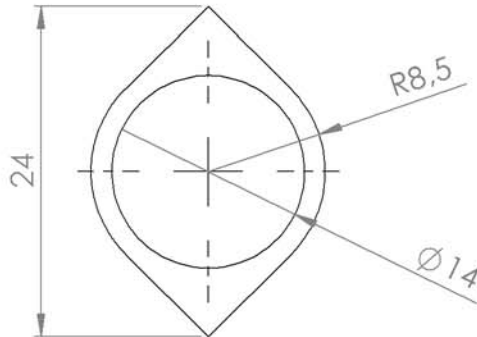
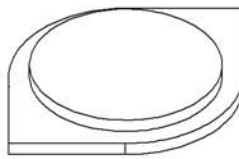
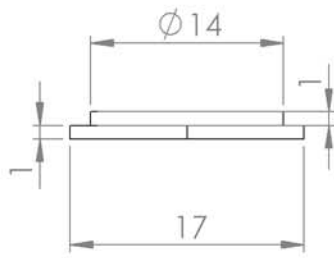
NUMBER OF PIECES: 8

NUMBER OF DRAWING:

8/36

A4

SCALE 5:1



**Licencia educacional de SolidWorks**  
**Sólo para uso académico**

*\*All distances in mm*



**LUNDS UNIVERSITET**  
 Lunds Tekniska Högskola

MATERIAL: Aluminum

NUMBER OF PIECES: 8

AUTHOR: ALBERT PLA RUIZ

DATE: May 2012

PROJECT: Temperature Control of a Scientific Instrument

TITLE:

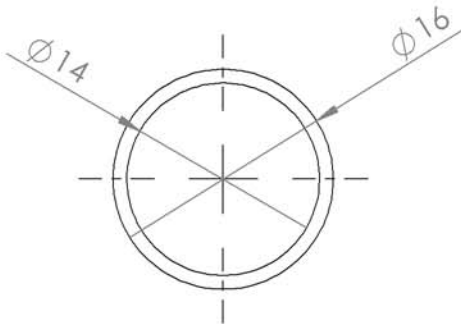
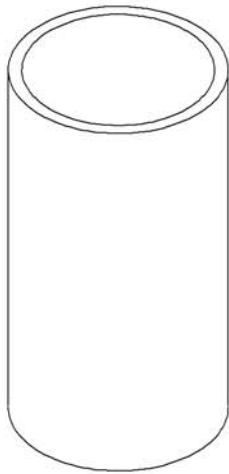
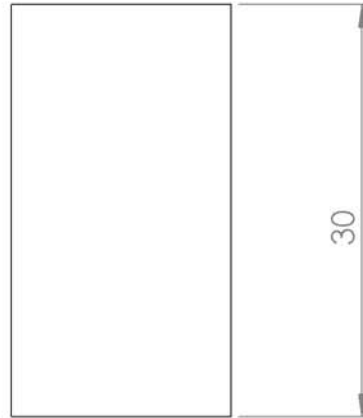
**Ampoule Holder Support**

NUMBER OF DRAWING:

**9/36**

A4

SCALE 2:1



**Licencia educacional de SolidWorks**  
**Sólo para uso académico**



**LUNDS UNIVERSITET**  
 Lunds Tekniska Högskola

MATERIAL: Aluminum

NUMBER OF PIECES: 8

*\*All distances in mm*

AUTHOR: ALBERT PLA RUIZ

DATE: May 2012

PROJECT: Temperature Control of a Scientific Instrument

TITLE:

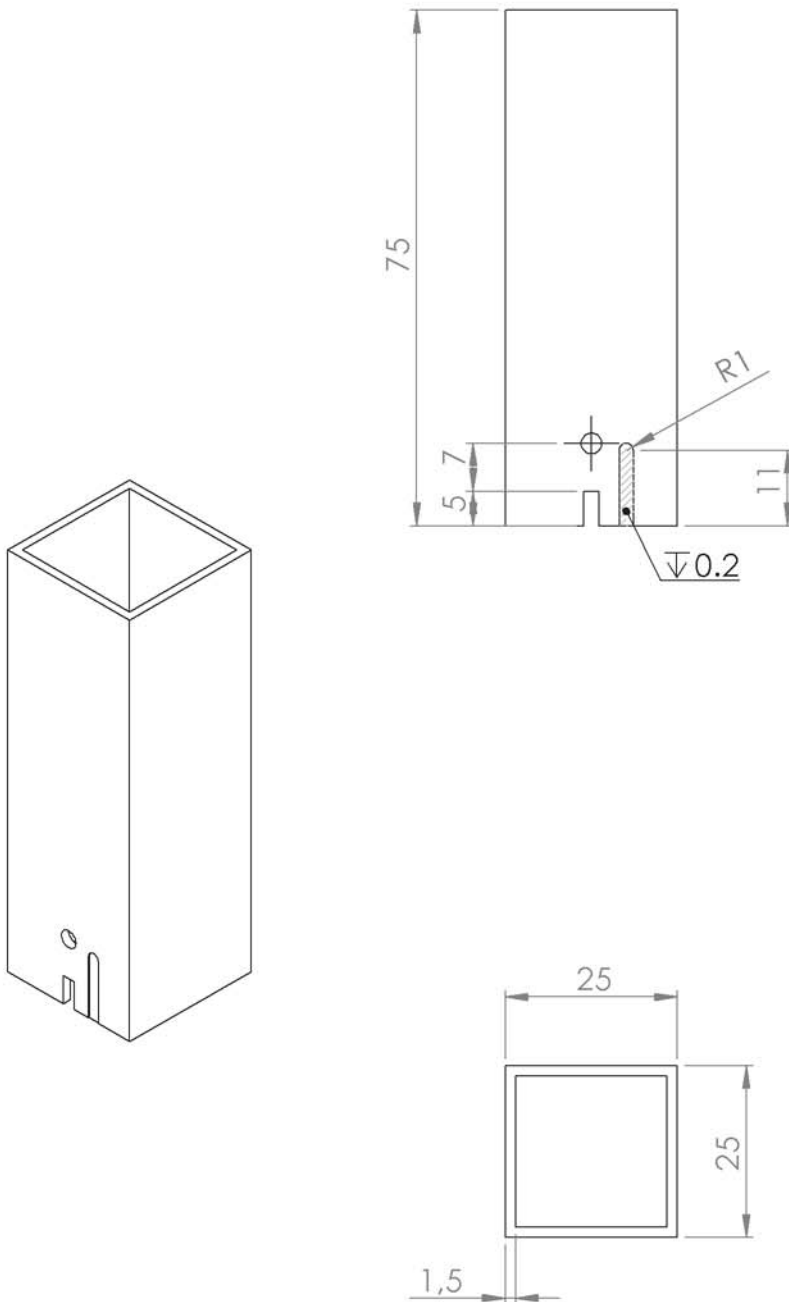
**Ampoule Holder**

NUMBER OF DRAWING:

**10/36**

A4

SCALE 2:1



**Licencia educacional de SolidWorks**  
**Sólo para uso académico**

*\*All distances in mm*



**LUNDS UNIVERSITET**  
 Lunds Tekniska Högskola

MATERIAL: Aluminum

NUMBER OF PIECES: 8

AUTHOR: ALBERT PLA RUIZ

DATE: May 2012

PROJECT: Temperature Control of a Scientific Instrument

TITLE:

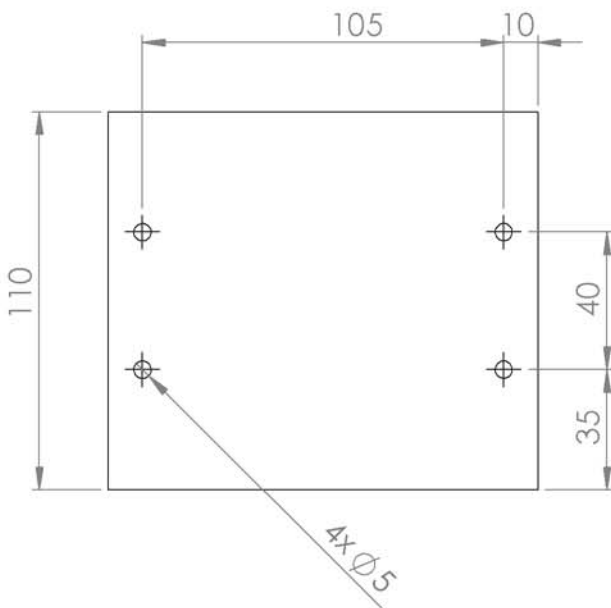
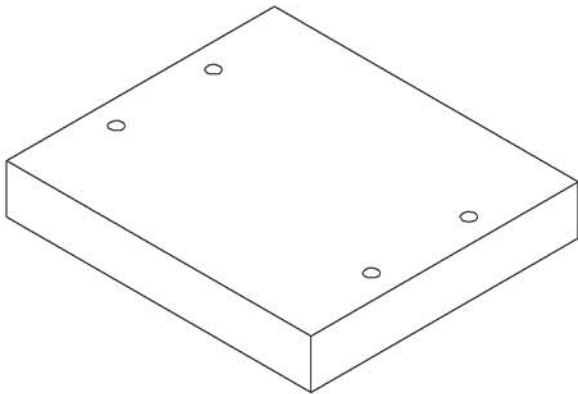
**Square Holder**

NUMBER OF DRAWING:

11/36

A4

SCALE 1:1



**Licencia educacional de SolidWorks**  
**Sólo para uso académico**

*\*All distances in mm*

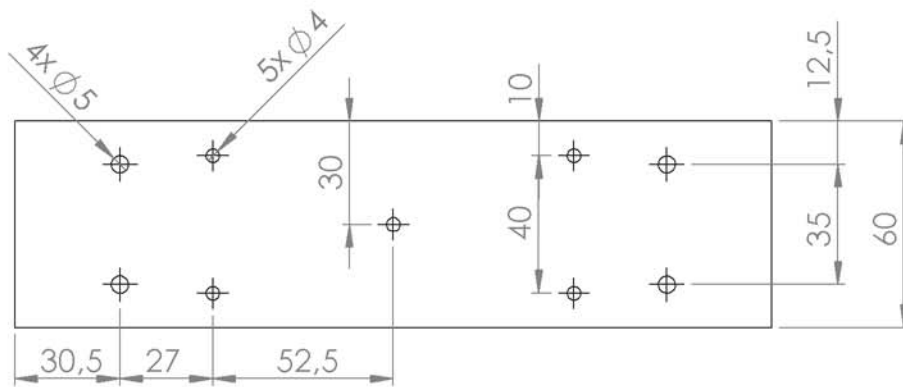
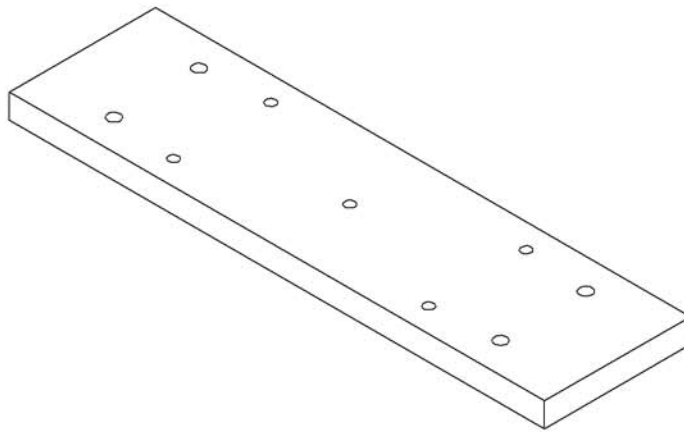


**LUNDS UNIVERSITET**  
 Lunds Tekniska Högskola

MATERIAL: Aluminum

NUMBER OF PIECES: 1

AUTHOR: ALBERT PLA RUIZ	DATE: May 2012
PROJECT: Temperature Control of a Scientific Instrument	
TITLE: <b>Aluminum Plate 1</b>	
NUMBER OF DRAWING:	12/36
	A4
	SCALE 1:2



**Licencia educacional de SolidWorks**  
**Sólo para uso académico**

\*All distances in mm



**LUNDS UNIVERSITET**  
 Lunds Tekniska Högskola

MATERIAL: Aluminum

NUMBER OF PIECES: 1

AUTHOR: ALBERT PLA RUIZ

DATE: May 2012

PROJECT: Temperature Control of a Scientific Instrument

TITLE:

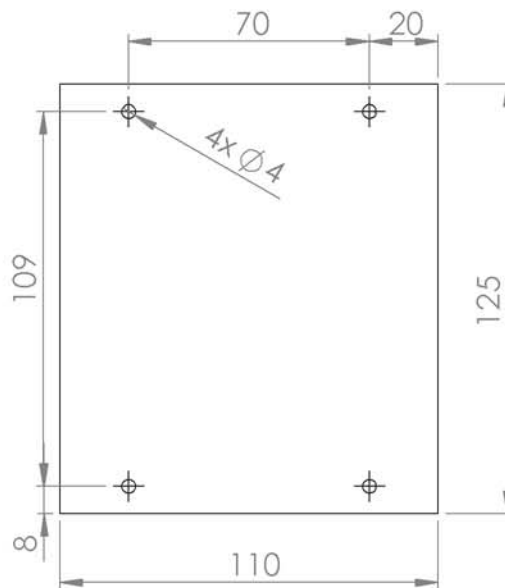
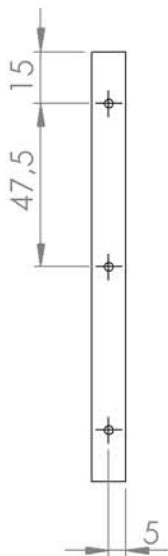
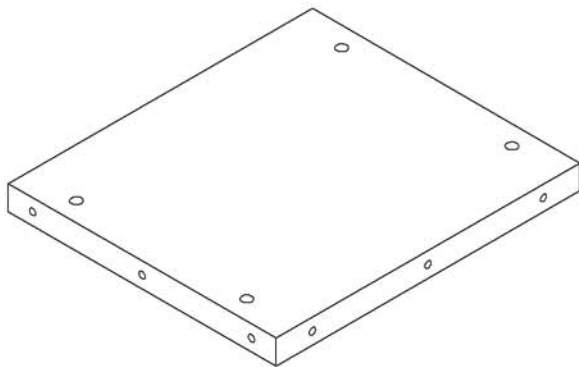
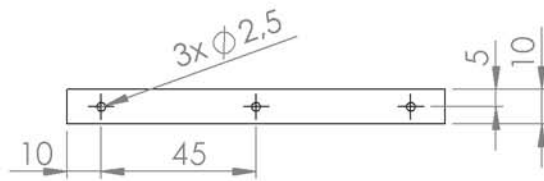
**Aluminum Plate 2**

NUMBER OF DRAWING:

**13/36**

**A4**

SCALE 1:2



**Licencia educacional de SolidWorks**  
**Sólo para uso académico**

*\*All distances in mm*



**LUNDS UNIVERSITET**  
 Lunds Tekniska Högskola

MATERIAL: Aluminum

NUMBER OF PIECES: 1

AUTHOR: ALBERT PLA RUIZ      DATE: May 2012

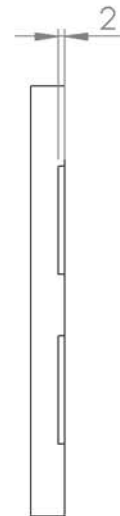
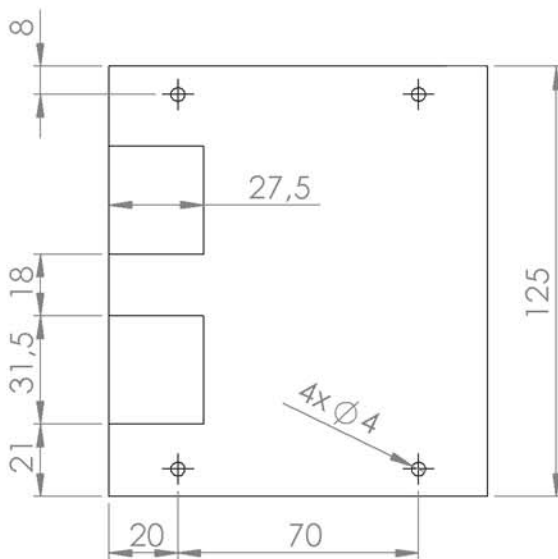
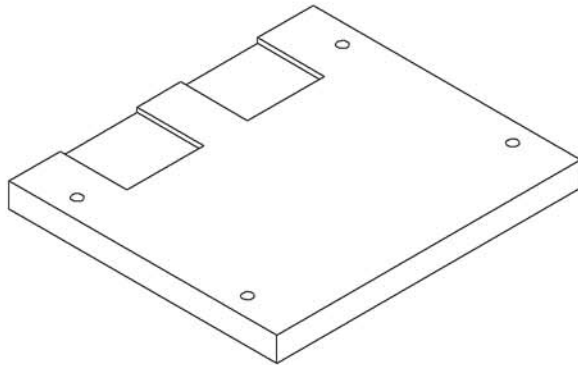
PROJECT: Temperature Control of a Scientific Instrument

TITLE:

**Aluminum Plate 3**

NUMBER OF DRAWING: 14/36

A4  
 SCALE 1:2



**Licencia educacional de SolidWorks**  
**Sólo para uso académico**

*\*All distances in mm*

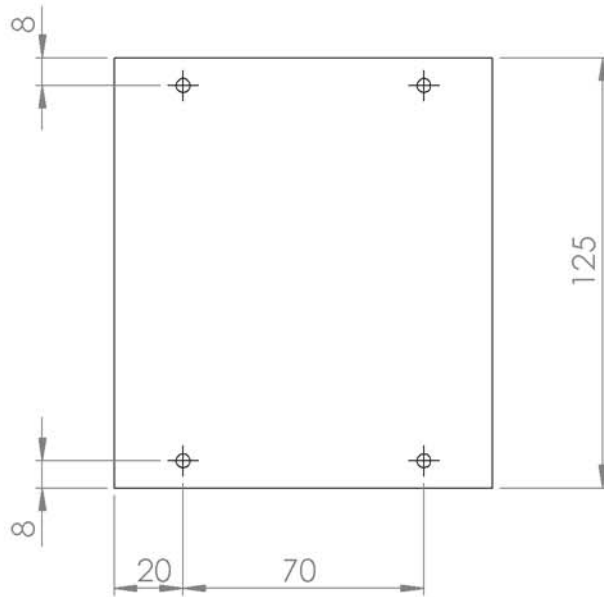
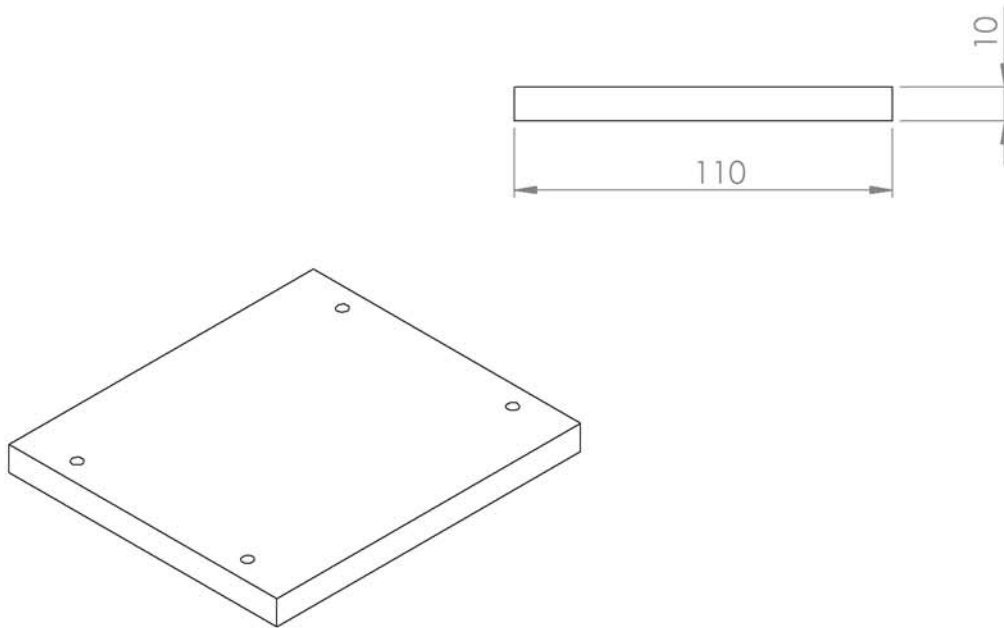


**LUNDS UNIVERSITET**  
 Lunds Tekniska Högskola

MATERIAL: Aluminum

NUMBER OF PIECES: 1

AUTHOR: ALBERT PLA RUIZ	DATE: May 2012
PROJECT: Temperature Control of a Scientific Instrument	
TITLE: <b>Aluminum Plate 4</b>	
NUMBER OF DRAWING:	15/36
	A4
	SCALE 1:2



**Licencia educacional de SolidWorks**  
**Sólo para uso académico**

*\*All distances in mm*

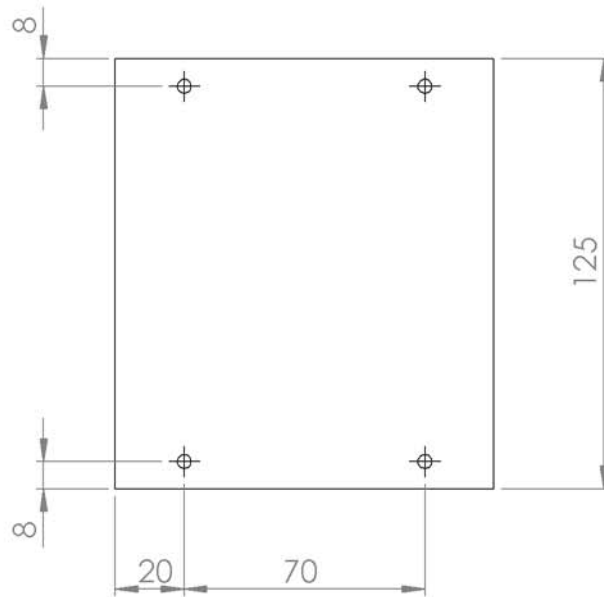
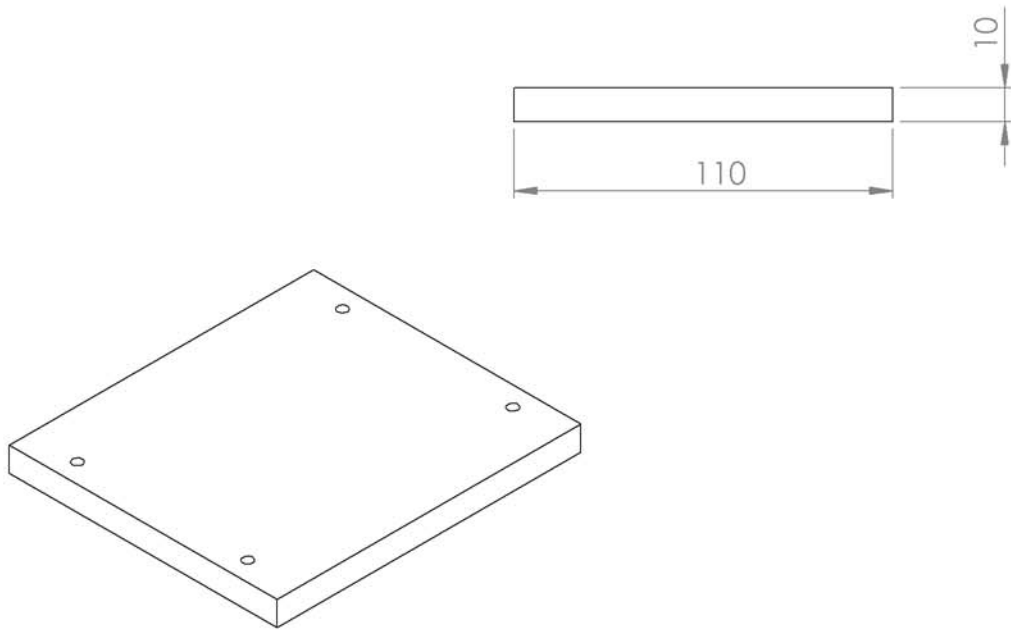


**LUNDS UNIVERSITET**  
 Lunds Tekniska Högskola

MATERIAL: Aluminum

NUMBER OF PIECES: 1

AUTHOR: ALBERT PLA RUIZ		DATE: May 2012	
PROJECT: Temperature Control of a Scientific Instrument			
TITLE: <b>Aluminum Plate 5</b>			
NUMBER OF DRAWING:		<b>16/36</b>	A4
			SCALE 1:2



**Licencia educacional de SolidWorks**  
**Sólo para uso académico**

*\*All distances in mm*

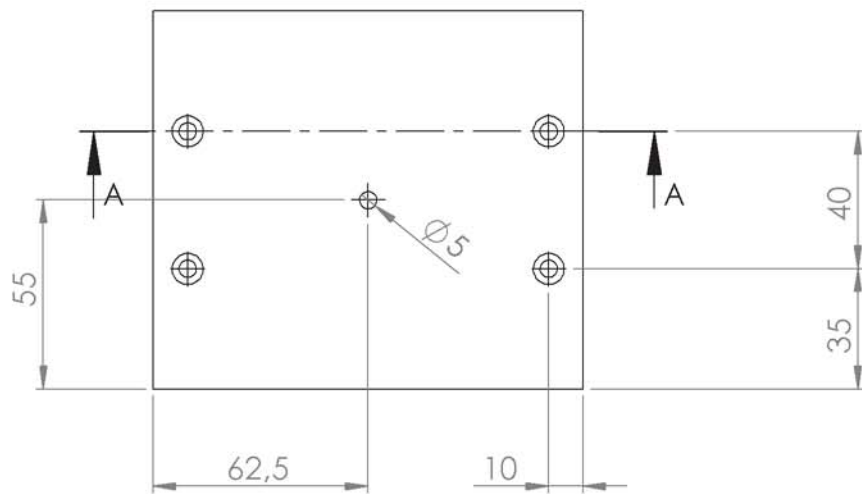
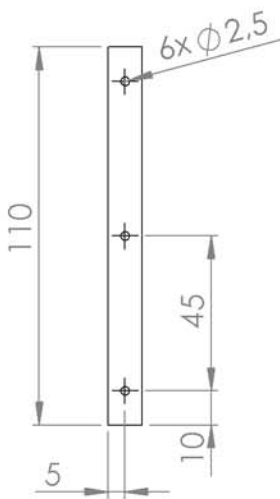
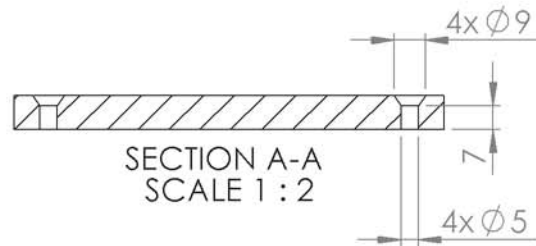
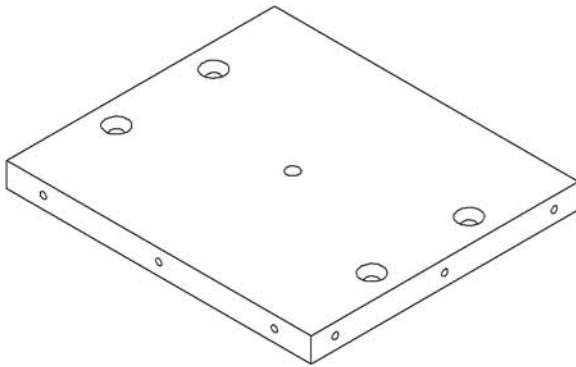
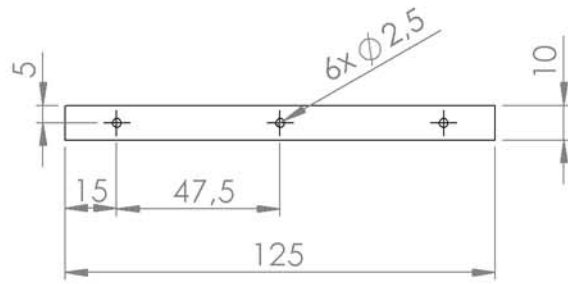


**LUNDS UNIVERSITET**  
 Lunds Tekniska Högskola

MATERIAL: Aluminum

NUMBER OF PIECES: 1

AUTHOR: ALBERT PLA RUIZ		DATE: May 2012
PROJECT: Temperature Control of a Scientific Instrument		
TITLE: <b>Aluminum Plate 6</b>		
NUMBER OF DRAWING:	<b>17/36</b>	A4
		SCALE 1:2



**Licencia educacional de SolidWorks**  
**Sólo para uso académico**

*\*All distances in mm*



**LUNDS UNIVERSITET**  
 Lunds Tekniska Högskola

MATERIAL: Copper

NUMBER OF PIECES: 1

AUTHOR: ALBERT PLA RUIZ

DATE: May 2012

PROJECT: Temperature Control of a Scientific Instrument

TITLE:

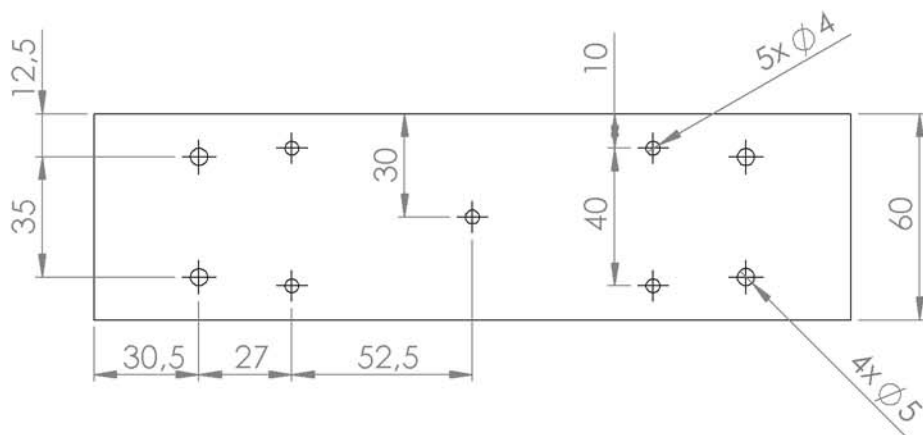
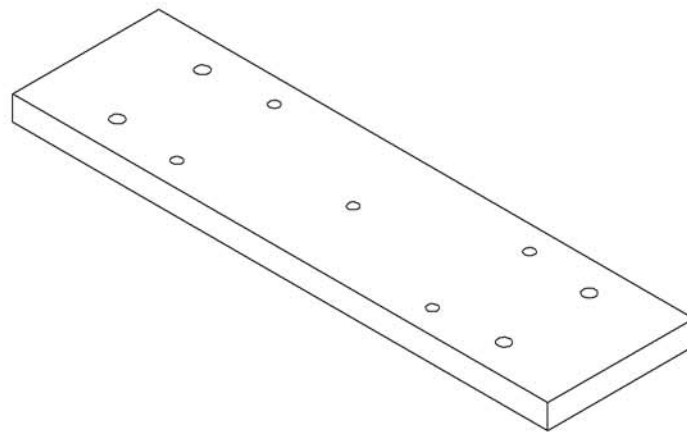
**Copper Plate 1**

NUMBER OF DRAWING:

**18/36**

**A4**

SCALE 1:2



**Licencia educacional de SolidWorks**  
**Sólo para uso académico**

*\*All distances in mm*

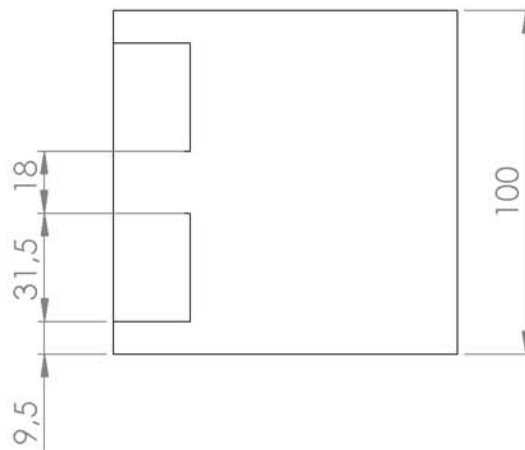
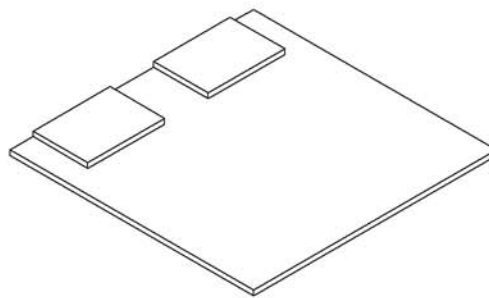
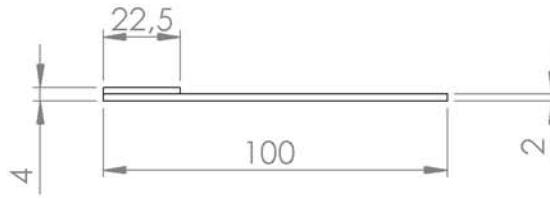


**LUNDS UNIVERSITET**  
 Lunds Tekniska Högskola

MATERIAL: Copper

NUMBER OF PIECES: 1

AUTHOR: ALBERT PLA RUIZ	DATE: May 2012
PROJECT: Temperature Control of a Scientific Instrument	
TITLE: <b>Copper Plate 2</b>	
NUMBER OF DRAWING:	19/36
	A4
	SCALE 1:2



**Licencia educacional de SolidWorks**  
**Sólo para uso académico**

*\*All distances in mm*



**LUNDS UNIVERSITET**  
 Lunds Tekniska Högskola

MATERIAL:

NUMBER OF PIECES: 1

AUTHOR: ALBERT PLA RUIZ

DATE: May 2012

PROJECT: Temperature Control of a Scientific Instrument

TITLE:

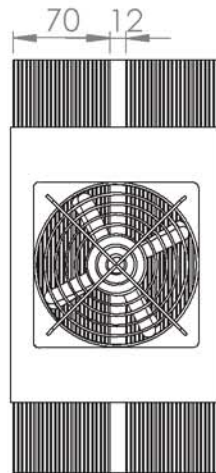
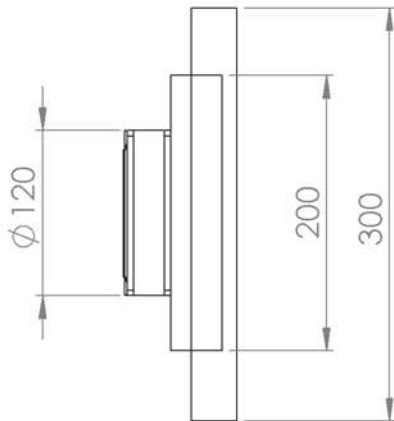
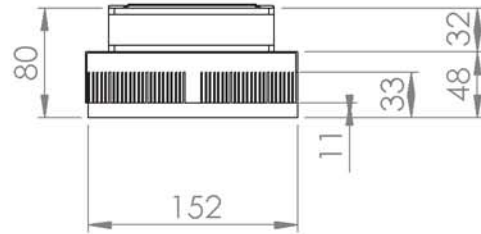
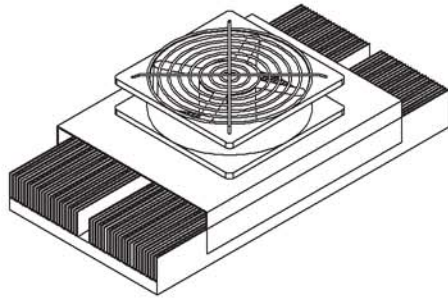
**Heater**

NUMBER OF DRAWING:

**20/36**

A4

SCALE 1:2



**Licencia educacional de SolidWorks**  
**Sólo para uso académico**

*\*All distances in mm*



**LUNDS UNIVERSITET**  
 Lunds Tekniska Högskola

MATERIAL: Aluminum

NUMBER OF PIECES: 1

AUTHOR: ALBERT PLA RUIZ

DATE: May 2012

PROJECT: Temperature Control of a Scientific Instrument

TITLE:

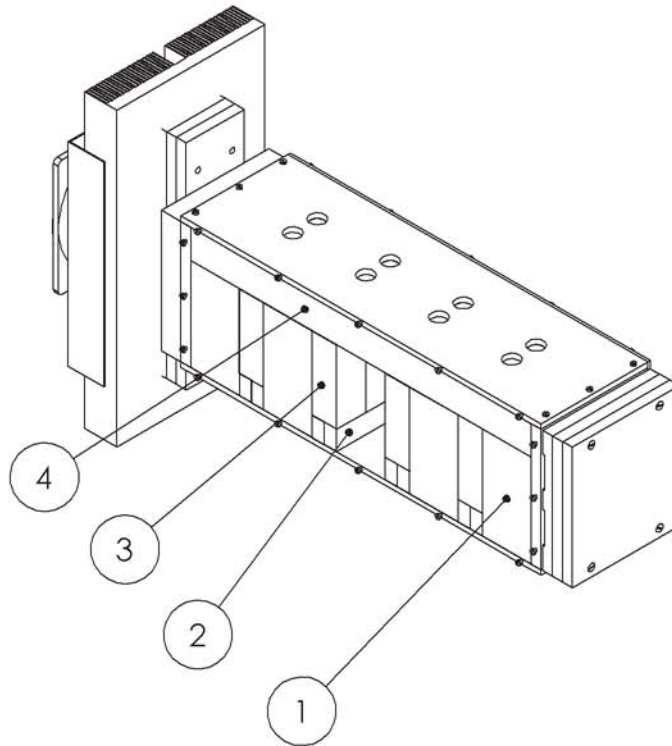
**TEC**

NUMBER OF DRAWING:

**21/36**

**A4**

SCALE 1:5



Number	Name	Quantity	Num Drawing
1	Inside insulation 1	4	23
2	Inside insulation 2	8	24
3	Inside insulation 3	8	25
4	Inside insulation 4	1	26

**Licencia educacional de SolidWorks**  
**Sólo para uso académico**



**LUNDS UNIVERSITET**  
 Lunds Tekniska Högskola

MATERIAL:

NUMBER OF PIECES: 1

AUTHOR: ALBERT PLA RUIZ

DATE: May 2012

PROJECT: Temperature Control of a Scientific Instrument

TITLE:

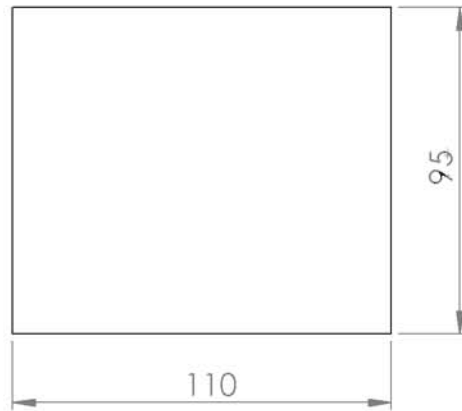
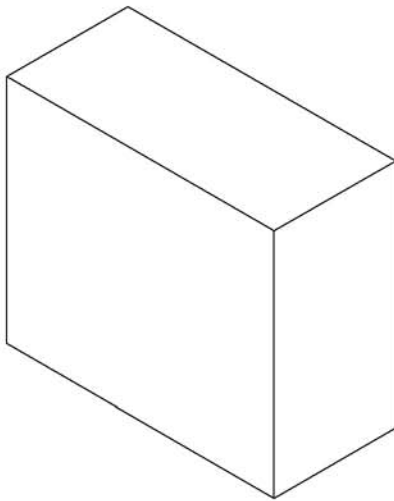
**STIC inside insulated**

NUMBER OF DRAWING:

**22/36**

A4

SCALE 1:5



**Licencia educacional de SolidWorks**  
**Sólo para uso académico**

*\*All distances in mm*

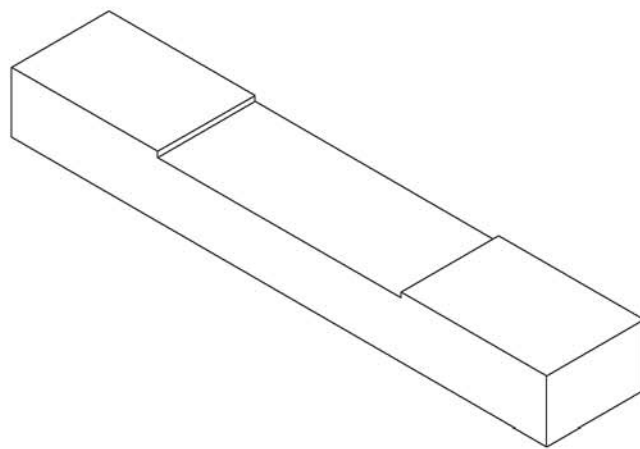
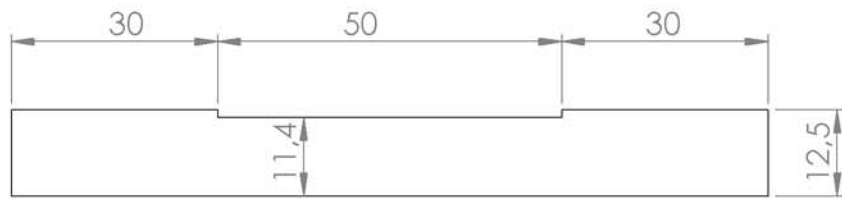


**LUNDS UNIVERSITET**  
 Lunds Tekniska Högskola

MATERIAL: Extruded Polystyrene Foam

NUMBER OF PIECES: 4

AUTHOR: ALBERT PLA RUIZ	DATE: May 2012
PROJECT: Temperature Control of a Scientific Instrument	
TITLE: <b>Inside Insulation 1</b>	
NUMBER OF DRAWING: <b>23/36</b>	A4
	SCALE 1:2



**Licencia educacional de SolidWorks**  
**Sólo para uso académico**

*\*All distances in mm*

AUTHOR: ALBERT PLA RUIZ      DATE: May 2012  
 PROJECT: Temperature Control of a Scientific Instrument

TITLE:  
**Inside Insulation 2**



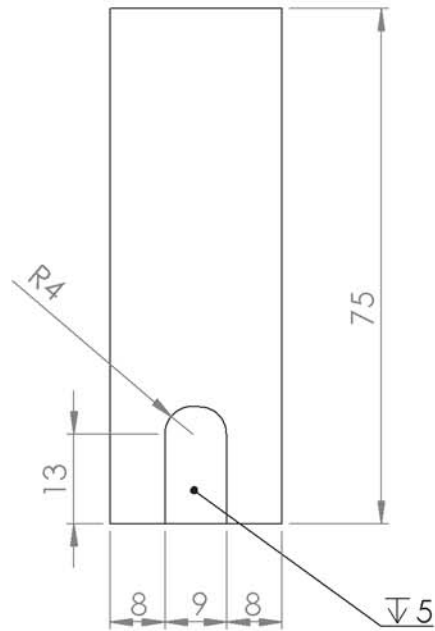
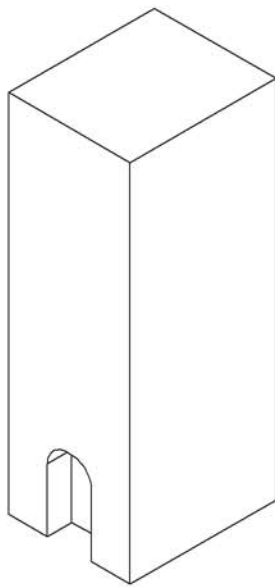
**LUNDS UNIVERSITET**  
 Lunds Tekniska Högskola

MATERIAL: Extruded  
 Polystyrene Foam

NUMBER OF PIECES: 8

NUMBER OF DRAWING: **24/36**

**A4**  
 SCALE 1:1



**Licencia educacional de SolidWorks**  
**Sólo para uso académico**

*\*All distances in mm*



**LUNDS UNIVERSITET**  
 Lunds Tekniska Högskola

MATERIAL: Extruded  
 Polystyrene Foam

NUMBER OF PIECES: 8

AUTHOR: ALBERT PLA RUIZ

DATE: May 2012

PROJECT: Temperature Control of a Scientific Instrument

TITLE:

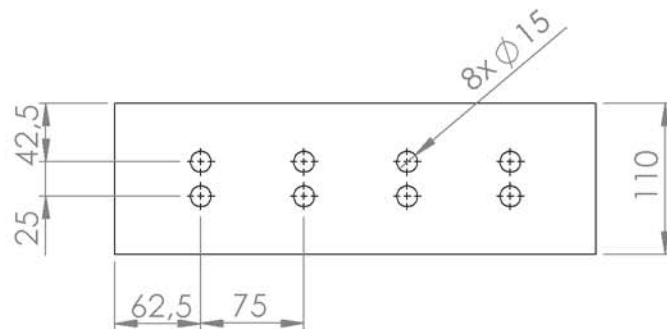
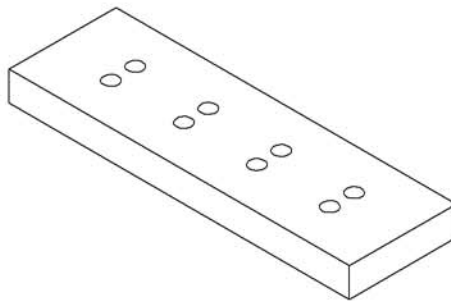
**Inside Insulation 3**

NUMBER OF DRAWING:

**25/36**

**A4**

SCALE 1:1



**Licencia educacional de SolidWorks**  
**Sólo para uso académico**

*\*All distances in mm*



**LUNDS UNIVERSITET**  
 Lunds Tekniska Högskola

MATERIAL: Extruded  
 Polystyrene Foam

NUMBER OF PIECES: 1

AUTHOR: ALBERT PLA RUIZ

DATE: May 2012

PROJECT: Temperature Control of a Scientific Instrument

TITLE:

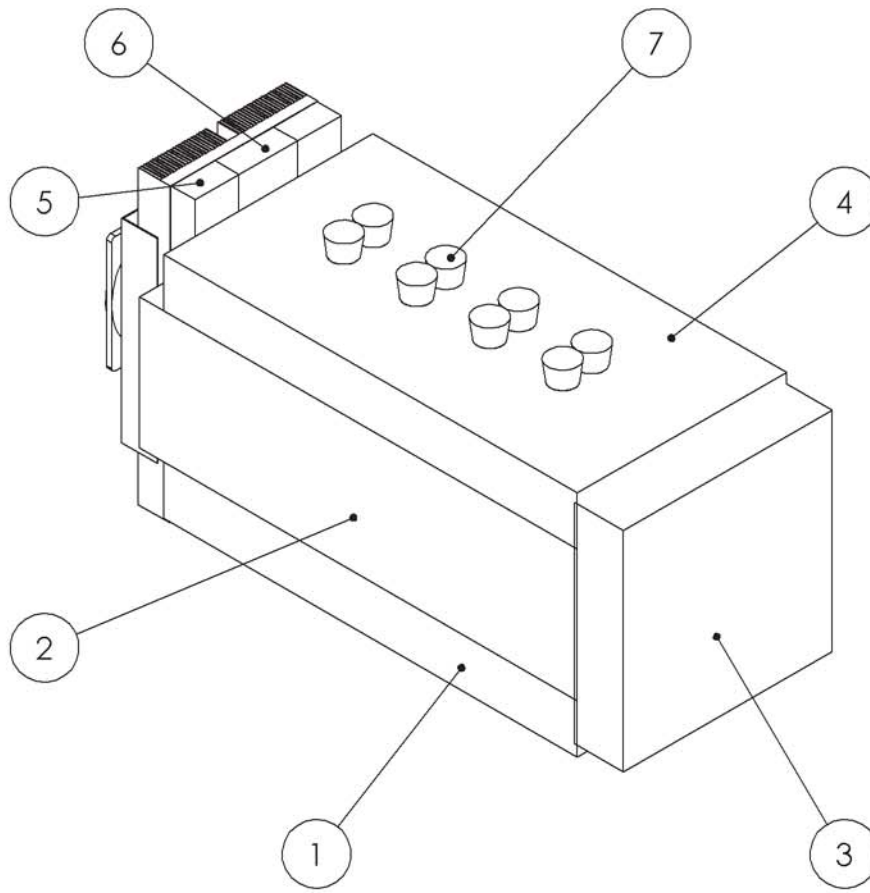
**Inside Insulation 4**

NUMBER OF DRAWING:

**26/36**

A4

SCALE 1:5



Number	Name	Quantity	Num Drawing
1	Outside Insulation 1	1	28
2	Outside Insulation 2	2	29
3	Outside Insulation 3	1	30
4	Outside Insulation 4	1	31
5	Outside Insulation 5	2	32
6	Outside Insulation 6	1	33
7	Outside Insulation 7	8	34

**Licencia educacional de SolidWorks**  
**Sólo para uso académico**



**LUNDS UNIVERSITET**  
 Lunds Tekniska Högskola

MATERIAL:

NUMBER OF PIECES: 1

AUTHOR: ALBERT PLA RUIZ

DATE: May 2012

PROJECT: Temperature Control of a Scientific Instrument

TITLE:

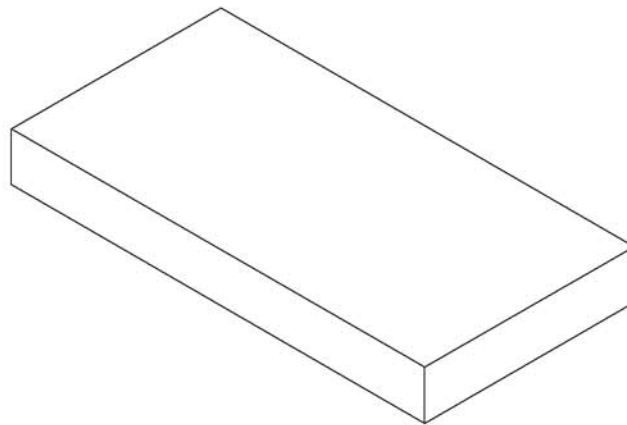
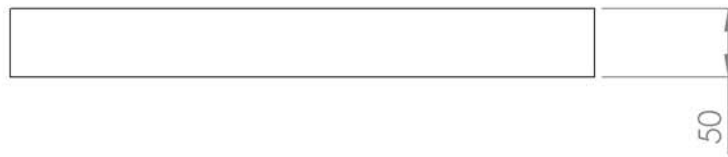
**STIC Outside Insulated**

NUMBER OF DRAWING:

**27/36**

A4

SCALE 1:5



**Licencia educacional de SolidWorks**  
**Sólo para uso académico**

*\*All distances in mm*



**LUNDS UNIVERSITET**  
 Lunds Tekniska Högskola

MATERIAL: Extruded  
 Polystyrene Foam

NUMBER OF PIECES: 1

AUTHOR: ALBERT PLA RUIZ

DATE: May 2012

PROJECT: Temperature Control of a Scientific Instrument

TITLE:

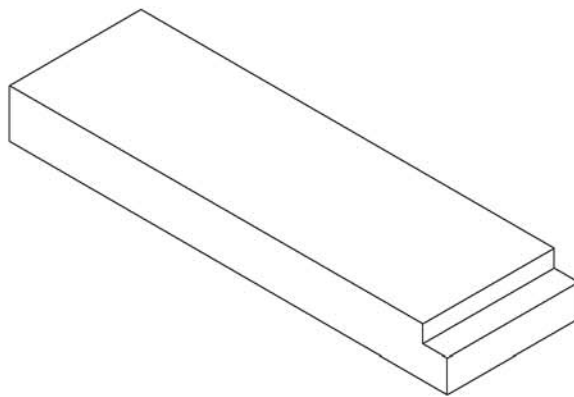
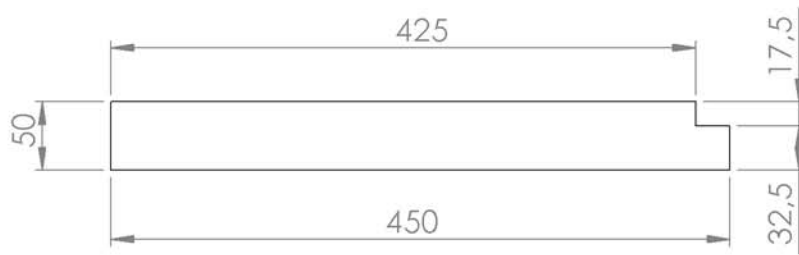
**Outside Insulation 1**

NUMBER OF DRAWING:

**28/36**

A4

SCALE 1:5



**Licencia educacional de SolidWorks**  
**Sólo para uso académico**

*\*All distances in mm*



**LUNDS UNIVERSITET**  
 Lunds Tekniska Högskola

MATERIAL: Extruded  
 Polystyrene Foam

NUMBER OF PIECES: 2

AUTHOR: ALBERT PLA RUIZ

DATE: May 2012

PROJECT: Temperature Control of a Scientific Instrument

TITLE:

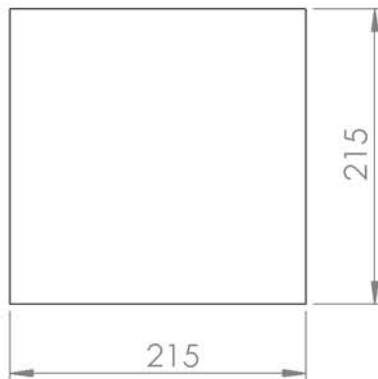
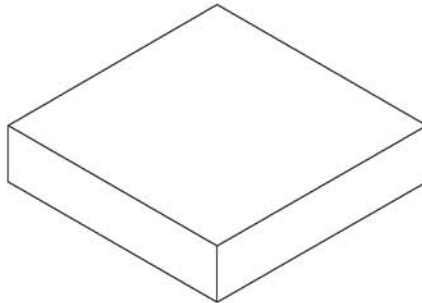
**Outside Insulation 2**

NUMBER OF DRAWING:

**29/36**

A4

SCALE 1:5



**Licencia educacional de SolidWorks**  
**Sólo para uso académico**

*\*All distances in mm*

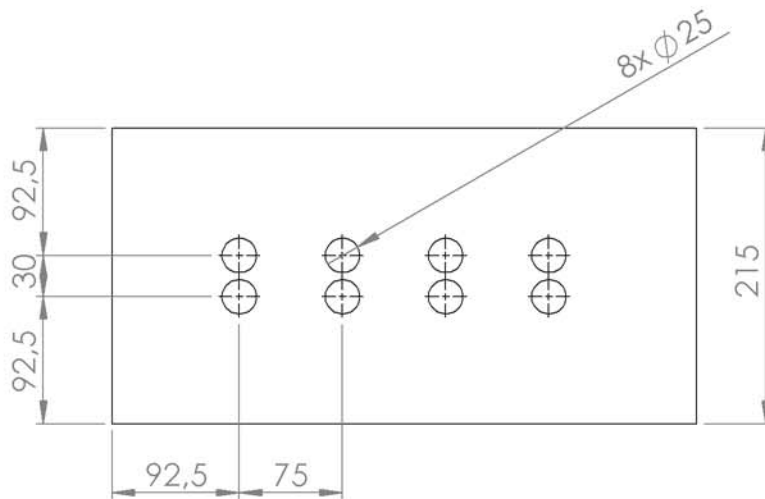
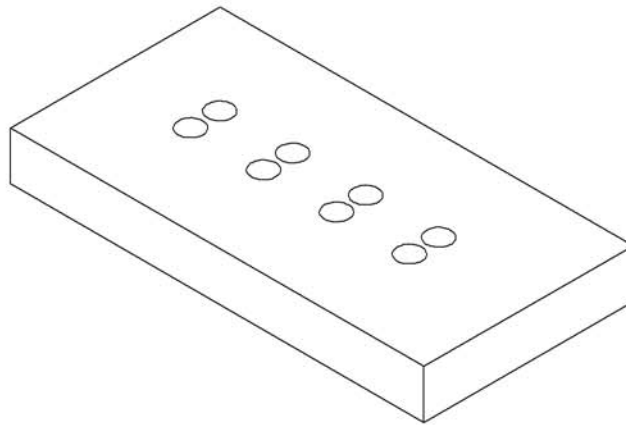


**LUNDS UNIVERSITET**  
 Lunds Tekniska Högskola

MATERIAL: Extruded  
 Polystyrene Foam

NUMBER OF PIECES: 1

AUTHOR: ALBERT PLA RUIZ		DATE: May 2012
PROJECT: Temperature Control of a Scientific Instrument		
TITLE: <h2 style="text-align: center;">Outside Insulation 3</h2>		
NUMBER OF DRAWING:	30/36	A4
		SCALE 1:5



**Licencia educacional de SolidWorks**  
**Sólo para uso académico**

\*All distances in mm



**LUNDS UNIVERSITET**  
 Lunds Tekniska Högskola

MATERIAL: Extruded  
 Polystyrene Foam

NUMBER OF PIECES: 1

AUTHOR: ALBERT PLA RUIZ

DATE: May 2012

PROJECT: Temperature Control of a Scientific Instrument

TITLE:

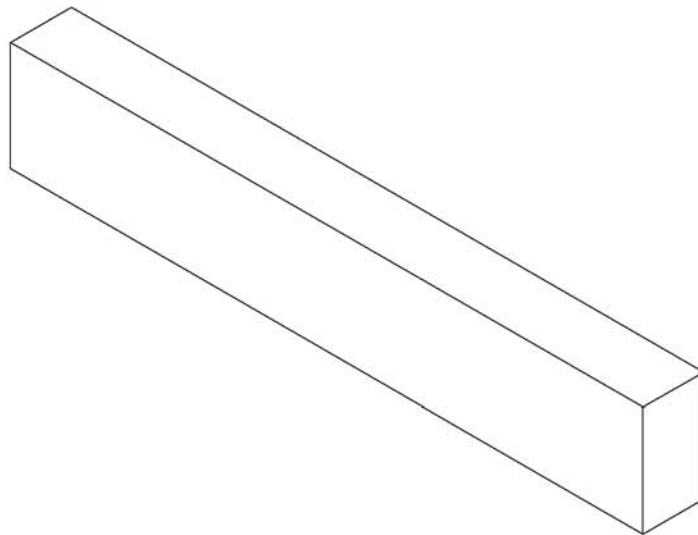
**Outside Insulation 4**

NUMBER OF DRAWING:

**31/36**

A4

SCALE 1:5



**Licencia educacional de SolidWorks**  
**Sólo para uso académico**

*\*All distances in mm*

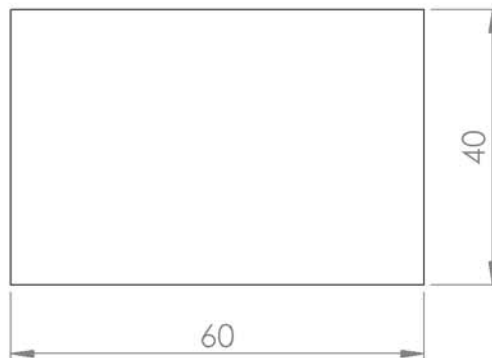
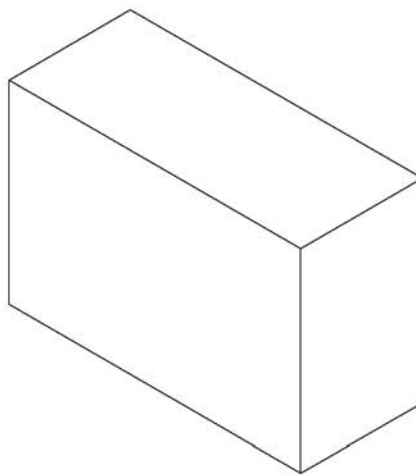


**LUNDS UNIVERSITET**  
 Lunds Tekniska Högskola

MATERIAL: Extruded Polystyrene Foam

NUMBER OF PIECES: 2

AUTHOR: ALBERT PLA RUIZ	DATE: May 2012
PROJECT: Temperature Control of a Scientific Instrument	
TITLE: <b>Outside Insulation 5</b>	
NUMBER OF DRAWING: <b>32/36</b>	A4
	SCALE 1:2



**Licencia educacional de SolidWorks**  
**Sólo para uso académico**

*\*All distances in mm*



**LUNDS UNIVERSITET**  
 Lunds Tekniska Högskola

MATERIAL: Extruded  
 Polystyrene Foam

NUMBER OF PIECES: 1

AUTHOR: ALBERT PLA RUIZ

DATE: May 2012

PROJECT: Temperature Control of a Scientific Instrument

TITLE:

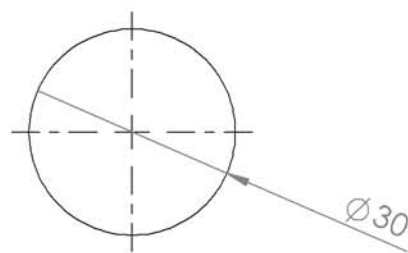
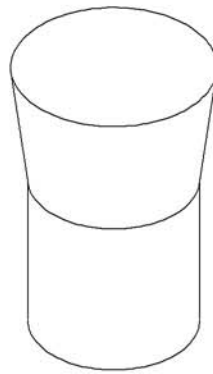
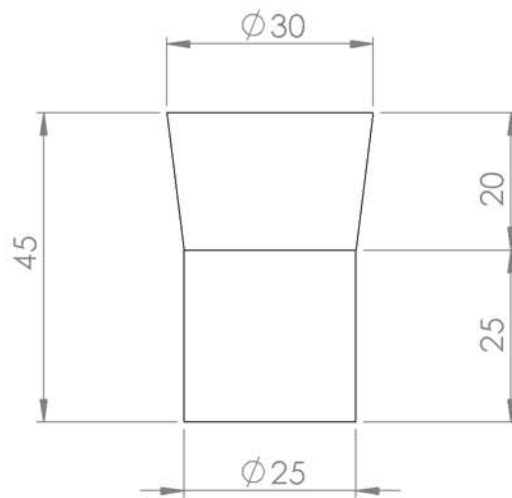
**Outside Insulation 6**

NUMBER OF DRAWING:

**33/36**

A4

SCALE 1:1



**Licencia educacional de SolidWorks**  
**Sólo para uso académico**

*\*All distances in mm*

AUTHOR: ALBERT PLA RUIZ

DATE: May 2012

PROJECT: Temperature Control of a Scientific Instrument

TITLE:

**Outside Insulation 7**

**LUNDS UNIVERSITET**  
 Lunds Tekniska Hogskola

MATERIAL: Extruded  
 Polystyrene Foam

NUMBER OF PIECES: 8

NUMBER OF DRAWING:

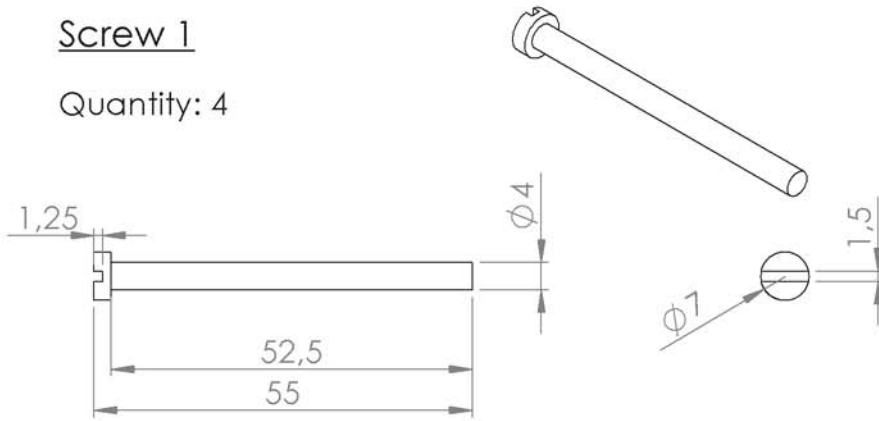
**34/36**

A4

SCALE 1:1

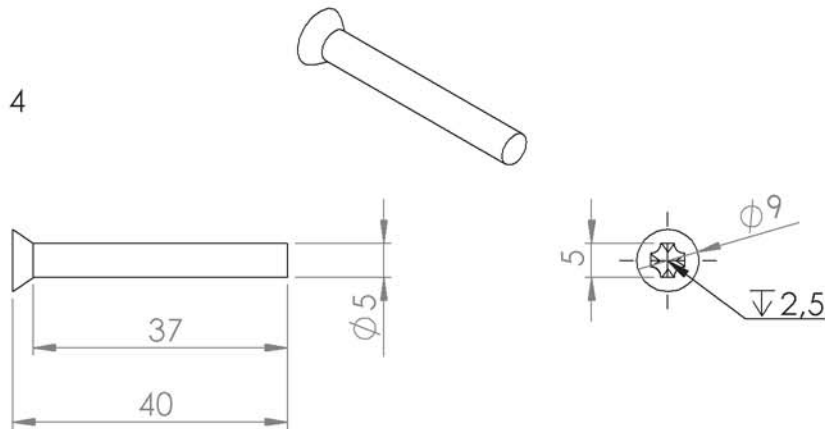
Screw 1

Quantity: 4



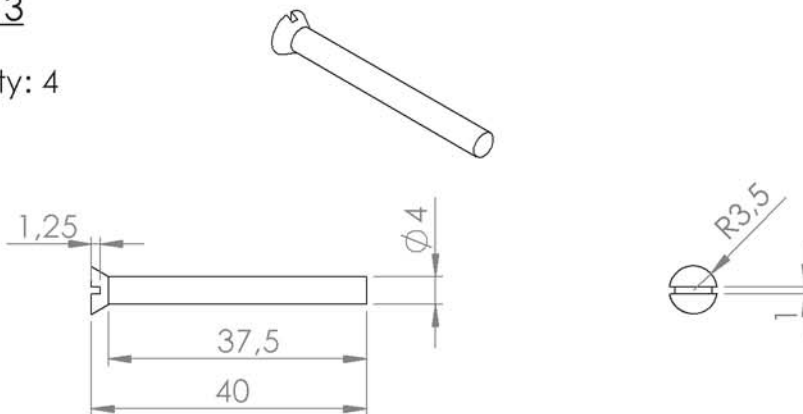
Screw 2

Quantity: 4



Screw 3

Quantity: 4



**Licencia educacional de SolidWorks**  
**Sólo para uso académico**



**LUNDS UNIVERSITET**  
 Lunds Tekniska Högskola

MATERIAL: Steel

NUMBER OF PIECES:

*\*All distances in mm*

AUTHOR: ALBERT PLA RUIZ      DATE: May 2012  
 PROJECT: Temperature Control of a Scientific Instrument

TITLE:

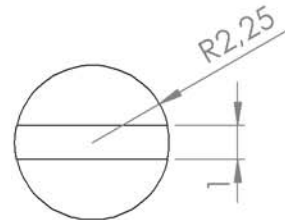
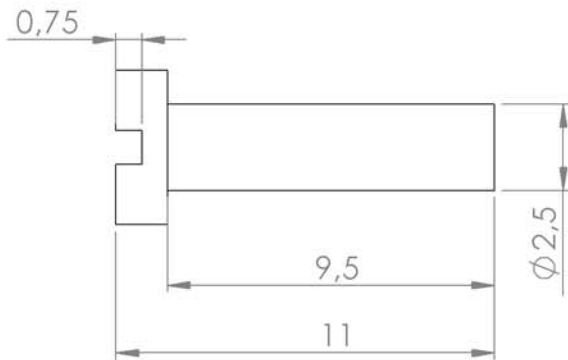
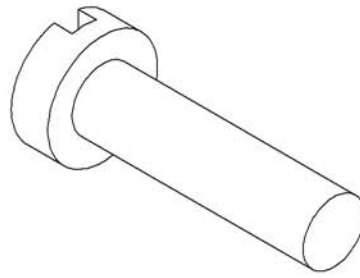
**Screws 1**

NUMBER OF DRAWING: **35/36**

**A4**  
 SCALE 1:1

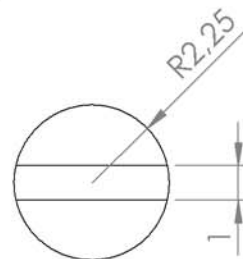
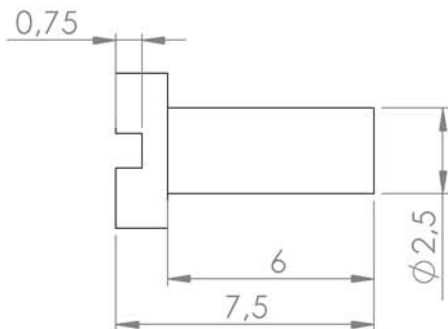
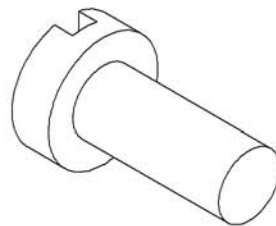
### Screw 4

Quantity: 12



### Screw 5

Quantity: 32



**Licencia educacional de SolidWorks**  
**Sólo para uso académico**

*\*All distances in mm*

AUTHOR: ALBERT PLA RUIZ

DATE: May 2012

PROJECT: Temperature Control of a Scientific Instrument

TITLE:

**Screws 2**



**LUNDS UNIVERSITET**  
Lunds Tekniska Högskola

MATERIAL: Steel

NUMBER OF DRAWING:

**36/36**

A4

NUMBER OF PIECES:

SCALE 5:1